

DISSERTATION

Titel der Dissertation

Modulation of cardiac sodium channel variants by Fyn tyrosine kinase

Verfasser

Gowri Shankar Bagavananthem Andavan, B.Tech, M.S.

angestrebter akademischer Grad

Doktor der Naturwissenschaften (Dr.rer.nat.)

Wien, 2011

Studienkennzahl lt. A 091 490

Studienblatt:

Dissertationsgebiet lt. Molekulare Biologie

Studienblatt:

Betreuerin / Betreuer: Ao.Univ.Prof. Mag. Dr. Rosa Lemmens-Gruber

Acknowledgements

Many thanks to my supervisor, ao.Univ.Prof. Dr. Rosa Lemmens-Gruber, for her tremendous job guiding me during this thesis, for spending so many hours, giving the right advice at the right time and for her outstanding contribution to my studies.

I would also thank the head of the Department and co-ordinator of the postgraduate program “Molecular Drug Targets” Univ.-Prof. Dr. Steffen Hering. I would thank my Masters supervisor Dr. Michael Charleston from University of Sydney, Sydney, Australia and my undergraduate supervisors Dr K. Sekar from Indian Institute of Science, Bangalore, India and Prof. P. Gautham from Anna University, Chennai, India for their continuous guidance and support.

I would also thank my fellow researchers in the Department of Pharmacology and Toxicology for their continuous support and fun.

Finally, I would like to thank my family who supported me so much during my whole period of studies.

Contents

Introduction -----	1
1.1 Background -----	1
1.1.1 Cardiac action potential-----	2
1.2 Voltage-gated ion channels -----	3
1.3 Voltage-gated sodium channels -----	4
1.3.1 Structure of voltage-gated sodium channels -----	4
1.3.2 Sodium channel gating -----	6
1.3.3 Voltage-gated sodium channel subtypes -----	6
1.4 Channelopathies -----	7
1.4.1 Cardiac sodium (SCN5A) channelopathies -----	9
1.5 Cardiac sodium channel splice variants -----	9
1.5.1 Functional Nav1.5 splice variants -----	11
1.5.2 Non-functional Nav1.5 splice variants-----	12
1.6 Src tyrosine kinase -----	12
1.6.1 Members of Src tyrosine kinase and its cellular location -----	13
1.6.2 Functional regions of Src tyrosine kinase -----	13
1.6.3 Structure of Src PTK and activation of tyrosine kinase -----	15
1.6.4 Mechanism of Src activation -----	17
1.7 Src kinase and ion channels-----	18
1.7.1 Src tyrosine kinase and voltage-gated sodium channels -----	19
1.7.2 Physiological relevance of cardiac sodium channels and Src family tyrosine kinase modulation -----	20
1.7.3 Modulation of sodium channel variants by Fyn tyrosine kinase -----	20
1.8 Nomenclature -----	21
Aims -----	22
Methods and Materials-----	23
3.1 Molecular Biology -----	23
3.1.1 DNA clones-----	23
3.1.2 DNA amplification and isolation -----	23
3.1.3 Site-directed mutagenesis-----	24
3.2 Cell Culture -----	26
3.2.1 Cells-----	26
3.2.2 Cell culture media -----	26
3.2.3 Sub-culturing cells-----	27
3.2.4 Transfection-----	28
3.3 Electrophysiology -----	28
3.3.1 Patch pipettes-----	28
3.3.2 Solutions -----	29
3.3.3 Experimental set-up -----	29
3.3.4 Pulse protocol -----	30
3.4 Bioinformatics Analysis-----	31

Results -----	32
4.1 Voltage-dependent kinetic parameters for Q1077 and Δ Q1077 cardiac sodium channel variants-----	32
4.2 Inactivation properties of Δ Q1077 and Q1077 with Fyn ^{CA} , Fyn ^{KD} and tyrosine kinase inhibitor PP2 -----	36
4.3 Activation properties of Δ Q1077 and Q1077 with Fyn ^{CA} -----	41
4.4 Sequence alignment of sodium channel subunits of the intracellular loop L _{DII-DIII} -----	43
4.5 Kinetics of Q1077 cardiac sodium channel mutants -----	45
4.6 Inactivation kinetics of Q1077 mutants with Fyn ^{CA} and Fyn ^{KD} -----	47
4.6.1 Modulation of inactivation kinetics of Q1077K mutant with Fyn ^{CA} and Fyn ^{KD} -----	47
4.6.2 Modulation of inactivation kinetics of Q1077A mutant with Fyn ^{CA} and Fyn ^{KD} -----	48
4.6.3 Modulation of inactivation kinetics of Q1077P mutant with Fyn ^{CA} and Fyn ^{KD} -----	48
4.6.4 Modulation of inactivation kinetics of Q1077Y mutant with Fyn ^{CA} and Fyn ^{KD} -----	48
4.6.5 Correlation between the mutant amino acid properties and the shift of inactivation curves. -----	51
Discussion -----	54
5.1 Splice variant specificity of Fyn modulation of cardiac sodium channels -----	54
5.2 Mutational effects at position 1077 -----	56
5.3 Uniqueness of cardiac sodium channel intracellular loop L _{DII-DIII} -----	57
5.4 Possible binding sites for the SH2 domain in the cardiac sodium channel -----	58
5.5 Putative SH3 domain binding sites in sodium channels -----	59
5.6 Importance of the tyrosine residues in the sodium channel for Fyn tyrosine kinase -----	62
Conclusion -----	64
Abbreviations -----	65
References-----	66
Appendix -----	78
9.1 Abstract -----	78
9.2 Zusammenfassung-----	78
9.3 Alignment -----	82
9.4 Curriculum vitae-----	89

List of Figures

Figure 1: Representation of an action potential from a ventricular myocardial cell showing all the possible currents responsible for different phases.....	2
Figure 2: A schematic representation of the voltage-gated sodium channel showing all four domains (DI-DIV) of the α -subunit and two β -subunits.....	5
Figure 3: Structure of Nav1.5 splice variants.	10
Figure 4: Organization of Src tyrosine kinase domain structure	13
Figure 5: Ribbon diagram illustrating the structure of human Src.	16
Figure 6: The activation mechanism of Src tyrosine kinase.	18
Figure 7: Original traces illustrating steady-state activation and steady-state inactivation of sodium channel currents of both (1) Q1077Present and (2) Δ Q1077.....	33
Figure 8: Boltzmann fitted steady-state inactivation and activation curves of (A) Q1077Present and (B) Δ Q1077 stably transfected cells.	35
Figure 9: Expression of catalytic active FynCA alters stably expressed Q1077Present and Δ Q1077 cells in the steady state inactivation curves. ...	39
Figure 10: Steady-state activation of stably expressed Q1077 and Δ Q1077 cardiac sodium channels.	42
Figure 11: Alignment of the intracellular loop of sodium channel subtypes connecting domain II and III (LDII-DIII).	44
Figure 12: Original traces illustrating steady state inactivation of all the transiently transfected mutants at position Q1077 in tsA-201 cells:	45
Figure 13: Expression of catalytic active Fyn ^{CA} alters steady state inactivation kinetics of Q1077 mutants.	50
Figure 14: Plot showing the linear relationship ($R^2 = 0.99$) between the hydrophobicity of an amino acid and the difference in shift of the inactivation curves	51
Figure 15: Plot showing the linear relationship between different properties of amino acids and the difference in shift of the inactivation curves	52
Figure 16: Amino acid sequence of the Q1077 (Accession Number AC137587) cardiac sodium channel.....	61
Figure 17: Amino acid sequence of the Nav1.2 (Accession Number NP_001035232) neuronal sodium channel.....	62

List of Tables

Table 1: Major currents during the cardiac ventricular action potential.....	3
Table 2: Different sodium channel isoforms and their associated channelopathies.	8
Table 3: Different cardiac sodium channel variants	21
Table 4: Forward and reverse primers for Q1077 mutations.....	25
Table 5: PCR cycling parameters Quick Change Site-Directed Mutagenesis.....	25
Table 6: Medium composition for culturing stably transfected cells.	27
Table 7: Voltage-dependent kinetic parameters for Q1077 and Δ Q1077 cardiac sodium channel variants.....	34
Table 8: Kinetic parameters for Q1077 and Δ Q1077 cardiac sodium channel variants with and without Fyn ^{CA}	37
Table 9: Half-maximal inactivation of both Q1077 and Δ Q1077 with Fyn ^{CA} , Fyn ^{KD} and with Fyn ^{CA} + PP2.....	38
Table 10: Half-maximal activation and slope of both Q1077 and Δ Q1077 with Fyn ^{CA}	41
Table 11: Kinetic parameters for all four mutants of the Q1077 cardiac sodium channel	46
Table 12: Half-maximal inactivation of all four Q1077 mutants with Fyn ^{CA} and Fyn ^{KD}	49

Introduction

1.1 Background

Ion channels are intrinsic membrane proteins that control the flow of specific ions across the cellular membrane. All ion channels are large transmembrane proteins. In living cells there are 300 types of ion channels (Gabashvili et al., 2007). Channels are ion selective and can differentiate between size and charge of the ions. Ion channels are classified based on the physical and chemical modulator of their gating properties. Some of the important groups of ion channels are listed below.

- Ligand-gated channels
- Voltage-gated channels
- Second messenger-gated channels
- Mechanosensitive channels
- Gap junctions

Voltage-gated ion channels in the cell membrane possess three different states: closed, open and inactivated. Ion channels in the cell membrane open or close depending on the cell membrane potential. Specific ions flow down their electrochemical gradient, when a channel is in an open state. The ion channel protein adopts different conformational states depending on the membrane potential. Ionic current is measured from the ion flow through an open channel. The best method to study this process is the patch clamp technique.

1.1.1 Cardiac action potential

The cardiac action potential is necessary for the electrical conduction system of the heart. Action potential of a single cardiac myocyte and the electrophysiological and mechanical function of the heart are interdependent. Various ion channels are responsible for the cardiac action potential.

The action potential is divided into five distinct phases corresponding to clearly recognizable landmarks in its contour.

Phase 0: Fast depolarization or upstroke

Phase 1: Fast initial repolarization

Phase 2: Plateau

Phase 3: Fast terminal repolarization

Phase 4: Electric diastole

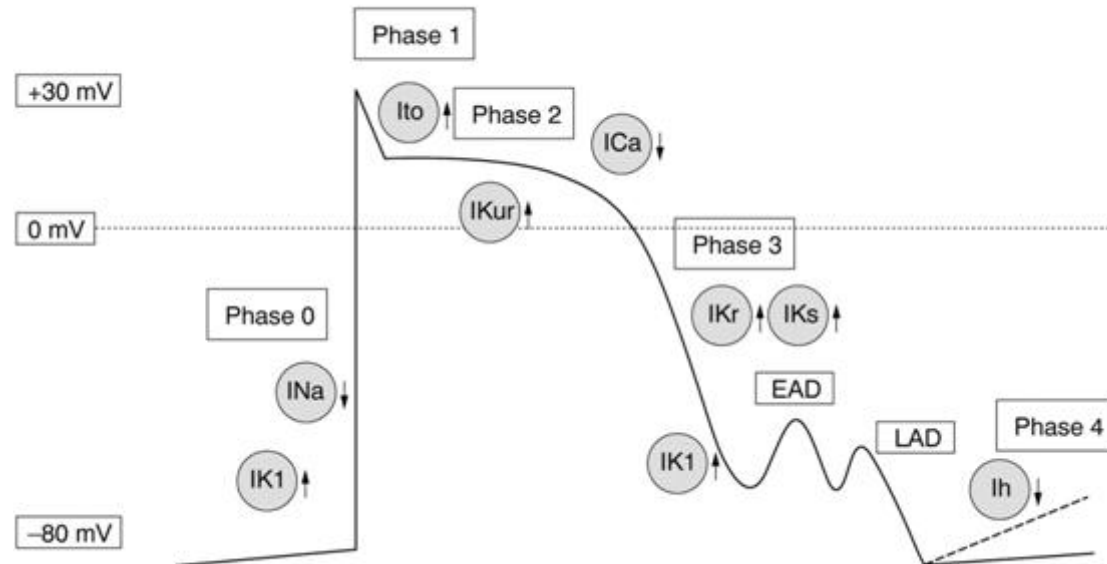


Figure 1: Representation of an action potential from a ventricular myocardial cell showing all the possible currents responsible for different phases.

An action potential is generated when the membrane potential is partially depolarized from the resting potential to the threshold potential.

Table 1: Major currents during the cardiac ventricular action potential.

Ions	Current	Protein	Gene	Phase/Role
Na⁺	I_{Na}	Na _V 1.5	SCN5A	0
Ca²⁺	$I_{\text{Ca(L)}}$	Ca _V 1.2	CACNA1C	0-2
K⁺	I_{to1}	K _V 4.2/4.3	KCND2/KCND3	1, notch
K⁺	I_{Ks}	K _V 7.1	KCNQ1	2,3
K⁺	I_{Kr}	hERG (K _V 11.1)	KCNH2	3
K⁺	I_{K1}	K _{IR} 2.1/2.2/2.3	KCNJ2/ KCNJ12/KCNJ4	3,4

1.2 Voltage-gated ion channels

Hodgkin and Huxley performed experiments on the ionic events responsible for the action potential, and with their classical equations they described the conductance and currents quantitatively (Hodgkin and Huxley, 1952b). The rising phase generation in the action potential was analyzed and explained by a conductance to sodium ions.

The eel electroplax, was the source where the first voltage-dependent ion channel was isolated and purified (Agnew et al., 1978). Several years later the sequence for the eel sodium channel was deduced from its mRNA (Noda et al., 1984). The voltage-dependent potassium channel (KvAP) from *Aeropyrum pernix* is the first X-ray crystallographic structure solved at a resolution of 3.2 Å (Jiang et al., 2003). Till now this forms the template for modelling other voltage-gated sodium, calcium and potassium channels. This research was awarded with the Nobel Prize in 2003. A basic pattern emerged from all these sequences: the functional channels are made up of four subunits (K^+ channels) or one protein with four homologous domains (Na^+ and Ca^{2+} channels).

In this thesis I will focus on the voltage-gated sodium channel.

1.3 Voltage-gated sodium channels

Voltage-gated sodium channels (Nav) belong to a family of membrane proteins that selectively conduct sodium due to changes in membrane potential. Sodium channels have various functional and pharmacological properties in different tissues and species (Mandel, 1992). Some sodium channels are not voltage-gated, such as the epithelial sodium channel (ENaC), which is responsible for sodium transport, and it is unrelated to other Nav channels (Catterall, 2000; Yu and Catterall, 2003).

1.3.1 Structure of voltage-gated sodium channels

Nav channels have a large, complex multimeric structure that is comprised of a core α -subunit and auxiliary function modifying β -subunits (Catterall, 2000) (Figure 2). These auxiliary subunits are involved in cellular signalling, channel trafficking, cell adhesion, stability of the membrane, gating modulation, and they may be targets for proteases involved in disease (Fahmi et al., 2001; Isom, 2001; Isom et al., 1994; Isom et al., 1992; Isom et al., 1995; Morgan et al., 2000; Zhou et al., 2000). Although Nav channels have auxiliary subunits, channel function, such as channel opening, ion selection and inactivation, is controlled by the core α -subunit. The central core is formed by a four domain-folding (DI-DIV) pattern, which determines the ion selectivity and conductance. Each domain is composed of six transmembrane helices (S1-S6). The S4 of each domain is the voltage sensor; it contains a distinct amino acid sequence, which has a positively charged residue followed by two hydrophobic residues. The re-entrant P-loop connecting S5-S6 forms a narrow and selective ion pore (Kass, 2006). Two negatively charged amino acids are present in an analogous position in all four domains, which form the receptor site and selectivity filter. The mammalian sodium channel resembles a subunit from the potassium channel of primitive bacteria (Ren et al., 2001). Substitution of a lysine at position 1,422 in repeat III and/or an alanine at position 1,714 in repeat IV of rat sodium channel II alters ion selectivity such that the channel takes on properties of a calcium channel. These data suggest that these residues constitute a portion of the selectivity filter (Heinemann et al., 1992).

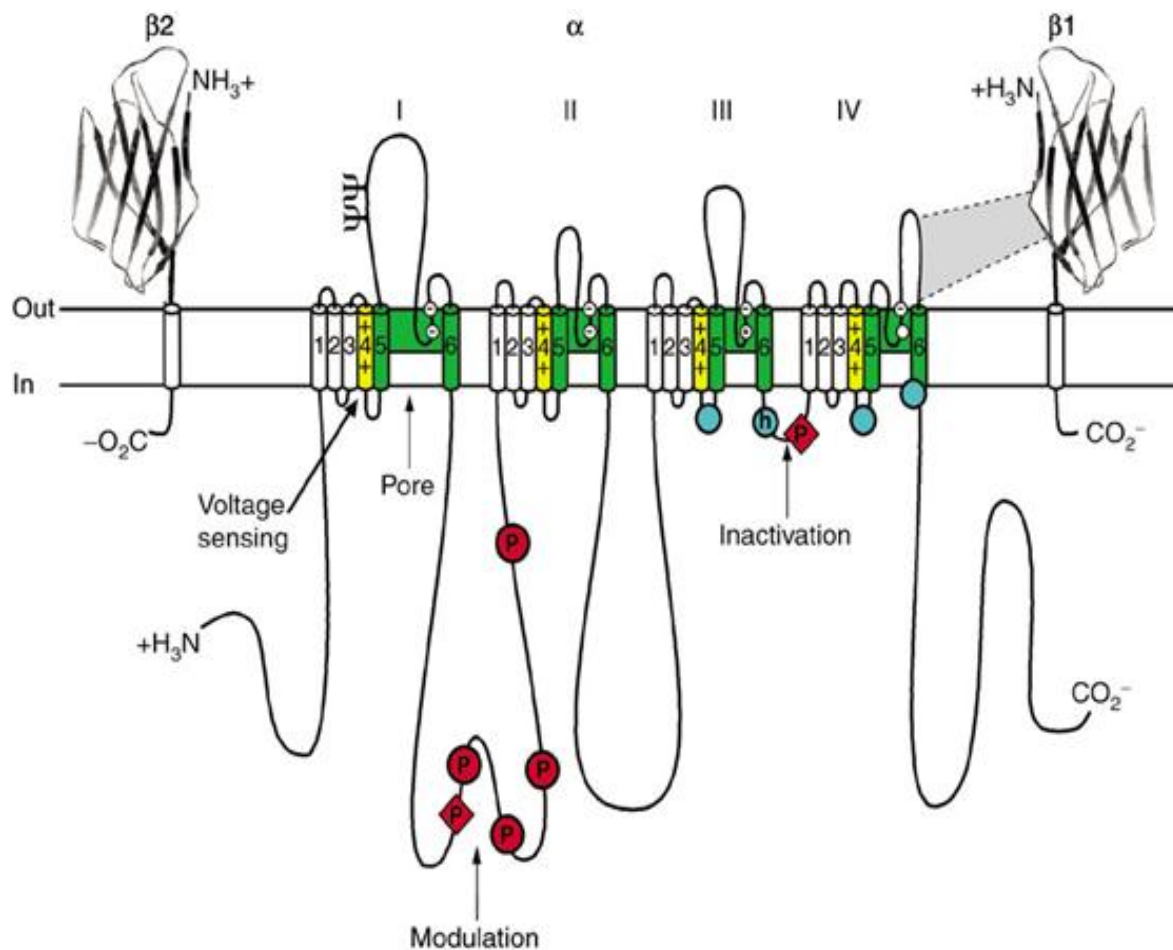


Figure 2: A schematic representation of the voltage-gated sodium channel showing all four domains (DI-DIV) of the α -subunit and two β -subunits.

Each domain has 6 transmembrane helices with a voltage sensor S4 (in yellow) and two pore lining segments S5 and S6 (in green). Blue circles in the intracellular loops of domains III and IV indicate the inactivation gate IFM motif and its receptor (h, inactivation gate); P, phosphorylation sites (in red circles: sites for protein kinase A; in red diamonds: sites for protein kinase C); ψ , probable N-linked glycosylation sites. Adapted from Yu and Catterall (2003).

1.3.2 Sodium channel gating

The sodium channel gates between three functional states: resting, active and inactivated – in a manner controlled by the membrane potential (Hodgkin and Huxley, 1952a). Channel opening (activation) is caused by the outward movement of the voltage sensors (S4) in each of the four domains in response to depolarization of the membrane potential. The movement of the voltage sensors is somehow coupled to opening of the channel, allowing entry of Na^+ ions. The short duration of channel activation is due to rapid inactivation. Inactivation is controlled by amino acids within the cytoplasmic loop between domains III and IV (George, 2005). Sodium channels undergo a slow inactivation if the membrane is depolarized for a long duration (Vilin and Ruben, 2001). This slower inactivation affects the amount of channels in the activation state. The detailed molecular mechanism of voltage-gated sodium channel gating is documented (Catterall, 1991, 2000; Denac et al., 2000; French and Horn, 1983; Hodgkin and Huxley, 1952a; Kuhn and Greeff, 1999; Marban et al., 1998; Mitrovic et al., 1995; Morgan et al., 2000; Romine et al., 1974; Tomaselli et al., 1995; Yang et al., 1996).

1.3.3 Voltage-gated sodium channel subtypes

There are nine sodium channel subtypes that are categorised by amino acid sequence and channel function (Table 1). These nine subtypes are broadly classified into three groups. The first group of channels is located in the central nervous system (CNS) and is comprised of the $\text{Na}_v1.1$, $\text{Na}_v1.2$, $\text{Na}_v1.3$ and $\text{Na}_v1.6$ sodium channels. The $\text{Na}_v1.3$ channel is highly expressed in the dorsal root ganglion (DRG). All four of the sodium channel subtypes are located on chromosome 2 (Catterall et al., 2005; Malo et al., 1994), and they are sensitive to tetrodotoxin (TTX) with a nanomolar IC_{50} value (Goldin, 2001). The next group of sodium channel subtypes is more diverse and is present on chromosome 3. This group is comprised of the cardiac $\text{Na}_v1.5$ channel subtype and the nociceptive neuron channel subtypes $\text{Na}_v1.8$ and $\text{Na}_v1.9$. These latter subtypes are TTX-resistant with micromolar IC_{50} values (Goldin, 2001). Single amino acid change from aromatic tyrosine or phenylalanine in chromosome 2 located subtypes to hydrophilic cystine, as present in $\text{Na}_v1.5$, reduces the TTX sensitivity 200 fold (Satin et al., 1992). On the other hand, change from phenylalanine to serine,

which is present in Nav1.8 and Nav1.9, results in even higher resistance to TTX (Sivilotti et al., 1997). TTX-resistant subtypes differ from TTX-sensitive subtypes in that they have slow inactivation kinetics and a single amino acid substitution in the pore-lining region of domain I (Catterall et al., 2005; Rogers et al., 2006). The third group of sodium channel subtypes is the intermediate group, which is composed of the TTX-sensitive skeletal muscle channel Nav1.4 and the DRG and sympathetic ganglion sodium channel Nav1.7 (Catterall et al., 2005; Rogers et al., 2006).

Sodium channels remain important targets for the development of novel drugs to treat many neurological, muscular and cardiac disorders. To date, numerous isoforms have been identified. Yet, it is unclear whether there are additional sodium channel isoforms. Advances in molecular biology have made it possible to discover channel mutations that occur in clinical disorders. However, additional analysis of the signalling pathways and molecules that modulate sodium channels is necessary. Proteins that are associated with sodium channels and the site of interaction should be identified in order to have a better understanding of channel function. Phenotype-based research should be performed to elucidate the role of sodium channels in physiology and disease. Lastly, since there is no crystal structure of mammalian sodium channels, understanding the structure-function relationship of sodium channels is hindered. Recent studies have shown that the sodium channel is far more complex than anticipated in terms of its function and association with other signalling molecules.

1.4 Channelopathies

Research of the molecular properties of sodium channels has elucidated mutations that cause multiple inherited hyper-excitability diseases in humans – considerably unexpected since *a priori* mutations might be expected to produce primarily hypo-excitability. These disorders are termed channelopathies. The first channelopathy involving sodium channels was found in skeletal muscle. Other channelopathies have been reported in cardiac and neuronal subtypes. A brief overview of review articles and original papers dealing with the various channelopathies is given in Table 2, followed by reviewing very recent publications in the subsequent section.

Table 2: Different sodium channel isoforms and their associated channelopathies.

Isoform	Gene	Location	Channelopathies	References
Na _v 1.1	SCN1A	CNS and DRG	<ul style="list-style-type: none"> Generalized epilepsy with febrile seizure Dravet syndrome 	(Heron et al., 2007; Lossin, 2009)
Na _v 1.2	SCN2A	CNS and DRG	<ul style="list-style-type: none"> Generalized epilepsy with febrile seizure Dravet syndrome Benign familial neonatal-infantile seizure 	(Herlenius et al., 2007; Heron et al., 2007; Misra et al., 2008; Sugawara et al., 2001)
Na _v 1.3	SCN3A	embryos, DRG and CNS		(Chen et al., 2000; Cummins and Waxman, 1997)
Na _v 1.4	SCN4A	skeletal muscle	<ul style="list-style-type: none"> Potassium-aggravated myotonia Paramyotonia congenita Hyperkalemic periodic paralysis Hypokalemic periodic paralysis 2 	(Heine et al., 1993; Orrell et al., 1998) (Koch et al., 1995; Ptacek et al., 1992; Wu et al., 2001) (Bendahhou et al., 1999; Ptacek et al., 1993) (Bendahhou et al., 2000; Bulman et al., 1999; Davies et al., 2001)
Na _v 1.5	SCN5A	heart, embryos and DRG	<ul style="list-style-type: none"> Long QT syndrome Brugada syndrome Conduction dysfunction Sinus node dysfunction SIDS Atrial fibrillation 	(Bennett et al., 1995; Goldenberg and Moss, 2008; Heron et al., 2009) (Benito et al., 2009; Brugada et al., 2009; Chen et al., 1998) (Schott et al., 1999) (Benson et al., 2003; Lei et al., 2008) (Makielski, 2006; Skinner et al., 2005; Wedekind et al., 2006) (Ellinor et al., 2008; McNair et al., 2004; Olson et al., 2005)
Na _v 1.6	SCN8A	DRG and CNS	In <i>jolting</i> mice- inherited cerebellar ataxias	(Kohrman et al., 1996)
Na _v 1.7	SCN9A	DRG and sympathetic ganglion	<ul style="list-style-type: none"> Primary erythermalgia Paroxysmal extreme pain disorder Insensitivity to pain 	(Drenth et al., 2005; Han et al., 2006; Harty et al., 2006; Yang et al., 2004) (Fertleman et al., 2006) (Cox et al., 2006)
Na _v 1.8	SCN10A	DRG	<ul style="list-style-type: none"> Neuropathic injury of DRG Trigeminal ganglia model of neuropathic pain In human cases radicular pain 	(Boucher et al., 2000; Coward et al., 2000; Dib-Hajj et al., 1998) (Eriksson et al., 2005) (Abe et al., 2002; Coward et al., 2000)
Na _v 1.9	SCN11A	DRG and CNS	<ul style="list-style-type: none"> Neuropathic injury of DRG Trigeminal ganglia model of neuropathic pain In human cases radicular pain 	(Boucher et al., 2000; Coward et al., 2000; Dib-Hajj et al., 1998) (Eriksson et al., 2005) (Abe et al., 2002; Coward et al., 2000)

1.4.1 Cardiac sodium (SCN5A) channelopathies

Impulse conduction in the atria, His-Purkinje system and the ventricle is sustained by the transient increase in sodium permeability (Hoffman and Cranefield, 1960). Cardiac sodium channels are the target of antiarrhythmic drugs (Grant et al., 1984; Hondeghem and Katzung, 1977). Disturbances in conduction and life-threatening arrhythmias are caused by decreased sodium channel function (Cascio, 2001; Tomaselli and Zipes, 2004).

Nav1.5 is a 2016 amino acid protein. Mutations in SCN5A, which encodes the primary sodium channel in cardiac tissues, cause sodium channel dysfunction and are associated with a number of unrelated arrhythmic syndromes, such as long QT syndrome (LQTS) (Bennett et al., 1995; Goldenberg and Moss, 2008), Brugada syndrome (BrS) (Benito et al., 2009; Brugada et al., 2009; Chen et al., 1998), conduction dysfunction (Schott et al., 1999), sinus node dysfunction (Benson et al., 2003; Lei et al., 2008), sudden infant death syndrome (SIDS) (Makielski, 2006; Skinner et al., 2005; Wedekind et al., 2006) and atrial fibrillation (Ellinor et al., 2008; McNair et al., 2004; Olson et al., 2005).

Sodium channel mutation causes cardiac arrhythmia by one of the two mechanisms:

- a) *Loss-of-function (LoF) mutations*: The consequences of these mutations are non-functional channels or rapidly inactivating channels. This results in a decrease of available sodium current during the fast depolarization phase.
- b) *Gain-of-function (GoF) mutations*: These mutations cause an increase in inactivation reversibility in the late component of the sodium current. In addition, these mutations prolong action potential duration and the QT interval.

1.5 Cardiac sodium channel splice variants

Exons coding for the cardiac sodium channel subtype undergo alternative splicing which eventually can produce biochemically, pharmacologically and functionally distinct sodium channels (Choi et al., 2010; Gazina et al., 2010; Kerr et al., 2008; Makielski et al., 2003; Schirmeyer et al., 2010; Schroeter et al., 2010; Tan et al., 2005). Figure 3 shows different splice variants of the cardiac sodium channel.

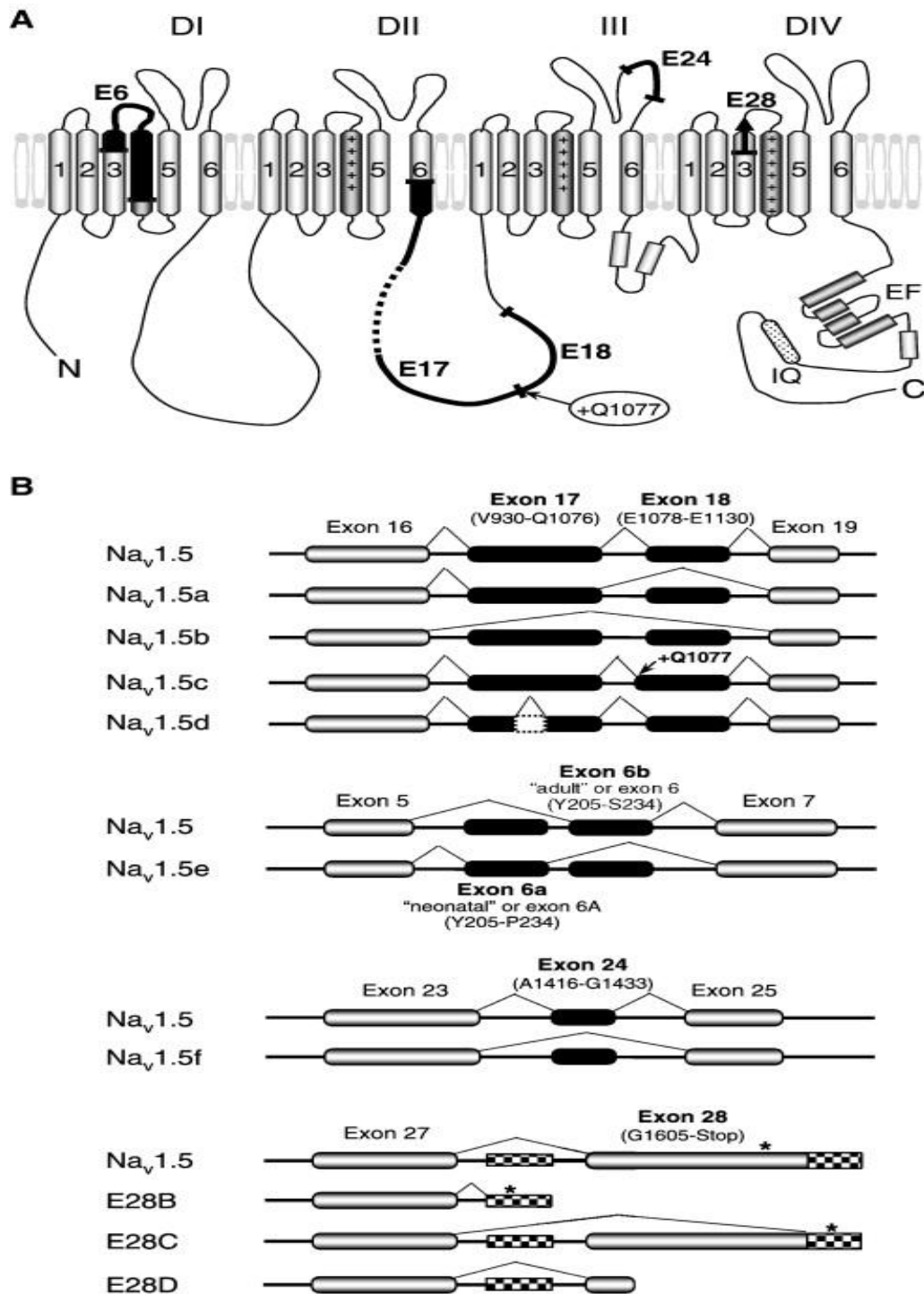


Figure 3: Structure of Nav1.5 splice variants.

(A) Proposed membrane topology of Nav1.5. (B) Alternative splicing of $\text{Na}_v1.5$ results in exon skipping ($\text{Na}_v1.5\text{a}$, $\text{Na}_v1.5\text{b}$, $\text{Na}_v1.5\text{f}$), in alternative usage of the exon 18 splice acceptor site and the extension of this exon by a CAG trinucleotide coding for Q1077 ($\text{Na}_v1.5\text{c}$), in partial deletion of exon 17 ($\text{Na}_v1.5\text{d}$), in the alternative usage of one of two exon 6 variants ($\text{Na}_v1.5\text{e}$), in abnormal exon 27/exon 28 splicing (variants E28B, E28C) or in premature transcript termination (E28D; last amino acid is G1642). The original numbering system of hH1 with 2016 amino acids (Gellens et al., 1992) is used in the sequence numbering. Reproduced from Schroeter et al. (2010).

1.5.1 Functional $\text{Na}_v1.5$ splice variants

$\text{Nav}1.5a$ was the first functional splice variant with the deletion of exon 18, which encodes for 53 amino acids of the D_{II-III} linker (Zimmer et al., 2002). This variant is a species-specific expression in the mammalian heart. It is not expressed in human, whereas it is expressed in pig, rat and mouse (Blechschmidt et al., 2008). Electrophysiological studies show similar kinetics to mouse Nav1.5 when expressed in HEK293 cells (Zimmer et al., 2002).

$\text{Nav}1.5c$ is the most abundant splice variant in the human heart. A glutamine at position 1077 by a 5'-extension of exon 18 (trinucleotide CAG), makes the splice variant Nav1.5c (Makielski et al., 2003). Electrophysiological properties of Q1077 and ΔQ1077 were alike (Makielski et al., 2003). Recent studies show that this splice variant plays an important role in SCN5A channelopathies like LQTS and BrS (Cocquet et al., 2006; Wang et al., 2007). The predicted phosphorylation site for CK2 ('Casein kinase 2', regulated through protein-protein interactions and changes in its concentration (Rodriguez et al., 2008)) is destroyed when Q1077 is included (Kerr et al., 2004). ΔQ1077 is the most abundant variant present in human heart. It is present in 45% of the human population (Makielski et al., 2003) (Table 3). Physiology of this splice variant is uncertain.

$\text{Nav}1.5d$ is a splice variant, with alternative exon 17 splicing as shown in Figure 3. Electrophysiological measurement shows that Nav1.5d significantly altered the kinetics, with depolarized steady-state activation and inactivation and 20% reduction in peak I_{Na} (Camacho et al., 2006; Schroeter et al. 2010).

Functional splice variant $\text{Nav}1.5e$ is present in human brain (Ou et al., 2005) and in human breast cancer cells (Brackenbury et al., 2007; Brackenbury et al., 2008; Fraser et al., 2005). Nav1.5e variant is alternative usage of 'neonatal' exon 6a. Shift of the steady-state activation to more depolarized potentials, slower recovery from inactivation and reduced availability are the electrophysiological differences between Nav1.5e and Nav1.5 (Onkal et al., 2008).

1.5.2 Non-functional $\text{Na}_V1.5$ splice variants

Non-functional splice variant $\text{Na}_V1.5b$ is generated by deletion of exon 17 and 18 which codes for the C-terminal end of DIIS6 that forms the large portion of the intracellular loop $L_{\text{DII-DIII}}$ (Zimmer et al., 2002). It is expressed in mouse heart but it is not expressed in rat, pig and human heart (Blechschmidt et al., 2008).

$\text{Na}_V1.5f$ is a non-functional splice variant present in various rat tissues and in human brain. $\text{Na}_V1.5f$ is characterized by deletion of exon 24 and thus removal of 18 amino acids in the DIII pore region (Schroeter et al., 2010; Wang et al., 2009; Wang et al., 2008).

C-terminal truncated splice variants (E28B, E28C and E28D) of $\text{Na}_V1.5$ were the splice variant which showed first evidence in the pathophysiology of the human heart (Shang et al., 2008; Shang et al., 2007). The mechanism of splicing is uncertain. All three novel C-terminal truncated splice variants were transcribed in human lymphoblasts, and one of them was expressed in human skeletal muscle (E28D). None of the truncated variants were observed in rats and mice (Schroeter et al., 2010; Shang et al., 2008; Shang et al., 2007).

1.6 Src tyrosine kinase

Tyrosine phosphorylation plays a vital role in the regulation of a variety of biological responses, which includes cell proliferation, migration, differentiation and survival (Thomas and Brugge, 1997). The protein tyrosine kinase (PTK) encompasses a diverse spectrum of proteins which mediate the above responses, as well as the receptors which activate them (Thomas and Brugge, 1997). There are many different distinct families of tyrosine kinases which execute the responses that lead to complex extensive cross talk between different receptor pathways. One such large family of cytoplasmic tyrosine kinases which is capable of communicating with a large number of different receptors is the Src protein tyrosine kinase (Src PTK) (Brugge and Erikson, 1977). The prototype of Src was first identified as the transforming protein (v-Src) of the oncogenic retrovirus, Rous sarcoma virus (Brugge and Erikson, 1977). V-Src is the mutant variant of a cellular protein ubiquitously expressed and highly

conserved over evolution. In 1978, two groups of researchers found that Src proteins possess protein tyrosine kinase activity, which led to deep investigation of Src on cell proliferation and its kinase activity (Collett and Erikson, 1978; Levinson et al., 1978).

1.6.1 Members of Src tyrosine kinase and its cellular location

Ten proteins were identified in this large Src PTK family which have structural features and significant amino acid sequence homology to Src. The ten members are Fyn, Yes, Yrk, Blk, Fgr, Hck, Lyn and the Frk subfamily proteins Frk/Rak and Iyk/Bsk (Brown and Cooper, 1996; Cance et al., 1994; Oberg-Welsh and Welsh, 1995; Thuvesson et al., 1995). The Src PTK is further divided into three major groups based on their expression. Src, Fyn and Yes are expressed in almost all tissues (Brown and Cooper, 1996). The second group consists of hematopoietic cell expressed Src PTK Blk, Fgr, Hck, Lck and Lyn (Bolen and Brugge, 1997). The third subgroup, Frk/Rak and Iyk/Bsk Src PTK, is expressed in epithelial-derived cells (Cance et al., 1994; Lee et al., 1994; Oberg-Welsh and Welsh, 1995; Thuvesson et al., 1995). Thus, Src-PTKs can function in many distinct cells and in distinct sub-cellular locations.

1.6.2 Functional regions of Src tyrosine kinase

Src PTKs are 52-62 kDa proteins composed of six distinct functional regions (Figure 4) (Brown and Cooper, 1996)

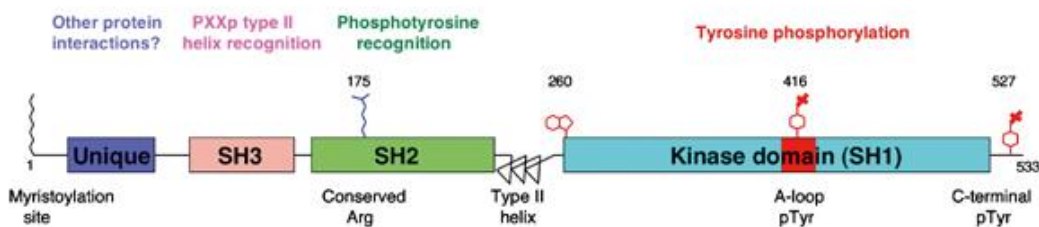


Figure 4: Organization of Src tyrosine kinase domain structure

The Figure shows all 6 different functional regions as explained in the text. Reproduced from Boggon and Eck (2004).

I. Src Homology (SH) 4 domain

This domain is a 15-amino acid sequence which contains signals for lipid modification of Src PTKs. Glycine at position 2 is responsible for the addition of myristic acid moiety, which is involved in targeting Src PTKs to cellular membranes (Resh, 1993). The cysteine residues in this domain are subjected to palmitylation (Resh, 1993; Thomas and Brugge, 1997).

II. Unique region

The name suggests its properties; this domain is unique and distinct for each member. It is proposed that this domain is involved in mediating interactions with receptors or proteins that are specific for each family member (Morgan et al., 1989; Winkler et al., 1993). It is also speculated that this region is involved in modulating proteins: protein interactions or regulation of catalytic activity (Thomas and Brugge, 1997).

III. SH3 domain

SH3 domains of Src PTK are composed of 50 amino acids. It is very important for intra- and intermolecular interactions that regulate Src catalytic activity, Src localization and recruitment of substrates. All SH3 domains target a proline-rich core consensus motif P-X-X-P (Feng et al., 1994; Rickles et al., 1995; Yu et al., 1994). Amino acids surrounding the prolines play a vital role in additional affinity and specificity for individual SH3 domains. Binding affinities of SH3 domains are in the micro-molar range. These affinities are strengthened *in vivo* by additional contacts with the target protein and other domains of Src (Cohen et al., 1995; Thomas and Brugge, 1997).

IV. SH2 domain

The SH2 domain is also an important domain involved in the regulation of the catalytic activity of Src PTKs, as well as the localization of Src and its binding proteins (Cohen et al., 1995; Pawson, 1995). All SH2 domains bind to short contiguous amino acid sequences containing phosphotyrosine. The specificity of individual SH2 domains lies in the 3-5 residues following the phosphotyrosine (Pawson, 1995). Structural analysis of SH2 revealed that the ligand-binding surface of SH2 domains is composed of two pockets. One pocket contacts the phosphotyrosine , the other pocket contacts the +3 amino acid residue following the phosphotyrosine (Songyang et al., 1993).

V. *Kinase domain (SH1)*

This domain possesses tyrosine Y-416, specific for protein kinase activity. The autophosphorylation site is very important for the regulation of kinase activity (Hubbard et al., 1994; Johnson et al., 1996; Knighton et al., 1991a; Knighton et al., 1991b). Phosphorylation of Tyr-416 stimulates complete activation of Src and provides a binding site for SH2 domains of other cellular proteins. The SH3 domain interacts with sequences in the kinase domain, as well as with sequences in the linker region that lies between the SH2 and kinase domain (Sicheri et al., 1997; Xu et al., 1997).

VI. *Short negative regulatory region*

This segment plays an important role in the activation of src kinase. It has the critical tyrosine residue Tyr 527. The SH2 domain interacts with pTyr 527 (Src) and adjacent residues in the negative regulatory tail (Brown and Cooper, 1996). Y527 in c-Src, and the corresponding tyrosine in other Src PTKs, are the primary sites of tyrosine phosphorylation *in vivo*. Kinase activity is reduced when pTyr 527 is phosphorylated and bound to the SH2 domain (Brown and Cooper, 1996).

Apart from all these domains the very important SH2 and SH3 domains have four principal functions in the regulation of Src kinase (Brown and Cooper, 1996):

1. They constrain the activity of the enzyme via intramolecular contacts.
2. Proteins that contain SH2 or SH3 ligands can bind to the SH2 or SH3 domains of Src and attract them to specific cellular locations.
3. Displacement of the intramolecular SH2 or SH3 domains results in activation of Src kinase activity.
4. Proteins containing SH2 or SH3 ligands can enhance their ability to function as substrates for Src protein–tyrosine kinase.

1.6.3 Structure of Src PTK and activation of tyrosine kinase

The Src kinase domain consists of the characteristic bilobed protein kinase architecture as illustrated in Figure 5 (Glass et al., 1997; Xu et al., 1997). The human

Src gene encodes a protein of 536 amino acids, and the chicken Src gene encodes a 533-residue protein. The small amino-terminal lobe of the kinase consists of residues 267–337 and is involved in anchoring and orienting ATP. This smaller lobe has mainly antiparallel β -sheet structure (Roskoski, 2004). Residues 341–520 form the large carboxyl-terminal lobe which is responsible for binding the protein substrate, and part of the ATP-binding site occurs in this lobe. It has predominantly α -helical structure (Roskoski, 2004). The cleft between the two lobes is the catalytic site for Src kinase. The two lobes move relative to each other and can open or close the cleft. Active site residues are from both the small and large lobes of the kinase; hence changes in the orientation of the two lobes can promote or restrain activity (Roskoski, 2004).

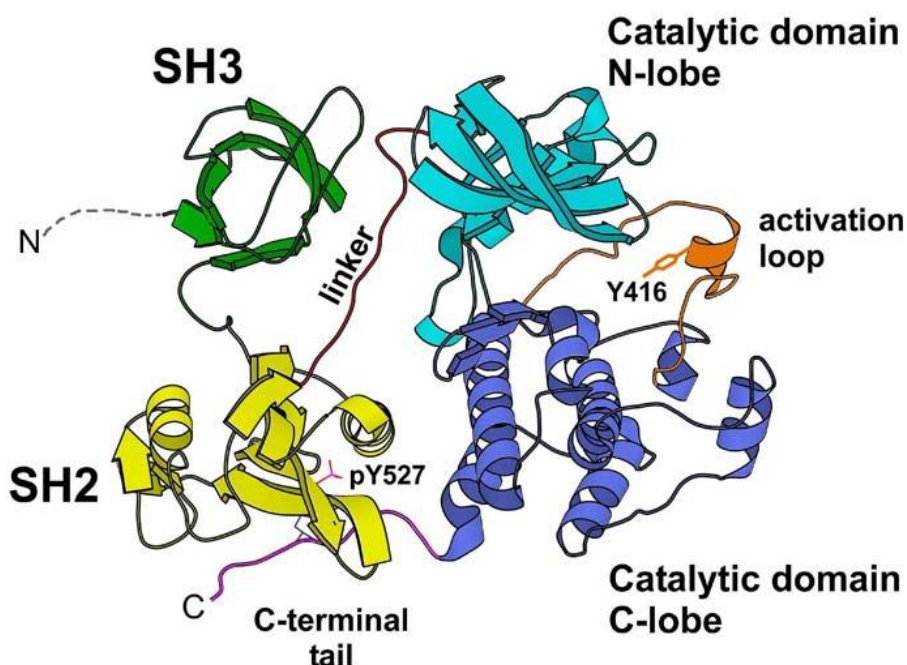


Figure 5: Ribbon diagram illustrating the structure of human Src.

This figure is reproduced from Roskoski (2004) and Xu et al. (1999).

The network controlling Src is a three step mechanism described by Harisson: the latch, the clamp, and the switch (Harrison, 2003).

A latch is formed when SH2 domain binds to phosphotyrosine 527 in the C-terminal tail. Tyr-527 is phosphorylated by *csk* kinase (Nada et al., 1991). This latch in turn stabilizes the attachment of the SH2 domain to the large lobe. Then the SH3 domain

contacts the small lobe. Prolines in the linker between the SH2 and kinase domains function as a motif that binds the SH3 domain and attaches the SH3 domain to the small kinase lobe. The assembly of the SH2 and SH3 domains behind the kinase domain is the clamp. This prevents the opening and closing of the cleft between the small and large lobes. The switch is the kinase-domain activation loop; the activation loop can switch between active and inactive conformations.

1.6.4 Mechanism of Src activation

Src tyrosine kinase is activated by unlatching, unclamping and switching. In the inactive state, Tyr 416, which is present in the activation loop, is segregated and is not a substrate for phosphorylation by another kinase (Roskoski, 2004). The protein is unlatched when phosphotyrosine 527 dissociates or is displaced from the SH2-binding pocket. When the protein is unlatched the clamp no longer locks the catalytic domain in an inactive conformation (Harrison, 2003; Xu et al., 1999). This dissociation allows dephosphorylation by enzymes such as protein tyrosine phosphatase- α (PTP α) (Brown and Cooper, 1996). This in turn allows the activation loop to assume their active conformations. Tyr416 can then undergo autophosphorylation by another Src kinase molecule. Following autophosphorylation, the enzyme is stabilized in its active state (Roskoski, 2004).

Studies show that substitution of Tyr-527 by another amino acid residue leads to activation of c-Src (Kmiecik and Shalloway, 1987). The inhibition of the csk gene activity also stimulates activity of PTK of the Src family (Imamoto and Soriano, 1993). Phosphorylation at Tyr-416 in Src (or homologous amino acid residues in other tyrosine kinases) is necessary for complete activation of most kinases studied so far. In the absence of phosphorylation, the activating loop acquires different conformations, which often inhibit protein-protein interactions. In this active conformation the loop forms a part of the site recognized by the substrates (Xu et al., 1997).

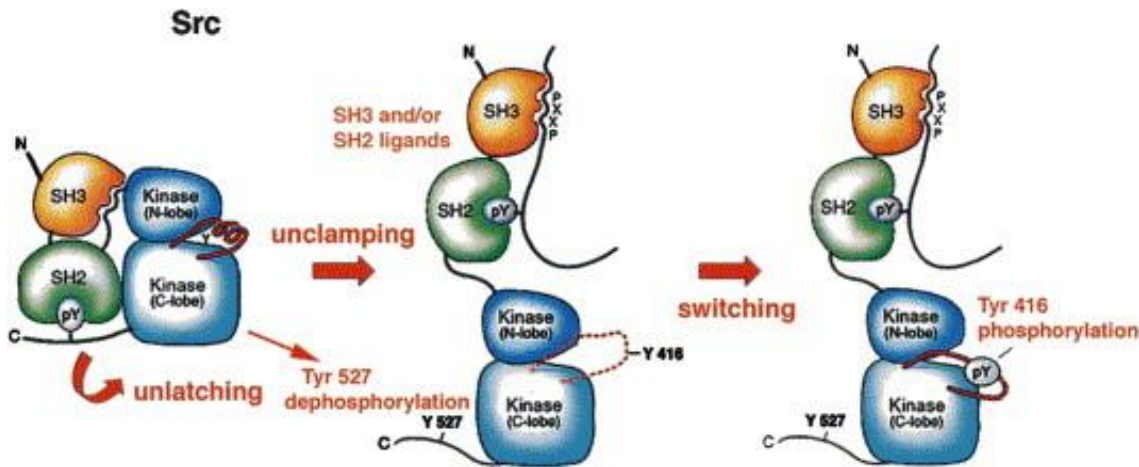


Figure 6: The activation mechanism of Src tyrosine kinase.

Reproduced from Roskoski (2004) and Xu et al. (1999).

1.7 Src kinase and ion channels

Both Src family and receptor tyrosine kinases are known to be potent modulators of ion channels (Levitin, 1994; Siegelbaum, 1994). Modulation by Fyn and other Src-family tyrosine kinases on potassium channels, calcium channels, sodium channels and glutamate receptors has been reported earlier. Studies show that potassium channel Kv2.1 is inhibited by Fyn tyrosine phosphorylation (Sobko et al., 1998; Tsai et al., 1999). Tyrosine phosphorylated Kv1.5 interacts with the SH3 domain of Src kinase (Holmes et al., 1996a; Nitabach et al., 2001). Kv1.2 currents are inhibited by tyrosine phosphorylation (Peretz et al., 2000; Wischmeyer et al., 1998). In 2003, Hou et al. showed that Src/Fyn binds and modulates voltage-gated calcium channels (Hou et al., 2003). Cellular plasticity, a form of plasticity that modifies the input–output relationships of the entire neuron, is mediated by modulation of voltage-gated sodium, calcium, and potassium channels by tyrosine phosphorylation/dephosphorylation (Cantrell and Catterall, 2001).

1.7.1 Src tyrosine kinase and voltage-gated sodium channels

Physiological and biochemical studies show that sodium channels are regulated by tyrosine kinase. Sodium channel studies have shown that the kinase activity enhances the intrinsic slow inactivation gating process, and thereby reduces the availability of channels (Cantrell and Catterall, 2001; Carr et al., 2003; Chen et al., 2006). Tyrosine phosphorylation and dephosphorylation have also been implicated in rapid sodium channel modulation (Hilborn et al., 1998; Ratcliffe et al., 2000). Tyrosine phosphorylation of these sodium channels is associated with a hyperpolarizing shift in steady-state inactivation, resulting in fewer available channels for generating an action potential. Recent studies done with sodium channels show that Fyn kinase binds to the rat brain sodium channel Nav1.2, enhances fast inactivation, and mediates inhibition of sodium currents by brain-derived neurotrophic factor (BDNF), acting through the neurotrophin receptor tyrosine receptor kinase B (TrkB) (Ahn et al., 2007). The molecular mechanism underlying the fast inactivation on Nav1.2 with Fyn tyrosine kinase is also reported. Fyn kinase binds to a Src homology 3 (SH3)-binding motif in the second half of the intracellular loop connecting domains I and II (L_{DI-DII}) of Nav1.2. Mutation of that SH3-binding motif prevents Fyn binding and Fyn enhancement of fast inactivation of sodium currents. Fast inactivation of the closely related Nav1.1 channel is not modulated by Fyn. These channels do not contain a SH3-binding motif in L_{DI-DII} .

In cardiac sodium channels, very few studies show that they behave oppositely from their neuronal counterparts. Hyperpolarizing shift is observed in the inactivation-voltage relationship, when tyrosine kinase inhibitors are added to cardiac myocytes (Wang et al., 2003). This suggests that the phosphorylated form of the cardiac channel displays enhanced excitability. In 2005, Richard Horn's group (Ahern et al., 2005) expressed SCN5A clones (hH1) in HEK cells. They found that Fyn shifts the inactivation-voltage relationship towards more hyperpolarizing potentials and the kinase activity dead mutant of Fyn reversed the effect.

1.7.2 Physiological relevance of cardiac sodium channels and Src family tyrosine kinase modulation

Cardiac sodium channel Nav1.5 (Maier et al., 2002) and Src tyrosine kinase (Holmes et al., 1996b; Toyofuku et al., 2001) are accumulated at the adherens junctions. Adherens junctions are made up of protein complexes linking the cell membranes and cytoskeletal elements within and between cells. Adherens junctions are responsible for the electrical coupling between cardiac myocytes (Ahern et al., 2005). Gap junctions in cardiac myocytes are reduced because of the c-Src-mediated tyrosine phosphorylation of Connexin-43. It also decreases the stability of Connexin-43 at the cell surface as well as in the whole cell (Toyofuku et al., 2001). Non-pathological stimulation of adrenergic ligands (Ma and Huang, 2002), angiotensin II (Sadoshima et al., 1995), epidermal growth factor (Wu et al., 2000) or insulin (Zhang and Hancox, 2003) are induced by tyrosine kinase activity in the heart.

1.7.3 Modulation of sodium channel variants by Fyn tyrosine kinase

In cardiac sodium channel variants, there is evidence which shows that sodium currents behave oppositely to their neuronal counterparts. In 2005, Ahern et al. showed that Fyn tyrosine kinase shifts the inactivation kinetics to more depolarizing potentials in HEK cells expressing Nav1.5 (hH1 clone). Later in 2007, Beacham et al. argued that the cardiac sodium channel does not have equivalent SH3 domain binding residues compared to the neuronal counterpart, so that the fast inactivation is shifted to more depolarizing potentials. Y1495 in the loop L_{DIII-DIV} is required for phosphorylation, in turn leading to the shift in inactivation. Equivalent Y1495 in the neuronal sodium channel is the site for phosphorylation.

1.8 Nomenclature

Table 3: Different cardiac sodium channel variants

International Human Genome Sequencing Consortium (IHGSC) sequence and reference sequence; hH1, hH1b and hH1c are previous cDNA clones of SCN5A; Accession No., GenBank nucleotide accession numbers, amino acid frequency (AAF), and variant name, name relative to SCN5A (defined herein as identical to IHGSC), AA No. indicates amino acid position number in the protein, using the full-length numbering consistent with the IHGSC databases. Population frequency indicates estimated percentage of channels in the study population.

Common Name	IHGSC	hH1	hH1b	hH1c	AAF
Accession No.	AC137587	M77235	AF482988	AY148488	
AA. No. 558	H	H	R	H	70% H
559	T	T	T	T	100% T
618	L	L	I	L	100% L
1027	R	Q	R	R	100% R
1077	Q	Q	Δ	Δ	65% Δ
Variant name	SCN5A [Q1077]	R1027Q	[H558R; L618I;Q1077del]	Q1077del	
Population Frequency	25%	0%	0%	45%	

Aims

The main aim of this project is to investigate the role of the Glutamate1077 residue in the intracellular loop ($L_{DII-III}$) connecting Domain II and III of the voltage-gated cardiac sodium channel in modulation by Fyn tyrosine kinase. In particular I address the following questions:

1. The role of Q1077 in $L_{DII-III}$ in the modulation of the sodium channel by Fyn tyrosine kinase?
2. Can Q1077 mutation affect the modulation by Fyn?
3. What is the potential SH3 binding motif in Nav1.5 which differs from Nav1.2 in modulation by Fyn kinase?
4. What are the potential residues involved in modulation of different sodium channel isoforms by Fyn kinase?
5. What are the unique amino acid sequences in the loop $L_{DII-III}$ of cardiac sodium channel, which makes it different from other sodium channel subtypes?

Methods and Materials

3.1 Molecular Biology

3.1.1 DNA clones

Q1077Pre and Q1077Del clones in *pcDNA3-N* were kindly provided by Prof. Jonathan C Makielski, University of Wisconsin, Madison. Fyn tyrosine kinase active (Δ Tyr 527) clone pCS2-c-Fyn^{CA} and tyrosine kinase dead (K299M) clone pCS2-c-Fyn^{KD} were gifts from Dr Richard Horn, Jefferson Medical College, USA. π H3-CD8 was a gift from Dr. B. Seed, Harvard Medical School, Boston, MA, USA

3.1.2 DNA amplification and isolation

Subcloning Efficiency™ DH5 α ™ (Invitrogen®) competent E. coli cells were used to transform the gifted cDNAs. Transformation was performed according to the manufacturer's protocol. The transformed cells were plated on LB Ampicilline plates. Then the transformed clones were picked from the LB plates and grown in SOC medium overnight. The overnight culture was used to isolate cDNA. Isolation of cDNA from the overnight culture was done using QIAGEN® mini and midiprep kits according to the manufacturer's protocol. Using Nanodrop spectrophotometer the concentration of the purified DNA from QIAGEN® mini and midiprep was obtained. cDNA were verified using restriction enzyme digestion and run on an agarose gel electrophoresis.

Methods and Materials

The components of the LB Ampicillin plates were:

- 10 g Tryptone Yeast Extract
- 5 g Yeast Extract
- 10 g NaCl
- 20 g Agar
- 1 l double distilled H₂O and autoclaved

10 ml of Ampicillin (concentration 100 mg/ml) was added and 7-10 ml were poured in each plate.

The components of the SOC medium were:

- 5 g Yeast Extract
- 20 g Tryptone
- 0.5 g NaCl
- 1 l double distilled H₂O and autoclaved

10 ml filter-sterilized (0.2 µm filter) solution of 1M MgCl₂, 1M MgSO₄ and 2M glucose was added.

3.1.3 Site-directed mutagenesis

Site-directed mutagenesis was performed using Stratagene Quick Change Site-Directed Mutagenesis Kit according to the manufacturer's protocol. Q1077Present (GenBank AC137587) Nav1.5 cDNA was used as the template for the mutation process. Both forward and reverse primers were designed using Stratagene primer design program. The forward primer and reverse primers for all the mutants are given in Table 4. Primers were ordered from Sigma® Life Sciences.

Table 4: Forward and reverse primers for Q1077 mutations.

Oligo Name	Sequence 5' to 3'
Q1077A Forward	CCAGCAAGCAGGCGGAATCCCAGC
Q1077A Reverse	GCTGGGATTCCGCCTGCTTGCTGGAC
Q1077K Forward	GAGTCCAGCAAGCAGAAGGAATCCCAGCC
Q1077K Reverse	CAGGCTGGGATTCCCTCTGCTTGCTGGACTC
Q1077P Forward	GTCCAGCAAGCAGCCGGATCCCAGCCTG
Q1077P Reverse	CAGGCTGGGATTCCGGCTGCTTGCTGGAC
Q1077Y Forward	GGAGTCCAGCAAGCAGTATGAATCCCAGCCTGTGT
Q1077Y Reverse	ACACAGGCTGGGATTCATACTGCTTGCTGGACTCC

The reagents were added according to the manufacturer's instruction manual in 200 µl Polymerase chain reaction (PCR) tubes. Then the tubes were placed in the PCR machine, with programmed cycling parameters given below in Table 5.

Table 5: PCR cycling parameters Quick Change Site-Directed Mutagenesis.

Segment	Cycle	Temperature	Time
1	1	95°C	2 minutes
2	18	95°C	20 seconds
		95°C	10 seconds
		95°C	6.1 minute
3	1	95°C	5 minutes

The PCR product was then transformed into the XL10-Gold ultra-competent cells according to the transformation protocol provided by the manufacturer. The transformed cells were plated on LB Ampicillin plates for more than 16 hours. Then

Methods and Materials

the transformed clones were picked from the LB plates and grown in SOC medium overnight. The overnight culture was used to isolate cDNA. Isolation of cDNA from the overnight culture was done using QIAGEN® mini and midiprep kits according to the manufacturer's protocol. Using Nanodrop spectrophotometer from Thermo Scientific, the concentration of the purified DNA from QIAGEN® mini and midiprep was obtained. The sequence of the DNA was verified using restriction enzyme digestion and sequencing.

3.2 Cell Culture

3.2.1 Cells

Human embryonic kidney tsA-201 cells with a passage number less than 25 were used for the experiments.

HEK293 stable cells encoding for Q1077Present (GenBank AC137587) and Q1077 Deleted (GenBank AY148488) were obtained from Prof. Jonathan C. Makielski, University of Wisconsin, Madison.

3.2.2 Cell culture media

DMEM-F-12 (Dulbecco's modified Eagle's medium/nutrient mixture F12 Ham) was purchased from Sigma-Aldrich GmbH for tsA-201cells. MEM (Modified Eagle's medium), MEM Sodium Pyruvate, L-Glutamine, Non-essential Amino Acids, and Geneticin were purchased from Sigma-Aldrich GmbH for stably transfected cells. Fetal calf serum (FCS) and Fetal bovine serum (FBS) was purchased from Sigma-Aldrich GmbH. PBS without $\text{Ca}^{2+}/\text{Mg}^{2+}$ 10X: 2.00 g KCl, 2.0 g KH_2PO_4 , 80.0 g NaCl, 27.07 g $\text{Na}_2\text{PO}_4 \cdot 2\text{H}_2\text{O}$, 1000 ml distilled H_2O . Mixed to dissolve, this solution was diluted 1:10 with distilled H_2O , sterile filtrated before use and stored at 4 °C. Trypsin/EDTA 10X: 0.25 g trypsin (1:250), 0.20 g EDTA, 10 ml PBS without $\text{Ca}^{2+}/\text{Mg}^{2+}$ 1X. Mix to dissolve. This solution was sterile filtrated and stored at -20 °C, and diluted 1:10 with sterile PBS without $\text{Ca}^{2+}/\text{Mg}^{2+}$ 1X before use.

3.2.3 Sub-culturing cells

3.2.3.1 Stably transfected cells

Stably transfected cells were grown on tissue culture flasks until 70% confluent cells. Medium was aspirated from plates, then cells were washed with 2 ml 1x PBS, twice. 2 ml trypsin (0.25% trypsin, 0.02% EDTA) was added and incubated for 2 min at 37°C. 3 ml of medium was added to quench and transferred to a 15 ml tube. The tube was centrifuged for 2 min at 1,000 RPM. After the medium was aspirated off the plates, 5 ml medium was added to resuspend the cells. 1/10 of the cell/media mixture was added to a new plate with fresh medium. The flask was placed in a 37°C incubator and checked every 2-3 days for growth. Cells for transfection were plated on Petri dishes (Falcon) at 30–50% confluence ~16 h before transfection. For cryostorage the resuspended cells were added to a medium (without antibiotics) containing 10% FBS and 5% DMSO.

Table 6: Medium composition for culturing stably transfected cells.

Reagent	Volume
MEM	500 ml bottle
MEM Sodium Pyruvate	5 ml
L-Glutamine	5 ml
MEM non-essential AA solution	5 ml
FBS (Fetal Bovine Serum)	50 ml

3.2.3.2 tsA Cells

Human embryonic kidney tsA-201 cells were grown at 5% CO₂ and 37 °C to 70% confluence in Dulbecco's modified Eagle's/F-12 medium supplemented with 10% fetal bovine serum (FBS). Cells were split using trypsin/ EDTA and plated on 35-mm Petri dishes (Falcon) at 30–50% confluence ~16 h before transfection.

3.2.4 Transfection

3.2.4.1 *Transient transfection of stably transfected HEK cells*

Before transfection, the medium was replaced with fresh medium, and the cells were transiently transfected with cDNAs of either 1 μ g cDNA of Fyn^{CA} or Fyn^{KD} with π H3-CD8 cDNA using the QIAGEN polyfect transfection reagents according to the manufacturer's protocol. Cells were incubated overnight at 37°C in 5% CO₂. After 12–16 h, the medium was replaced, and the cells were allowed to recover for 9–24 h before experiments. Anti-CD8-coated beads (Dynal, Oslo, Norway) were used to identify transfected cells (Jurman et al., 1994).

3.2.4.2 *Transient transfection of mutant clones*

Sodium channels were transiently expressed for electrophysiological analysis by transfecting tsA-201 cells in 35 mm dishes with 1.2 μ g of cDNA encoding the Nav1.5 (Genebank AC13758) α - subunit mutants Q1077A, Q1077P, Q1077Y, Q1077K and π H3-CD8 cDNAs with or without 0.1 μ g of Fyn^{CA} or Fyn^{KD} cDNA, using the QIAGEN polyfect transfection reagents according to the manufacturer's protocol. Anti-CD8-coated beads (Dynal, Oslo, Norway) were used to identify transfected cells (Jurman et al., 1994).

3.3 Electrophysiology

3.3.1 Patch pipettes

Patch pipettes were made in three stages: pipette pulling, heat polishing and filling. The patch pipettes were pulled from borosilicate glass 1.5mm O.D. X 0.86mm I.D. (Harvard Apparatus, UK) using a programmed Flaming/Brown micropipette puller (P-87, Sutter Instrument Company, CA, USA). The pipette tips were heat polished on a Micro-Forge model MF-79 (Narishige Scientific Instrument Lab., Tokyo, Japan). The pipette tip polishing was observed at 16 x 35 magnification using

Methods and Materials

a compound microscope with a long distance objective (Leitz Biomed, Wetzlar, Germany). This procedure further reduced the tip opening to a final resistance of $\leq 5\text{-}8 \text{ M}\Omega$. The pipette solution was back filled using hypodermic needles of size 0.60 X 60mm 23GX2-3/8" (Enosa, ROSE GmBh, Germany). The pipette solution must be filtered before using with a pore size equivalent to 0.2 mm in diameter (Sartorius, Göttingen, Germany). The pipette resistance was controlled before patch formation. Pipettes with a resistance lower than $1.5 \text{ M}\Omega$ were rejected and also pipettes with a resistance higher than $10 \text{ M}\Omega$. Usually, the pipette resistance between $1.5\text{-}3.5 \text{ M}\Omega$ was used for whole cell patch clamp experiments.

3.3.2 Patch clamp solutions

Macroscopic I_{Na} was recorded using the whole cell patch-clamp technique.

3.3.2.1 Stably transfected HEK cells

The bath (extracellular) solution contained (in mM) 20 NaCl, 120 $\text{C}_5\text{H}_{14}\text{ClNO}$, 4 KCl, 1.8 CaCl_2 , 0.75 MgCl_2 , and 5 HEPES (pH 7.4 with NaOH). The pipette solution contained (in mM) 120 CsF, 20 CsCl, 5 EGTA, and 5 HEPES (pH 7.4 set with CsOH).

3.3.2.2 tsA-20I cells with Q1077 mutants

The bath (extracellular) solution contained (in mM) 140 NaCl, 4 KCl, 1.8 CaCl_2 , 0.75 MgCl_2 , and 5 HEPES (pH 7.4 with NaOH). The pipette solution contained (in mM) 120 CsF, 20 CsCl, 5 EGTA, and 5 HEPES (pH 7.4 set with CsOH).

3.3.3 Experimental set-up

The patch clamp set-up consisted of the microscope (Axiovert 100, Carl Zeiss, Germany), amplifier (Axopatch 200B, Axon Instruments, CA, USA), headstage (CV 203BU Axon Instruments, CA, USA), pipette holder (HL-U, Axon Instruments, Inc.,

Foster City, Ca, USA), micromanipulator (Patchman, Eppendorf, Hamburg, Germany), computer, metal cage and vibration isolation table (Newport Corporation, Irvine, CA, USA). The silver wire was chlorinated every week before using as an electrode.

Membrane currents were recorded with an Axopatch 200B amplifier (Axon Instruments). Data were acquired using pCLAMP 10.2. Peak I_{Na} was obtained after passive leak subtraction. Data were digitized at 100 kHz and were low pass filtered at 10 kHz. Parameter fits were obtained using Origin 7.0.

3.3.4 Pulse protocol

Pulse protocol for activation curves

Current was elicited by a clamp from a holding potential of -140 mV to various test pulses (-60, -55, -50, -45, -40, -35, -30, -25, -20, -15, -10, 0, +10, +20, +30, +40, +50, +60, +70 mV) for 24 ms. 10 s was given between each sweep.

Pulse protocol for inactivation curves

Current recordings were obtained when the cells were clamped from a holding potential of -140 mV to 100 ms prepulses at -130, -120, -110, -105, -100, -95, -90, -85, -80, -75, -70, -65, -60, -50, -40, -30, -20, -10, and 0 mV, followed by a 24 ms test pulse to 0 mV.

3.3.5 Data acquisition and analysis

For the study of peak current-voltage relationships, data were normalized to the peak I_{Na} in each data set. The current-voltage (I-V) curves were fitted according to the following modified Boltzmann function: $G_{Na} = [1 + \exp(V_{1/2}-V)/k_{act}]^{-1}$, where $V_{1/2}$ and k_{act} are the mid-point and the slope factor, respectively, and $G_{Na} = I_{Na}/(V - V_{rev})$ where V_{rev} is the reversal potential. For voltage dependence of “steady-state” inactivation, I_{Na} was obtained in response to a test depolarization to 0 mV from a holding potential of -150 mV, followed by a 1 sec conditioning step to the various conditioning potentials (V_c). In order to normalize the capacity transients a 0.2 ms step back to -150 mV was applied before a test depolarization. The voltage dependent

Methods and Materials

availability from inactivation was determined by fitting the data to the Boltzmann function: $I_{Na} = I_{Na\text{-max}} [1 + \exp(V_c - V_{1/2})/k_{inact}]^{-1}$, where $V_{1/2}$ and k_{inact} are the midpoint and the slope factor, respectively, and V is the membrane potential.

3.4 Bioinformatics Analysis

Sequences of all the sodium channel variants were obtained from NCBI protein database. Later the sequences were aligned using the CLUSTALX: Multiple sequence alignment program (Larkin et al., 2007; Thompson et al., 1994) with default parameter. Then the aligned sequence was corrected manually if there was a mismatch.

Results

Previous results published on the modulation of the sodium channel by Fyn show that active Fyn shifts the steady-state inactivation in $\text{Na}_V1.2$ (Beacham et al., 2007) and $\text{Na}_V1.5$ (Ahern et al., 2005) without affecting the steady-state activation kinetics. Therefore, particular attention was payed on studies of the steady-state inactivation kinetics of cardiac sodium channel variants (Q1077 and $\Delta\text{Q}1077$) in presence and absence of Fyn.

4.1 Voltage-dependent kinetic parameters for Q1077 and $\Delta\text{Q}1077$ cardiac sodium channel variants

Modulation of sodium current kinetics by Fyn tyrosine kinases on stably expressed Q1077 and $\Delta\text{Q}1077$ variants in HEK-293 cells was investigated. Figure 7 shows the original current traces obtained with Q1077 and $\Delta\text{Q}1077$ variants. From the Figure it is evident that $\Delta\text{Q}1077$ has an increased peak I_{Na} compared to the Q1077 variant.

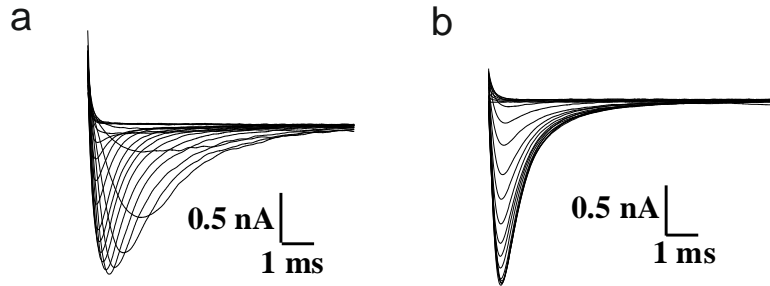
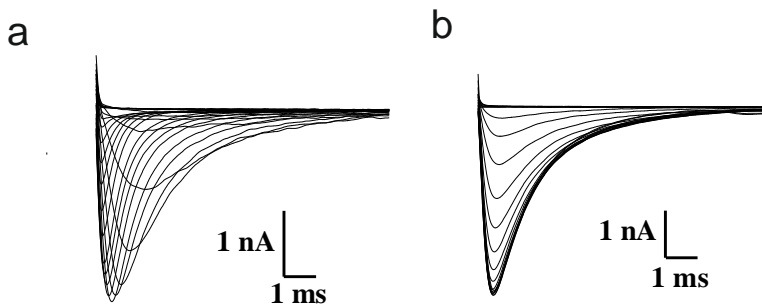
1. Q1077Present**2. ΔQ1077**

Figure 7: Original traces illustrating steady-state activation and steady-state inactivation of sodium channel currents of both (1) Q1077Present and (2) ΔQ1077.

In both variants, (1) and (2), (a) represents the activation current elicited from a holding potential of -140 mV to various test pulses (-60, -55, -50, -45, -40, -35, -30, -25, -20, -15, -10, 0, +10, +20, +30, +40, +50, +60, +70) for 24 ms. 10 s was given between each sweep. (b) In both (1) and (2) current recordings are shown, which were obtained when the cells were clamped from a holding potential of -140 mV to 100 ms prepulses at -130, -120, -110, -105, -100, -95, -90, -85, -80, -75, -70, -65, -60, -50, -40, -30, -20, -10, and 0 mV, followed by a 24 ms test pulse to 0 mV.

Table 7 shows the voltage-dependent kinetic parameters for both Q1077 and ΔQ1077 variants. There was no significant difference in the activation kinetics among both the variants. However, the $V_{1/2}$ steady-state inactivation of ΔQ1077 was observed at more depolarized potentials (-79.39 ± 0.38 mV) than that of the Q1077 variant (-88.21 ± 0.31 mV) ($p < 0.001$). The slope (K_{inact}) of the inactivation curve of ΔQ1077 (5.20 ± 0.27 mV) also differs from that of Q1077 (6.55 ± 0.21 mV) ($p < 0.001$). These results indicate that the glutamate residue (Q) at position 1077 plays a role in the steady-state inactivation of the cardiac sodium channel. As shown in Figure 7 and Table 7 the

peak I_{Na} of $\Delta Q1077$ (3.78 ± 0.11 nA) was larger than that of the Q1077Present variant (1.92 ± 0.10 nA) ($p < 0.001$). The decay of I_{Na} at 0 mV, for the portion of the I_{Na} trace after 90% of peak, was fitted using double exponential decay function. The values obtained from the fit are also tabulated in Table 7. The results on the decay of I_{Na} indicate that the fast component of the time constant (τ_f) in $\Delta Q1077$ (1.69 ± 0.14 ms) is significantly different ($p < 0.001$) from that of the Q1077Present variant (0.79 ± 0.46 ms) (Table 7, Figure 7).

Table 7: Voltage-dependent kinetic parameters for Q1077 and $\Delta Q1077$ cardiac sodium channel variants.

Data are given as the means \pm SEM, obtained from curve fitting to n experiments. Activation, inactivation, and decay were obtained according to the protocol described in the Materials and Methods section. For the decay of I_{Na} at 0 mV, the portion of the I_{Na} trace after decay to 90% of the peak current was fit to a sum of exponentials: $I_{Na}(t) = A_f X \exp -t/\tau_f + A_s X \exp -t/\tau_s + \text{offset}$, where t is time, τ_f and τ_s represent the time constants of the fast and slow components, and A_f and A_s are amplitudes of fast and slow components, respectively.

* Significant difference (ANOVA) for Q1077 and $\Delta Q1077$ stably transfected cells $p < 0.001$

	$\Delta Q1077$	Q1077Present
Inactivation		
$V_{1/2}$, mV	$-79.39 \pm 0.38^*$	-88.21 ± 0.31
Slope, mV	$5.20 \pm 0.27^*$	6.55 ± 0.21
n	9	8
Activation		
$V_{1/2}$, mV	-48.16 ± 0.20	-47.65 ± 0.29
Slope, mV	3.44 ± 0.10	3.60 ± 0.10
n	5	4
Peak Current		
I_{Na} , nA	$3.78 \pm 0.11^*$	1.92 ± 0.10
n	8	4
Decay (0 mV)		
A_f	0.87 ± 0.11	0.85 ± 0.03
τ_f , ms	$1.69 \pm 0.14^*$	0.79 ± 0.46
τ_s , ms	3.78 ± 0.15	4.09 ± 0.90
n	7	5

Figure 8 shows the Boltzmann fitted curves of both steady-state activation and inactivation of (A) Q1077 and (B) Δ Q1077 cells on the normalized I_{Na} and G_{Na} obtained from the original traces using the inactivation and activation pulse protocol as described in Material and Methods.

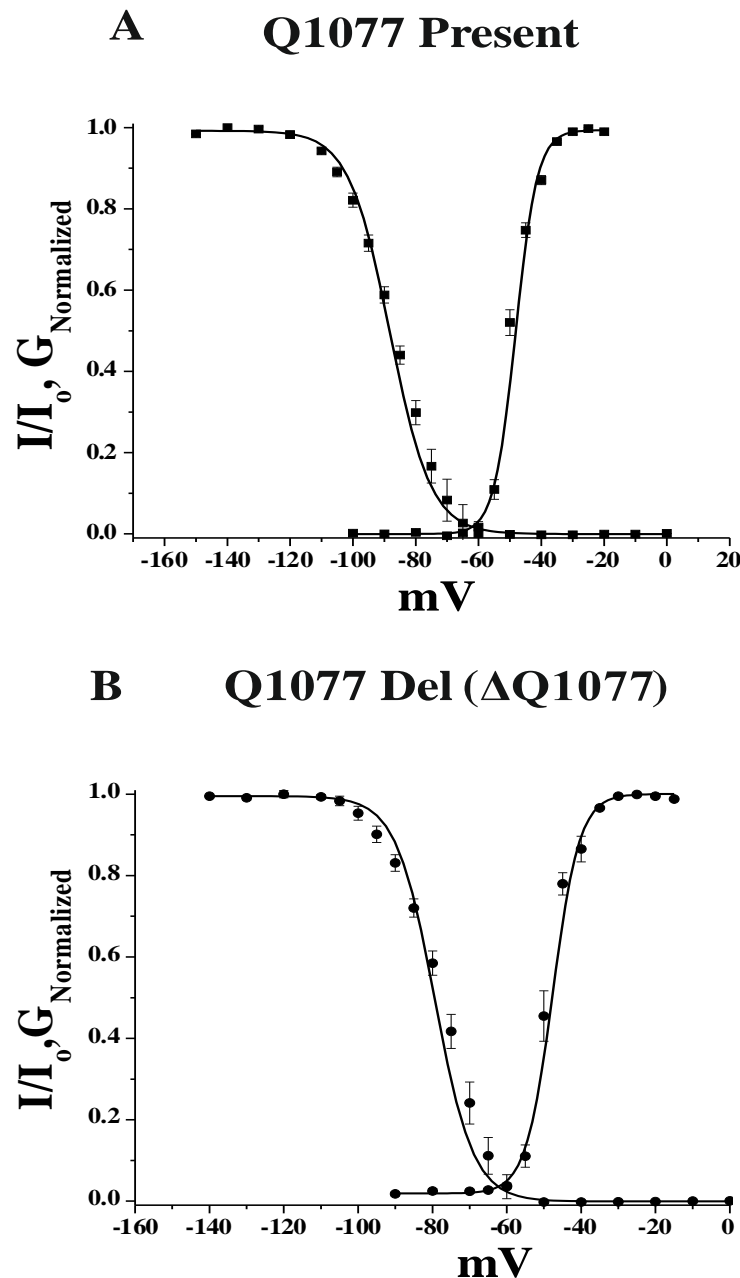


Figure 8: Boltzmann fitted steady-state inactivation and activation curves of (A) Q1077 Present and (B) Δ Q1077 stably transfected cells.

Boltzmann fitting, using the functions as described above, was done on the normalized values from original traces.

4.2 Inactivation properties of Δ Q1077 and Q1077 with Fyn^{CA}, Fyn^{KD} and tyrosine kinase inhibitor PP2

To test whether Fyn tyrosine kinase can differently modulate Δ Q1077 and Q1077, the stably transfected cells were transiently transfected with Fyn^{CA} and Fyn^{KD}. The constitutively active mutant, Fyn^{CA} lacks its inhibitory carboxyl terminus (amino acids upstream of 525 were deleted), whereas the kinase dead mutant Fyn^{KD} has a single point mutation at position K299M (Ahern et al., 2005; Nitabach et al., 2001). Figure 9 shows the steady-state inactivation curves of the sodium current from stably expressed cells (Δ Q1077 and Q1077), either alone or transiently transfected with active Fyn^{CA} or dead Fyn^{KD}, or Fyn^{CA} incubated with the potent Src tyrosine kinase inhibitor PP2.

Experiments with Fyn^{CA} on Q1077Present caused a 16-mV depolarizing shift of the steady-state inactivation curve (Figure 9 and Table 9). The $V_{1/2}$ inactivation of Q1077Present was -88.21 ± 0.31 mV (n=8) and the $V_{1/2}$ inactivation of Q1077Present with Fyn^{CA} was shifted to -72.98 ± 0.06 mV ($p < 0.001$, n=6). This result indicates that the shift in steady-state inactivation of Q1077Present in presence of Fyn^{CA} is similar to the hH1 cardiac sodium channel variant modulation by Fyn^{CA}. In the hH1 cardiac sodium channel, Fyn^{CA} caused a 5-mV shift of the steady-state inactivation curve from a $V_{1/2}$ of -94.9 ± 2.4 mV to -89.4 ± 0.9 mV (Ahern et al., 2005). To prove that this shift was due to Fyn, Q1077Present cells were transiently transfected with Fyn^{KD}. The data were confirmed as no shift was observed with Fyn^{KD} (-87.13 ± 0.29 , n=4). Further evidence was obtained with the kinase inhibitor PP2. PP2 inhibited the Fyn action and reversed back the depolarizing shift from -72.98 ± 0.06 mV caused by Fyn^{CA} to -88.41 ± 0.09 mV (n=3). These results obtained with Q1077Present in presence of Fyn^{CA}, Fyn^{KD} and Src tyrosine inhibitor PP2 show that the depolarizing shift was caused by Fyn tyrosine kinase.

Our experiments with Fyn^{CA} on Δ Q1077 caused a 9-mV hyperpolarizing potential shift of the steady-state inactivation curve (Figure 9 and Table 9) from an average $V_{1/2}$ of -79.39 ± 0.38 mV (n=9) for Δ Q1077 stably expressed cells to -88.51 ± 0.31 mV in the presence of Fyn^{CA} (n=5) ($p < 0.001$). The hyperpolarizing shift caused by Fyn^{CA} was similar to that observed in the Nav1.2 channel, in which a 5-mV shift from -64.2 ± 0.42 mV to -70.1 ± 0.32 mV was caused by Fyn (Beacham et al., 2007). When the

Results

$\Delta Q1077$ cells were transiently transfected with Fyn^{KD} no shift of the steady-state inactivation curve was observed (n=6). This study confirms that the hyperpolarizing shift was caused by Fyn^{CA}. To substantially confirm that the shift in the inactivation of $\Delta Q1077$ was due to Fyn, the cells which were transfected with Fyn^{CA} were treated with 1 μ mol/L of the Src kinase inhibitor PP2. The kinase inhibitor PP2 inhibited the Fyn action and reversed back the Fyn^{CA}-caused hyperpolarizing shift from -88.51 ± 0.31 mV to -78.52 ± 0.14 mV. This clearly confirms that the hyperpolarizing shift was caused by Fyn tyrosine kinase.

No significant difference was seen in the peak I_{Na} and the decay of current in both Q1077Present and $\Delta Q1077$ with and without Fyn^{CA} (Table 9). However, from analysis of steady-state inactivation it was evident that Q1077Present and $\Delta Q1077$ cardiac sodium channels behave differently in the modulation by Fyn tyrosine kinase.

Table 8: Kinetic parameters for Q1077 and $\Delta Q1077$ cardiac sodium channel variants with and without Fyn^{CA}.

	$\Delta Q1077$	$\Delta Q1077 + Fyn^{CA}$	Q1077Present	$Q1077 + Fyn^{CA}$
Peak Current				
I_{Na} , nA	3.78 ± 0.11	3.97 ± 0.28	1.92 ± 0.10	1.71 ± 0.26
n	8	3	4	4
Decay (0 mV)				
A_f	0.87 ± 0.11	0.84 ± 0.12	0.85 ± 0.03	0.89 ± 0.49
τ_f , ms	1.69 ± 0.14	1.45 ± 0.21	0.79 ± 0.46	0.96 ± 0.38
τ_s , ms	3.78 ± 0.15	4.13 ± 0.63	4.09 ± 0.90	4.62 ± 0.16
n	7	3	5	4

Table 9: Half-maximal inactivation of both Q1077 and ΔQ1077 with Fyn^{CA}, Fyn^{KD} and with Fyn^{CA} + PP2.

Data are derived from fits of Boltzmann function to normalized inactivation curves determined from individual cells as described in Materials and Methods. * p<0.001.

Variant	Half-maximal inactivation ($V_{1/2}$) (mV)	K_{Inact} (mV)	n
Q1077Present	-88.21 ± 0.31	5.55 ± 0.21	8
Q1077Present + Fyn ^{CA}	-72.98 ± 0.06*	6.73 ± 0.35*	6
Q1077Present + Fyn ^{KD}	-87.13 ± 0.29	5.18 ± 0.24	4
Q1077Present + Fyn ^{CA} + PP2	-88.41 ± 0.09	5.91 ± 0.63	3
ΔQ1077	-79.13 ± 0.38	5.76 ± 0.27	9
ΔQ1077 + Fyn ^{CA}	-88.21 ± 0.31*	7.63 ± 0.18*	5
ΔQ1077 + Fyn ^{KD}	-80.61 ± 0.36	5.97 ± 0.28	6
ΔQ1077 + Fyn ^{CA} + PP2	-78.88 ± 0.14	6.28 ± 0.37	2

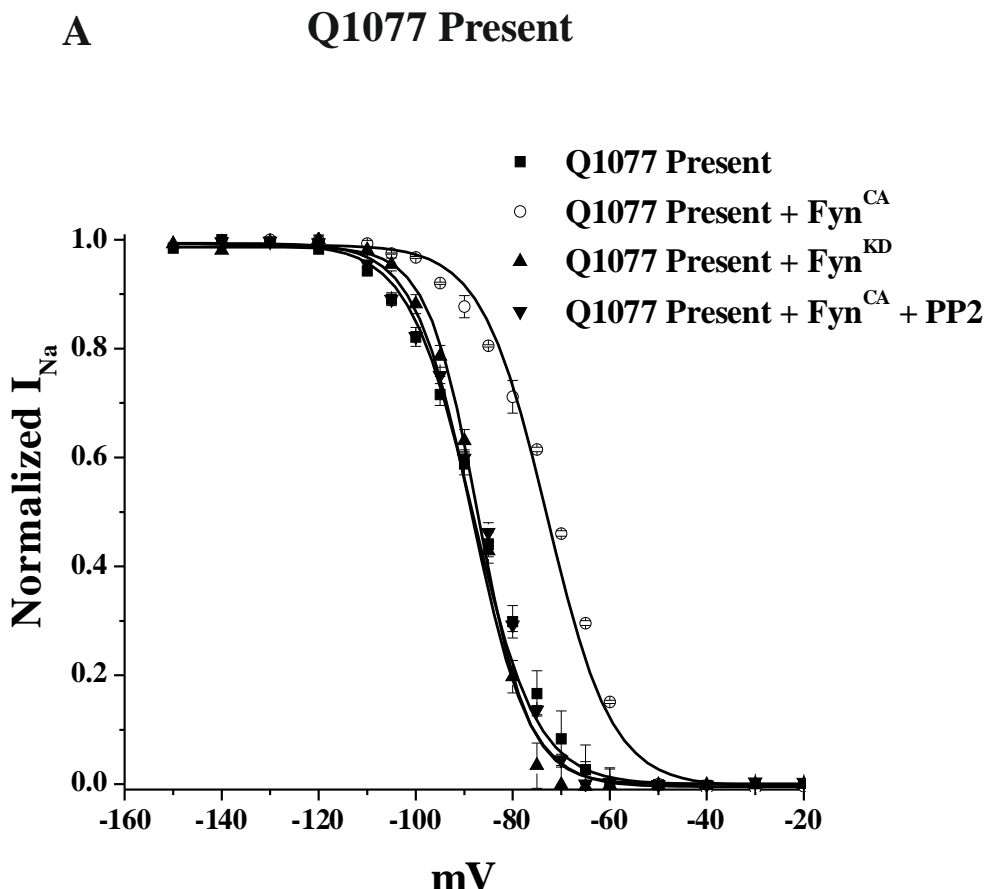
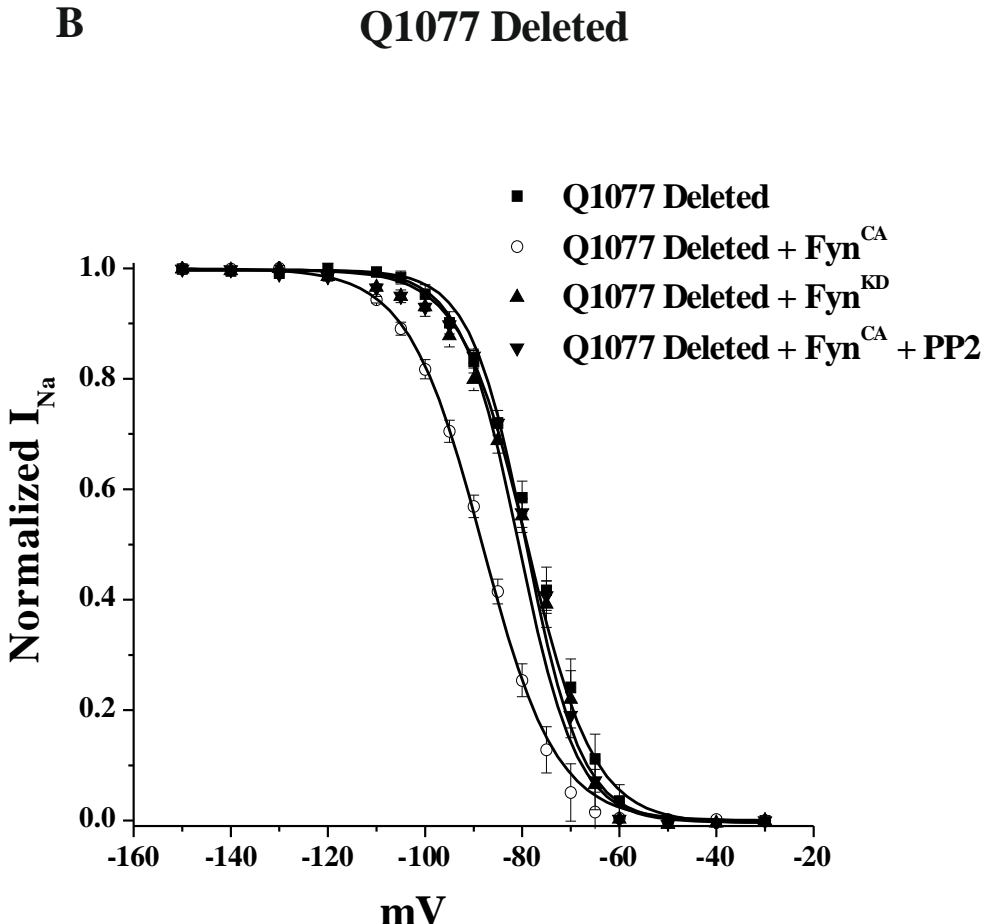


Figure 9A: Expression of catalytic active Fyn^{CA} alters steady state inactivation curves in stably expressed Q1077Present and ΔQ1077 cells.

A. Steady-state inactivation properties of stably expressed Q1077Present cardiac sodium channel current with Fyn^{CA}. Solid line in (A) with filled squares corresponds to the Boltzmann fit of current recorded from stably expressed Q1077Present cells. The $V_{1/2}$ of Q1077Present is -88.21 ± 0.31 mV. The Boltzmann fit curve with open circles represents data obtained from stably expressed Q1077Present cells with Fyn^{CA}. $V_{1/2}$ of Q1077Present expressed with Fyn^{CA} is -72.98 ± 0.06 mV. When Q1077Present cells were expressed with Fyn^{KD}, represented by filled up-pointing triangles, the $V_{1/2}$ is -87.13 ± 0.29 mV. To test the Src tyrosine kinase inhibitor action, the Q1077Present cells transfected with Fyn^{CA} were incubated with the specific tyrosine kinase inhibitor PP2 (1 μmol/L) for 30 minutes before current recording. The curve with filled down-pointing triangles denotes the Boltzmann fit of Q1077Present in presence of Fyn^{CA} and the specific tyrosine kinase inhibitor PP2; the $V_{1/2}$ is -88.41 ± 0.09 mV.

**Figure 9B:**

B. Similar inactivation curves for Δ Q1077 cells are shown as explained above for Q1077Present cells. Boltzmann fit of stably expressed Δ Q1077 cells is denoted with filled squares. The $V_{1/2}$ inactivation of Δ Q1077 is -79.39 ± 0.38 mV. The inactivation curve of stably expressed Δ Q1077 with Fyn^{CA} is represented by open circles. $V_{1/2}$ for Δ Q1077 expressed with Fyn^{CA} is -80.76 ± 0.36 mV. The inactivation curve for Δ Q1077 cells expressed with Fyn^{KD} is represented by filled up-pointing triangles; the $V_{1/2}$ is -80.76 ± 0.36 mV. The Boltzmann fitted inactivation curve for the Δ Q1077 cells in presence of Fyn^{CA} and PP2 is depicted with filled down-pointing triangles. $V_{1/2}$ inactivation, when treated with PP2, is -78.52 ± 0.14 mV.

4.3 Activation Properties of $\Delta Q1077$ and $Q1077$ with Fyn^{CA}

To determine whether Fyn^{CA} can modulate the steady-state activation of $\Delta Q1077$ and $Q1077$, the cells were transfected with Fyn^{CA} , and the normalized conductance of $\Delta Q1077$ and $Q1077$ with or without Fyn^{CA} was analysed. The steady-state activation of $\Delta Q1077$ and $Q1077$ in presence or absence of Fyn^{CA} is shown in Figure 10 and Table 10.

Table 10: Half-maximal activation and slope of both $Q1077$ and $\Delta Q1077$ with Fyn^{CA} .

Data derived from fits of a Boltzmann function to normalized activation curves, determined from individual cells as described in Materials and Methods.

Variant	Half-maximal activation ($V_{1/2}$) (mV)	K_{Act} (mV)	n
Q1077	-48.91 ± 0.22	3.87 ± 0.13	5
Q1077 + Fyn^{CA}	-49.17 ± 0.23	4.05 ± 0.23	3
$\Delta Q1077$	-47.65 ± 0.29	3.69 ± 0.10	4
$\Delta Q1077 + Fyn^{CA}$	-48.56 ± 0.63	4.07 ± 0.59	3

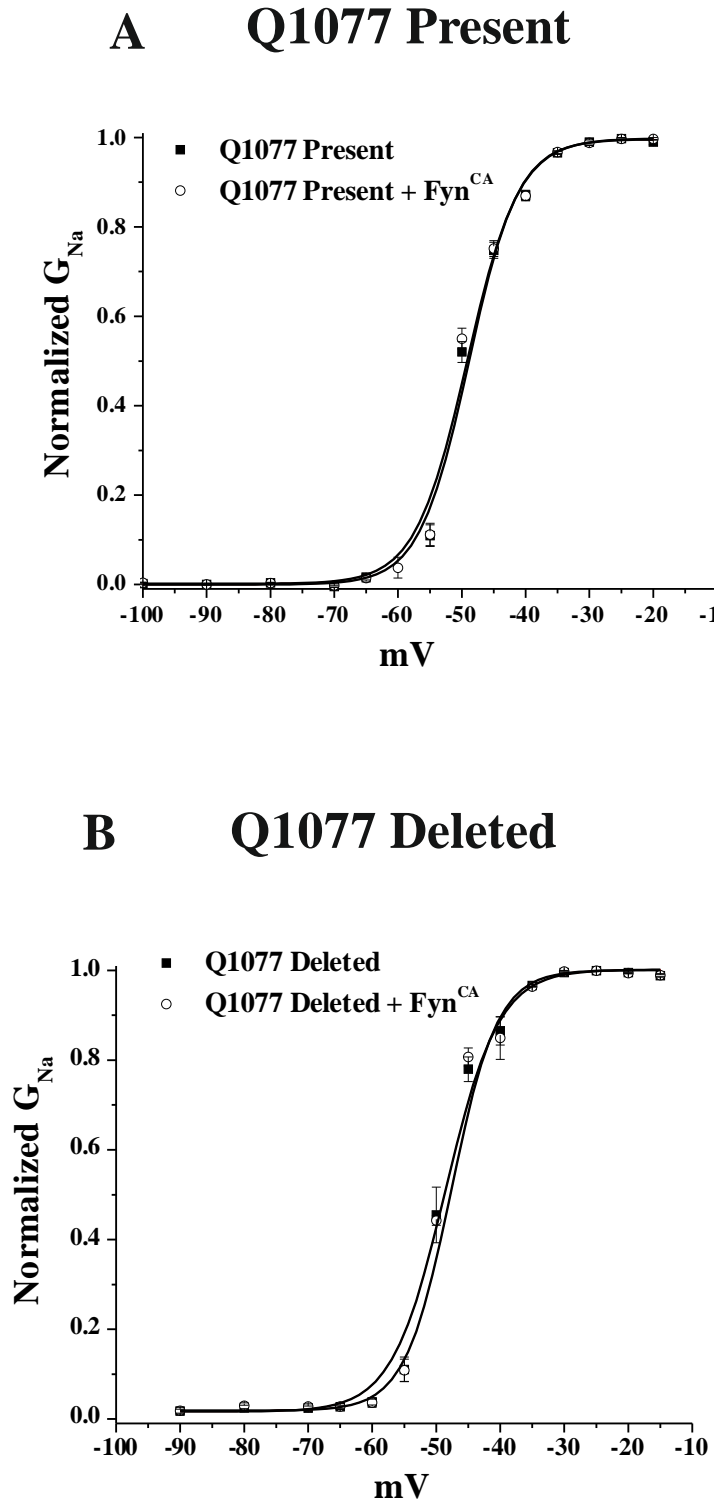


Figure 10: Steady-state activation curves of stably expressed Q1077 and Δ Q1077 cardiac sodium channels.

Boltzmann functions fit to normalized conductance were determined from individual cells as described in Materials and Methods.

Figure 10 shows the activation curves of Q1077Present in absence and presence of Fyn^{CA}. Fyn^{CA} did not cause any shift of the activation curve. Similarly, in ΔQ1077 Fyn^{CA} also did not alter the activation curve (Table 10).

These data clearly show that activation kinetics of the two variants, Q1077Present and ΔQ1077, is not modulated by Fyn. These results were consistent with earlier published results on Fyn modulation of steady state activation of Nav1.2 and Nav1.5 (hH1) sodium channels (Ahern et al., 2005; Beacham et al., 2007).

4.4 Sequence alignment of sodium channel subunits of the intracellular loop L_{DII-DIII}

To ascertain the uniqueness of cardiac sodium channel sequence, the amino acid sequences of all the nine sodium channel isoforms were aligned using the multiple sequence alignment CLUSTAL X program. The Pfam database is a large collection of protein families, each represented by multiple sequence alignments and hidden Markov models (Finn et al., 2010). According to pfam06512 database (Marchler-Bauer et al., 2011), amino acids of the cardiac sodium channel between positions 953-1214 form one of the sodium ion-transport associated regions of the channel. In the predicted cardiac sodium channel structure (George et al., 1992), amino acids from position 953 to 1214 also form the intracellular loop connecting the DII and DIII region (L_{DII-DIII}) of the cardiac sodium channel. Since Q1077 is present in the intracellular loop connecting domains II and III, amino acid sequences of this loop of all the sodium channel isoforms were aligned and analysed (Figure 11).

From Figure 11 it is evident that the Q1077 residue is located in the amino acid sequence 1075-KQQESQP-1081, which is unique in the cardiac sodium channel. In L_{DII-DIII} the amino acid sequences 1047-GEQPGQGTPGDPEPVCVPIAAE-1053 and 1116-QQWKAEPQAPGCGETP-1132 are also unique among different sodium channel isoforms (Figure 11).

Results

Nav1.1	DDDNEMNNLQIAVDRMHKGVAYVKRKIYEFIQQSF
Nav1.8	DDDNEMNNLQIAVDRMHKGVAYVKRKIYEFIQQSF
Nav1.9	DDDNEMNNLQIAVDRMHKGVAYVKRKIYEFIQQSF
Nav1.2	DDDNEMNNLQIAVGRMQKGIDFVKRKIREFIQKAF
Nav1.3	DDDNEMNNLQIAVGRMQKGIDYVKNKMRECQKAF
Nav1.7	EEDPDANNLQIAVTRIKKGINYVKQLREFILKAF
Nav1.6	DDDGEMLNLQISVIRIKKGVAWTKLVHAFMQAHF
Nav1.4	DEDGEMNNLQIAIGRIKLGIGFAKAFLLLGLHGKI
Nav1.5(Q1077)	950 DEDREMNNLQLALARIQRGLRFFVKRTTWDGCCGLL ::*: * **; :: * : * : .. *
Nav1.1	IRKQKILDEIKPLDDLNNKKDSCMS--NHT-AEIGKLDYLKDVGNTTSGIGT-----
Nav1.8	IRKQKILDEIKPLDDLNNKKDSCMS--NHT-AEIGKLDYLKDVGNTTSGIGT-----
Nav1.9	IRKQKILDEIKPLDDLNNKKDSCMS--NHT-AEIGKLDYLKDVGNTTSGIGT-----
Nav1.2	VRKQKALDEIKPLEDLNNKKDSCIS--NHTTIEIGKDLNYLKDGNGTTSGIG-----
Nav1.3	FRKPKVIEIHE----GNKIDSCMS--NNTGIEISKE NYLRDGNNGTTSGVGT-----
Nav1.7	SKKPKSREIRQAEDLNTKKENYIS--NHTLAEMSKGHNFKE-KDKISGFG-----
Nav1.6	KQRE--ADEVKPLDELYEKKANCIA--NHTGADIHRNGDFQKNGNGTTSGIG-----
Nav1.4	LSPKDIMLSLGEADGAGEAGEAGET--APEDEKKEPPEEDLKKDNHILNHMG-----
Nav1.5(Q1077)	RQRPKPAALAAQQLPSCIATPYSPPPPTEKVPPTRKETRFEEGEQPGQGTPGDPEPV *: . . . : :
Nav1.1	-----GSSVEKYIIDESDYMSFINNPS-----LTVTVPPIAVGESDFENLNTEDFSSE
Nav1.8	-----GSSVEKYIIDESDYMSFINNPS-----LTVTVPPIAVGESDFENLNTEDFSSE
Nav1.9	-----GSSVEKYIIDESDYMSFINNPS-----LTVTVPPIAVGESDFENLNTEDFSSE
Nav1.2	-----SSVEKYVVDESODYMSFINNPS-----LTVTVPPIAVGESDFENLNTEEFSSE
Nav1.3	-----GSSVEKYVIDENDYMSFINNPS-----LTVTVPPIAVGESDFENLNTEEFSSE
Nav1.7	-----SSVDKHLMEDSDGQSFHNPN-----LTVTVPPIAPGESDFLENMNAELSSD
Nav1.6	-----SSVEKYIID-EHMSFINNPN-----LTVRVPIAVGESDFENLNTEEDVSSE
Nav1.4	-----LADGPPSSLELDHNLNFINNPN-----LTIQVPIASEEESDLEMPTEEETDTF
Nav1.5(Q1077)	CVPIAVAEASDQDQEEDDEENSLGTEEEESSKQQESQPVSGGPEAPPDSRTWSQVSATASSE : : . . . : . * * : * . : . :
Nav1.1	SDLEESKE--KLNE-----SSSSSEGSTVDIGAPVE--EQPVVEPEETLEPE
Nav1.8	SDLEESKE--KLNE-----SSSSSEGSTVDIGAPVE--EQPVVEPEETLEPE
Nav1.9	SDLEESKE--KLNE-----SSSSSEGSTVDIGAPVE--EQPVVEPEETLEPE
Nav1.2	SDMEESKE--KLN-----ATSSSEGSTVDVVLIPREG-EQAETEPEEDLKPE
Nav1.3	SELEESKE--KLN-----ATSSSEGSTVDVVLIPREG-EQAETEPEEDLKPE
Nav1.7	SDSEYSKV--RLN-----RSSSSECSTVDNPLPEG-EAAEAEPMNSDEPE
Nav1.6	SDPEGSKD--KLD-----DTSSSEGSTIDIKPEVE--EVPVQEPEEYLDPD
Nav1.4	SEPEDDSKPKPQPLY-----DGNSSVCSTADYKPPPEEDPEEQAEENPEGEQPE
Nav1.5(Q1077)	AEASASQADWRQQWKAEPQAPGCGETPEDSCSEGSTADMTNTAELLEQIPDLGQDVKDPE : : . * : : . * * * * * * : . * :
Nav1.1	ACFTEGCVQRFKCCQINVEEGRGKQWWNLRRTCFRIVEHNWFETFIVFM
Nav1.8	ACFTEGCVQRFKCCQINVEEGRGKQWWNLRRTCFRIVEHNWFETFIVFM
Nav1.9	ACFTEGCVQRFKCCQINVEEGRGKQWWNLRRTCFRIVEHNWFETFIVFM
Nav1.2	ACFTEDCVRKFKCCQISIEEGKGKLWWNLRKTCYKIVEHNWFETFIVFM
Nav1.3	ACFTEGCIKKFPFCQVSTEEGKGKIIWWNLRKTCYSIVEHNWFETFIVFM
Nav1.7	ACFTDGCVRFRFSCCQVNIESGGKGKIIWWNLRKTCYKIVEHHSWFESFIVLM
Nav1.6	ACFTEGCVQRFKCCQVNIEEGLGKSWWLRLKTCFLIVEHNWFETFIVFM
Nav1.4	ECFTEACVQRWPCLYVDISQGRGKKWWTLRRACFKIVEHNWFETFIVFM
Nav1.5(Q1077)	DCFTEGCVRRCPCCAVDTTQAPGKWWWRRLKTCYHIVEHSWFETFIVFM 1214 ***: *::: : . . . * * * : *::: * ***: ***: ***: *:

Figure 11: Alignment of the intracellular loop of sodium channel subtypes connecting Domain II and III ($L_{DII-DIII}$).

Amino acid numbering of cardiac sodium channel and the proposed structure (George et al., 1992) forms the base of the alignment. Corresponding $L_{DII-DIII}$ residues of the other sodium channel subtypes were used for the alignment.

Asterisks denote consensus amino acids, colons denote high similarity of amino acids, and dots denote less similarity among the aligned amino acids. No symbol denotes lack of similarity among amino acids.

4.5 Kinetics of Q1077 cardiac sodium channel mutants

To analyse the importance of Q1077 in the cardiac sodium channel, the amino acid glutamate was replaced with different amino acids using the Stratagene Quick Change Site-Directed Mutagenesis Kit with the Q1077Present cDNA as the template. The Q1077 was mutated to lysine (Q1077K), alanine (Q1077A), proline (Q1077P), and tyrosine (Q1077Y). The steady-state inactivation kinetics was obtained as described in the Materials and Methods section.

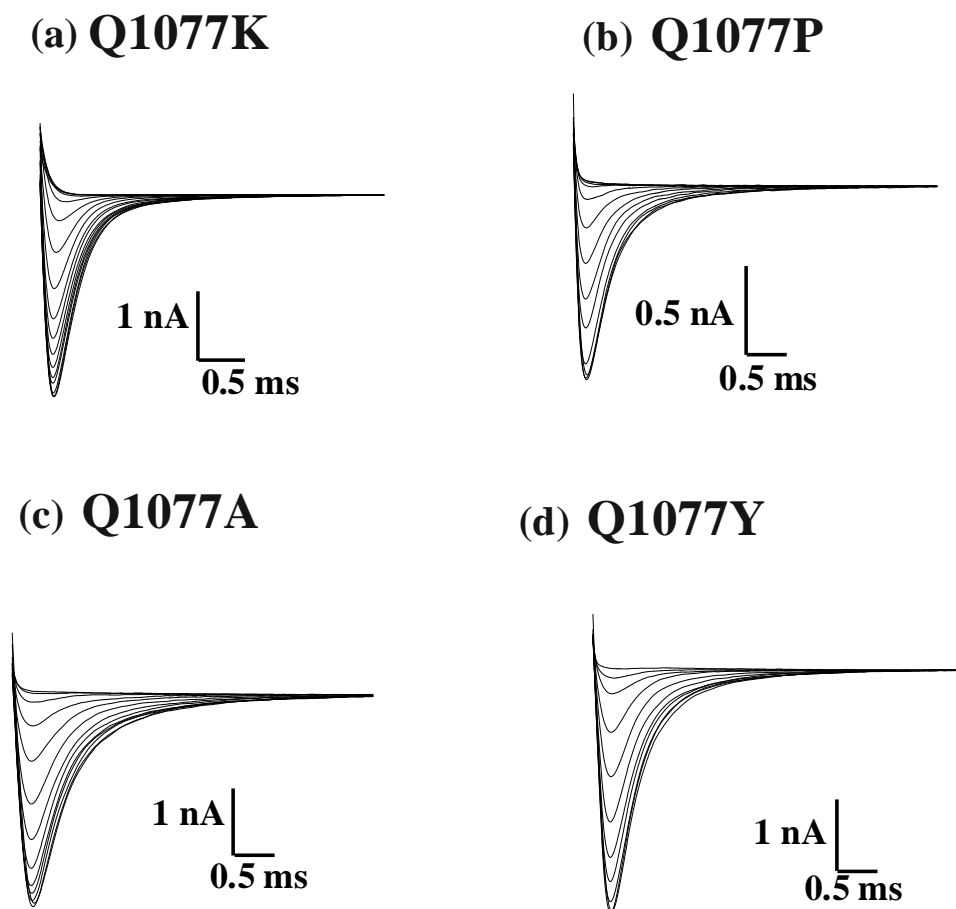


Figure 12: Original traces illustrating steady-state inactivation of the transiently transfected mutants at position Q1077 in tsA-201 cells:

(a) Q1077K, (b) Q1077P (c) Q1077A (d) Q1077Y. Current recordings are shown, which were obtained when the cells were clamped from a holding potential of -140 mV to 100 ms prepulses at -150, -140, -130, -120, -110, -105, -100, -95, -90, -85, -80, -75, -70, -65, -60, -50, -40, -30, -20, -10, and 0 mV, followed by a 24 ms test pulse to 0 mV.

Results

From Figure 12 it is evident that the peak I_{Na} of Q1077P was smaller than that of the other counterparts. To obtain detailed inactivation kinetics, the original traces were fitted with Boltzmann functions as done for Q1077Present and Δ Q1077 (Table 11).

Table 11: Kinetic parameters for all four mutants of the Q1077 cardiac sodium channel.

§ (p<0.001) Significant difference (ANOVA) of the mutants relative to Q1077Present.
 * (p<0.001) Significant difference (ANOVA) among all 4 different Q1077 mutants.

	Q1077K	Q1077P	Q1077A	Q1077Y
Inactivation				
$V_{1/2}$, mV	$-97.47 \pm 0.23^{\ast\ast}$	-88.21 ± 0.47	$-101.61 \pm 0.30^{\ast\ast}$	-90.43 ± 0.35
Slope, mV	6.13 ± 0.22	7.16 ± 0.32	6.39 ± 0.25	6.49 ± 0.32
n	3	4	6	4
Peak Current				
I_{Na} , nA	-3.59 ± 0.92	$0.81 \pm 0.09^{\ast}$	-4.48 ± 0.87	-3.24 ± 0.51
n	4	3	3	3
Decay (0 mV)				
A_f	0.94 ± 0.27	0.64 ± 0.26	0.69 ± 0.25	0.86 ± 0.43
τ_f , ms	0.53 ± 0.76	0.76 ± 0.11	0.65 ± 0.24	0.78 ± 0.63
τ_s , ms	2.84 ± 0.33	2.44 ± 0.44	$5.45 \pm 0.70^{\ast}$	2.13 ± 0.14
n	3	4	3	3

As illustrated in Table 11 the steady-state inactivation of mutants Q1077A and Q1077K was shifted to more hyperpolarizing potentials. The $V_{1/2}$ inactivation of Q1077K was -97.47 ± 0.23 mV (n=3) and for Q1077A it was -101.61 ± 0.30 mV (n=6), which was statistically different (p<0.001) from the Q1077Present variant (-88.21 ± 0.31 mV, n=8). In contrast, there was no statistically significant difference in the steady-state inactivation kinetics of Q1077P (-88.21 ± 0.47 mV, n=4) and Q1077Y (-90.43 ± 0.35 mV, n=4) compared to the Q1077Present variant (-88.21 ± 0.3 mV, n=8). This indicates that the mutation at position 1077 with alanine and lysine (Q1077A and Q1077K) altered the $V_{1/2}$ inactivation. The peak I_{Na} of Q1077P

(0.81 ± 0.09 nA, n=3) was statistically different ($p<0.001$) from that of the other mutants Q1077K (-3.59 ± 0.92 nA, n=4), Q1077A (-4.48 ± 0.87 nA, n=3) and Q1077Y (-3.24 ± 0.51 nA, n=3). Thus, the mutation from glutamine at position 1077 to proline significantly reduced the peak I_{Na} . For the decay of I_{Na} at 0 mV, the portion of the I_{Na} trace measured after 90% of peak was fit to a sum of exponentials and the parameters are listed in Table 11. The decay time constant of the slow component (τ_s) for Q1077A was significantly ($p<0.001$) different from that of the other 1077 mutants (Q1077K, Q1077P and Q1077Y).

4.6 Inactivation kinetics of Q1077 mutants with Fyn^{CA} and Fyn^{KD}

To test the modulation of Q1077 mutants by Fyn^{CA} and Fyn^{KD}, the mutant clones were co-transfected with Fyn^{CA} and Fyn^{KD} in tsA-201 cells. Original traces were obtained using the inactivation protocol as described in the Materials and Method section. The obtained traces were then analysed and fitted using Boltzmann function. The results were plotted (Figure 13) and tabulated (Table 12). The difference in the modulation by Fyn^{CA} among different Q1077 mutants is presented in the following sections.

4.6.1 Modulation of inactivation kinetics of Q1077K mutant with Fyn^{CA} and Fyn^{KD}

When the neutral amino acid glutamine at position Q1077 was replaced with the basic residue lysine (Q1077K), the inactivation was shifted to more hyperpolarizing potentials (-97.47 ± 0.23 mV, n=6). Cells co-transfected with Fyn^{CA} produced a statistically significant ($p<0.001$) hyperpolarizing shift from -97.47 ± 0.23 mV to -102.95 ± 0.43 mV (n=3). This result was similar to that of the Nav1.2 sodium channel modulation by Fyn and Δ Q1077 stably transfected cell modulation by Fyn. Q1077K with Fyn^{KD} ($V_{1/2}$: -97.63 ± 0.98 mV, n=3) did not produce any shift of the inactivation curve. This strongly emphasises that the modulation in inactivation was due to Fyn.

4.6.2 Modulation of inactivation kinetics of Q1077A mutant with Fyn^{CA} and Fyn^{KD}

The polar glutamine residue at position 1077 was replaced with the unpolar residue alanine (Q1077A). Q1077A also produced a hyperpolarizing shift, which was even larger (13.4 mV) compared to the other three mutants (Table 12). Cells co-transfected with Fyn^{CA} produced a statistically significant hyperpolarizing shift from -101.61 ± 0.30 mV (n=6) to -118.02 ± 0.36 mV (n=3). When the cells were co-transfected with Fyn^{KD} no statistically significant shift in the inactivation ($V_{1/2}$: -105.33 ± 0.51 mV) was observed. The results obtained for inactivation of I_{Na} of Q1077A were in line with the Q1077K mutant, but the shift caused due to Q1077A mutant was larger (Table 12).

4.6.3 Modulation of inactivation kinetics of Q1077P mutant with Fyn^{CA} and Fyn^{KD}

The aliphatic glutamine residue at position 1077 in the cardiac sodium channel was replaced with the heterocyclic amino acid residue proline (Q1077P). The steady-state inactivation of the Q1077P mutant (-88.21 ± 0.47 mV, n=6) was not shifted. When the Q1077P mutant was co-transfected with Fyn^{CA}, a statistically significant ($p<0.001$) hyperpolarizing shift from -88.21 ± 0.47 mV to -97.71 ± 0.38 mV (n=4) was produced. The hyperpolarizing shift was not observed in the Q1077P mutant transfected with Fyn^{KD} (-88.85 ± 0.89 mV, n=4). This hyperpolarizing shift caused by the mutant Q1077P with Fyn^{CA} was less compared to the Q1077A mutant, but more pronounced than with the Q1077K mutant.

4.6.4 Modulation of inactivation kinetics of Q1077Y mutant with Fyn^{CA} and Fyn^{KD}

The aromatic amino acid residue tyrosine was substituted instead of the aliphatic glutamine residue at position 1077 (Q1077Y). Similar to mutant Q1077P, the steady-state inactivation of Q1077Y was also not shifted (-90.43 ± 0.35 mV, n=4). When the Q1077Y mutant was co-transfected with Fyn^{CA}, a statistically significant

Results

($p < 0.001$) hyperpolarizing shift from -90.43 ± 0.35 mV to -99.79 ± 0.18 mV ($n=3$) was observed. Such a hyperpolarizing shift was not seen when the cells were co-transfected with Fyn^{KD} (-90.45 ± 0.32 mV, $n=3$).

Table 12: Half-maximal inactivation of all four Q1077 mutants with Fyn^{CA} and Fyn^{KD}.

Data are derived from fits of Boltzmann function to normalized inactivation curves.

Mutant	Half-maximal inactivation ($V_{1/2}$) (mV)	K_{Inact} (mV)	n
Q1077Y	-90.43 ± 0.35	6.49 ± 0.32	4
Q1077Y + Fyn ^{CA}	$-99.79 \pm 0.18^*$	$7.98 \pm 0.13^*$	3
Q1077Y + Fyn ^{KD}	-90.45 ± 0.32	6.62 ± 0.59	3
Q1077P	-88.21 ± 0.47	7.16 ± 0.32	6
Q1077P + Fyn ^{CA}	$-97.71 \pm 0.38^*$	7.41 ± 0.14	4
Q1077P + Fyn ^{KD}	-88.85 ± 0.89	6.65 ± 0.53	4
Q1077K	-97.47 ± 0.23	6.13 ± 0.22	6
Q1077K + Fyn ^{CA}	$-102.95 \pm 0.43^*$	$8.96 \pm 0.24^*$	3
Q1077K + Fyn ^{KD}	-97.63 ± 0.98	6.82 ± 0.63	3
Q1077A	-101.61 ± 0.30	6.39 ± 0.25	6
Q1077A + Fyn ^{CA}	$-118.02 \pm 0.36^*$	6.84 ± 0.17	3
Q1077A + Fyn ^{KD}	-105.33 ± 0.51	5.73 ± 0.28	5

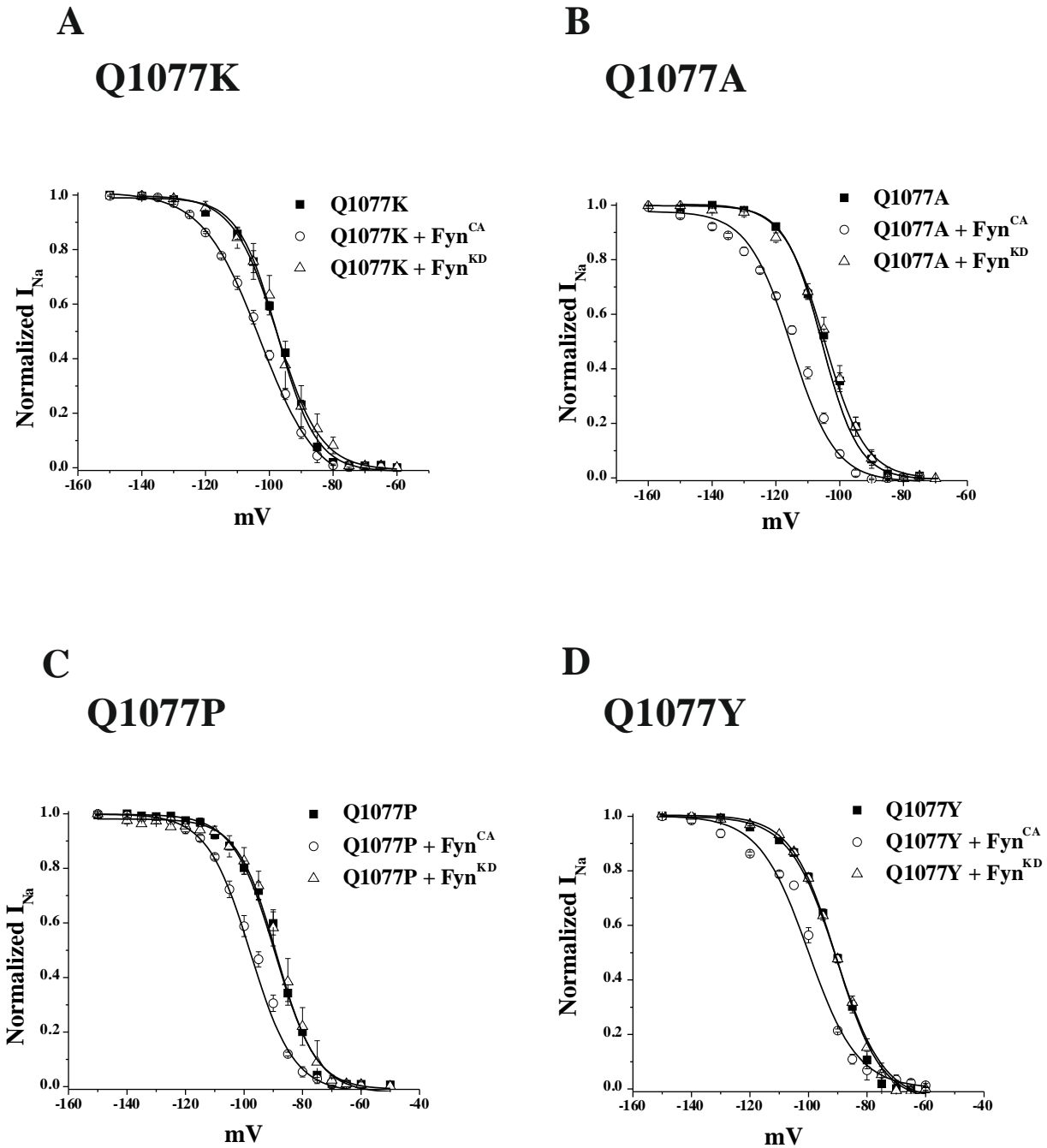


Figure 13: Expression of catalytic active Fyn^{CA} alters steady-state inactivation kinetics of Q1077 mutants.

Boltzmann function fitted steady-state inactivation curves of four Q1077 mutants - (A) Q1077K, (B) Q1077A, (C) Q1077P, (D) Q1077Y with Fyn^{CA} and Fyn^{KD} are shown. Solid lines with filled squares correspond to Boltzmann fits of the respective transiently transfected mutant. Cells expressing both, Q1077 mutants and Fyn^{CA}, are represented by open circles. Q1077 mutants expressed with Fyn^{KD} are represented by open triangles. Number of experiments is given in Table 12.

Thus, the steady-state inactivation curves of all four different Q1077 mutants were shifted to more hyperpolarizing potentials when they were co-expressed with Fyn^{CA}. This hyperpolarizing shift in inactivation is similar to the modulation of Nav1.2 and ΔQ1077 cardiac sodium channels caused by Fyn tyrosine kinase.

4.6.5 Correlation between the mutant amino acid properties and the shift in inactivation curves.

There is a linear correlation ($R^2 = 0.99$) when the hydrophobicity of an amino acid side chain is plotted against the difference in shifts of the inactivation curves in presence and absence of Fyn^{CA} (Figure 14).

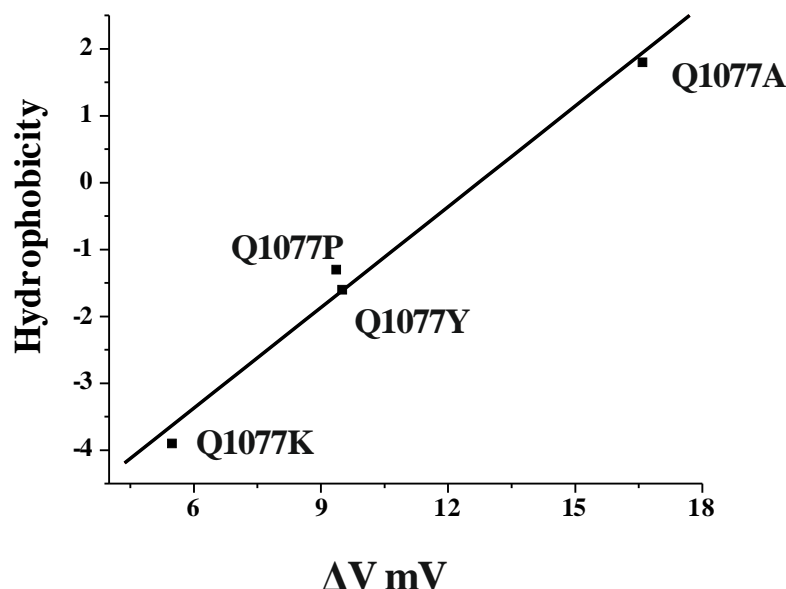


Figure 14: Plot showing the linear relationship ($R^2 = 0.99$) between the hydrophobicity of an amino acid and the difference in shift of the inactivation curves ($\Delta V = V_{1/2, \text{Mutant}} - V_{1/2, \text{Mutant} + \text{Fyn}^{\text{CA}}}$).

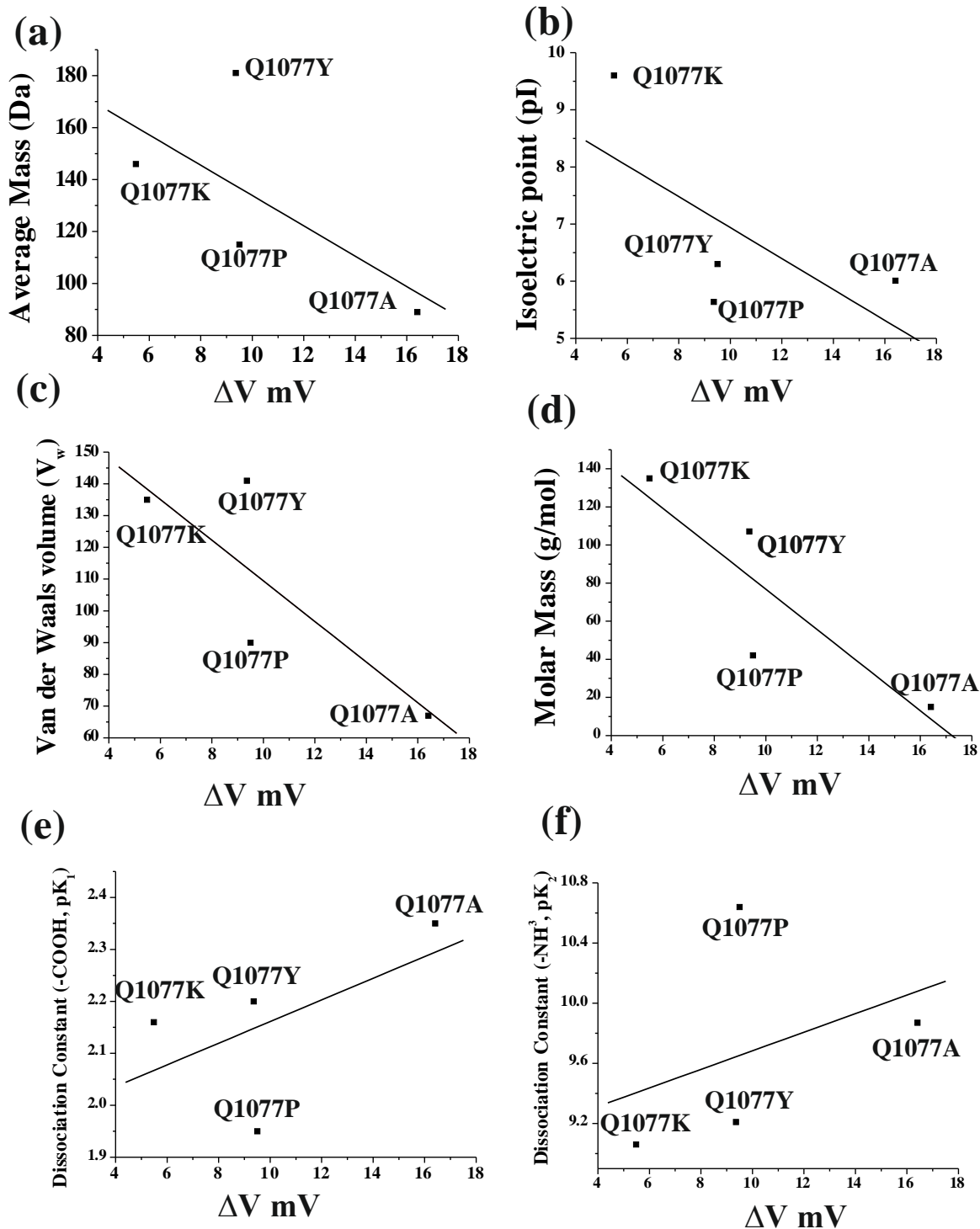


Figure 15: Plot showing the linear relationship between different properties of amino acids and the difference in shift of the inactivation curves

(a) average mass ($R^2 = 0.45$), (b) isoelectric point ($R^2 = 0.45$), (c) Van der Waals volume ($R^2 = 0.67$), (d) molar mass ($R^2 = 0.76$), (e) dissociation constant ($\alpha\text{-COOH}$) pK_1 ($R^2 = 0.33$) and (f) dissociation constant ($\alpha\text{-NH}_3^+$) pK_2 ($R^2 = 0.16$) of an amino acid and the difference in shift of the inactivation curves ($\Delta V = V_{1/2, \text{Mutant}} - V_{1/2, \text{Mutant} + \text{CA}}$) is shown.

Results

Linear correlation graphs of different properties of the amino acids plotted against the difference in shift of the inactivation curves (ΔV mV) show weak or no correlation (Figure 15). Only molar mass ($R^2 = 0.76$) and the Van der Waals volume (V_w) ($R^2 = 0.67$) were weakly correlated, whereas the other parameters like average mass ($R^2 = 0.45$), isoelectric point ($R^2 = 0.45$), dissociation constant pK_1 ($R^2 = 0.33$) and pK_2 ($R^2 = 0.16$) were poorly correlated.

Discussion

In this study, it is shown that the voltage-gated sodium channel variants are modulated differently by Fyn, which is a member of the large Src tyrosine kinase family. The effect of Fyn tyrosine kinase has been evaluated by shifts observed in the steady-state inactivation curves of the sodium channel variants. The evidence of this difference in the modulation by Fyn tyrosine kinase is further supported by mutating the glutamine residue (Q1077) in the intracellular loop ($L_{DII-DIII}$) to four different residues (A, P, K and Y). The amino acid sequence of the intracellular loop ($L_{DII-DIII}$) of all the sodium channel isoforms was analyzed and the uniqueness of the cardiac sodium channel to other sodium channel isoforms is documented. Lastly, a search for putative Src tyrosine kinase SH3 and SH2 binding motifs in the amino acid sequence of the cardiac sodium channel was performed.

5.1 Splice variant specificity of Fyn modulation of cardiac sodium channels

Our results indicate that Fyn regulates inactivation of different cardiac sodium channel variants differently. The Q1077Present variant shifted the inactivation curve to more depolarizing potentials (15 mV), while the $\Delta Q1077$ variant shifted the inactivation curve to more hyperpolarizing potentials (9 mV). Studies on the hH1 polymorphic cardiac sodium channel variant shifted the inactivation curve with Fyn to more depolarizing potentials (5 mV) (Ahern et al., 2005). The hH1 sodium channel variant is composed of 2016 amino acids, and it has a glutamine residue at position

1027 compared to Q1077Present, which has an arginine residue at this position. Δ Q1077 (Q1077del) is a splice variant of the Q1077Present variant where an additional glutamine is inserted at position 1077 by a 5'-extension of exon 18 by the trinucleotide CAG (Makielski et al., 2003). The peak I_{Na} of Δ Q1077 is larger than in hH1, and $V_{1/2}$ inactivation appeared at more depolarized potentials (+5 mV) than in the hH1 variant. The activation curve is not shifted in both the Δ Q1077 and hH1 variant (Makielski et al., 2003). This suggests that Q1077 and surrounding residues may play a role in the steady-state inactivation kinetics of the cardiac sodium channel. There is also evidence that the Δ Q1077 variant behaves differently in the background of cardiac mutations causing channelopathies. The loss of function mutation G1406R in the cardiac sodium channel, which causes Brugada syndrome, shows difference in the partial expression defect with Δ Q1077 and Q1077 in the background. These data suggest that there might be a partial trafficking defect, expression defect or gating abnormalities due to loss of function of the G1406R mutation (Tan et al., 2006). Therefore, intracellular trafficking might play an important role in the difference of modulation.

The putative site for CK2 (casein kinase 2) phosphorylation is reported to be (S/T)XX(E/D) (Meggio and Pinna, 2003). This sequence -SKQE- is present in loop L_{DII-DIII} in the Δ Q1077 variant of the Nav1.5 cardiac sodium channel at position 1074 to 1077. Inserting a glutamine residue (Q1077Present) abolishes the putative phosphoacceptor site for CK2 (Kerr et al., 2004).

There is also a study which reports that Δ Q1077 is present in 45% of the Nav1.5 transcript in human hearts, and the Q1077Present variant transcript is present in 25% of the human hearts (Makielski et al., 2003). The hH1 cardiac sodium channel transcript (Accession No. M77235), on which modulation by Fyn was studied (Ahern et al., 2005), is not present (0%) in the human population (Makielski, 2006). Thus, based on these previously published data and our own results on the modulation of inactivation of Δ Q1077 and Q1077Present by Fyn, we speculate that the glutamine residue at position 1077 and the neighbouring residues in loop L_{DII-DIII} could play a role in the difference of modulation of the cardiac sodium channel by Fyn.

5.2 Mutational effects at position 1077

Our results indicate that substitution of aliphatic glutamine at position 1077 to aromatic tyrosine or heterocyclic proline does not have any effect on inactivation kinetics, as it was similar to the Q1077Present variant. Whereas, when aliphatic and polar glutamine was mutated to aliphatic and hydrophobic alanine or to the polar and basic amino acid lysine there was a shift in $V_{1/2}$ inactivation observed compared to Q1077Present. In the case of Q1077A, alanine is a hydrophobic residue and it is ambivalent; that means it can be inside or outside the protein accessible area. This could lead to different hydrophobic interactions between other nearby residues, in turn hindering the inactivation process. In Q1077K, lysine substitution shifted the $V_{1/2}$ inactivation to more hyperpolarizing potentials compared to the Q1077Present variant. The lysine residue has the ability to interact with the solvent readily, which might have played a role in shifting the inactivation curve to more hyperpolarizing potentials. Q1077P and Q1077Y, which are bulky residues, could hinder the folding of loop L_{DII-DIII} which is the ion transport associated region.

Our results on mutation at position 1077 revealed that all the amino acid mutations from glutamine to alanine, lysine, tyrosine and proline caused a shift of the respective inactivation curves to more hyperpolarizing potentials with Fyn as observed in Δ Q1077 (Figure 9) and Nav1.2 (Beacham et al., 2007). However, there is different extent of the hyperpolarizing shift among different mutations. The mutation with alanine caused a very large hyperpolarizing shift by Fyn, and the least hyperpolarizing shift was produced by the positively charged residue lysine. There was also a strong linear correlation ($R^2=0.99$) between the hydrophobicity of the mutated amino acids and the extent of the Fyn-caused hyperpolarizing shift. Highly hydrophobic residues are present in the SH2 domain of the Src tyrosine kinase, and in addition also the peptide binding site of SH3 is composed of a hydrophobic groove. When Q is present at position 1077 there might be hindrance to the hydrophobic interaction between the SH domains and the cardiac sodium channel. There is weak linear correlation observed with molar mass ($R^2=0.76$) or the Van-der-Waals volume (V_w) (volume of the union of overlapping spheres) ($R^2=0.67$), respectively, and the difference in the hyperpolarizing shifts caused by Fyn. V_w plays an important role in the packing and folding of a protein (Richards, 1977). Thus, from our mutational analysis we can

conclude that hydrophobicity, and to a lesser extent, the Van-der-Waals volume (V_w) of the amino acids is vital in the different modulation of the sodium channel by Fyn.

5.3 Uniqueness of cardiac sodium channel intracellular loop L_{DII-DIII}

From the performed sequence analysis it is obvious that the glutamine residue at position 1077 is unique among different sodium channel isoforms (Figure 11). There are three short unique amino acid sequences present in the cardiac sodium channel compared to other sodium channel isoforms. The glutamine at position 1077 is present in one of these unique sequences of the cardiac sodium channel as shown in the Figure 11. Glutamine at position 1076 and 1077 is surrounded by the charged amino acids lysine at position 1075 and glutamic acid at position 1078. In turn, both of these charged amino acids are surrounded by the polar residue serine. Thus, the two glutamine residues are hidden in between the two polar serine residues, which might hinder the flexibility of the sodium channel. This serine residue has the ability to form a hydrogen bond with other polar residues. It has the property of either accepting or donating a hydrogen bond. So, an additional glutamine at position 1077 might hinder the flexibility of the loop L_{DII-DIII}. This might play an anchoring role in facilitating the SH domains of the Src tyrosine kinase to bind to the cardiac sodium channel.

Recent studies on MOG1 (multicopy suppressor of *gsp1*), which is present in the nucleus and the cytosol of cardiac cells (Marfatia et al., 2001), demonstrate that it plays an important role in the regulation of nuclear protein trafficking (Wu et al., 2008). It showed that MOG1 is an important cofactor for optimal expression of Nav1.5 at the cell membrane. When MOG1 and Nav1.5 were co-expressed in HEK293 cells, there was only an increase in the peak I_{Na} with no change in the biophysical characteristics. The interaction site for MOG1 in Nav1.5 is the loop connecting domain II and domain III (L_{DII-DIII}) (Abriel and Kass, 2005; Wu et al., 2008). Ankyrins are intracellular proteins which target and stabilize the membrane proteins including ion channels, transporters, exchangers and cell adhesion molecules in various tissues (Cunha and Mohler, 2006). Ankyrin-G binds to the -VPIAXXSD-motif in loop L_{DII-DIII} of the cardiac sodium channel (Abriel and Kass, 2005; Mohler et al., 2004). SCN5A mutation (pE1053K) in Brugada syndrome patients leads to

disruption of the interaction between Nav1.5 and ankyrin-G (Mohler et al., 2004). Thus, these studies on different intracellular proteins, which modulate the sodium channel, reveal that L_{DII-DIII} is an essential target. From our results on cardiac sodium channel variants, modulation by Fyn suggests that the protein-protein interaction site for the sodium channel and Fyn should be present in L_{DII-DIII}.

5.4 Possible binding sites for the SH2 domain in the cardiac sodium channel

Our results on the possible SH3 domain binding, poly-proline motif show that there are five such motifs in loop L_{DII-DIII}. As shown in Figure 15, the Nav1.2 does not contain any proline-rich motif in L_{DII-DIII}. Thus, this loop L_{DII-DIII} could play an important role in SH3 binding and modulation of the cardiac sodium channel by Fyn. In Nav1.2 the consensus sequence for the potential binding site of the Fyn SH2 domain, after phosphorylation, is present in the N- and C-terminal (Beacham et al., 2007). The sequence for the potential SH2 binding site in Nav1.2 is reported as 66-YGDI-69 in the N-terminal, and 1893-YEPI-1896 in the C-terminal. In the cardiac sodium channel corresponding sites were analysed using the sequence alignment program. There, the C-terminal -YGDI- is replaced by 68-YGNP-, whereas the N-terminal has a corresponding 1988-YEPI-1992 sequence (Beacham et al., 2007). Similarly, in the Nav1.2 channel there is a Y730 which is located in L_{DII-DIII} near the SH3 binding motif (-RVLPILP-), which is required for optimal regulation by Fyn (Beacham et al., 2007). This Y730 residue is conserved in all other sodium channel isoforms except the cardiac sodium channel. In the cardiac sodium channel the corresponding Y730 is replaced by N688 (asparagine). In Nav1.2, it was speculated that the SH2 motifs in the N- and C-terminal and the SH3 motif in L_{DII-DIII} play a role in maintaining a high local concentration of Fyn. But in the cardiac sodium channel there is only one SH2 binding motif in the C-terminal and several putative SH3 binding motifs in L_{DII-DIII}. Earlier studies show that the Fyn SH2 domain binds to the -pYQQI- motif of the target protein (Songyang et al., 1993). However, there are some other SH2 domains which bind to different patterns. The growth factor receptor-bound protein 2 (Grb2) SH2 domain binds to the -pYXNX- motif of the target protein

(Rahuel et al., 1996), whereas the SH2 domain of the growth factor phospholipase C- γ 1 (PLC- γ 1) binds to hydrophobic residues that follow pTyr (Ji et al., 1999). Thus, Fyn could also bind to different SH2 motifs in the cardiac sodium channel other than the putative SH2 binding motif in Nav1.2. Putative SH2 binding motifs are situated in the C-terminal of the cardiac sodium channel, because there are motifs (1811-YDSV-1814 and 1977-YSVL-1980) apart from the conserved -YEPI-, which have a hydrophobic residue at the pY+3 residue. The pY+3 residue is tightly bound to the hydrophobic pocket, and this pocket is critical for the peptide specificity (Brändén and Tooze, 1999). Thus, valine in the 1811-YDSV-1814 motif and leucine in the 1977-YSVL-1980 motif might form a tight hydrophobic interaction with the hydrophobic pocket of the SH2 domain. Mutational studies on these motifs will give an insight view on the SH2 binding pockets of the cardiac sodium channel.

5.5 Putative SH3 domain binding sites in sodium channels

The SH3 domain consists of a five-stranded up-and-down antiparallel β sheet. The peptide binding site is made up of a hydrophobic groove (Brändén and Tooze, 1999). The SH3 domain of the Src tyrosine kinase binds to the target peptides which have proline-rich motifs (Lim, 1996; Yu et al., 1994). When the peptide binds to the SH3 domain, proline-rich segments adopt a left-handed poly-proline type II helix with three amino acids per turn. There are three ridges in the poly-proline helix of which two contact the SH3 domain of the protein tyrosine kinase. The SH3 domain of the Src tyrosine kinase contains a group of acidic amino acids and less hydrophobic amino acid residues (Brändén and Tooze, 1999). All known SH3 target proteins carry a consensus sequence -PXXP-. When v-src is expressed with the human voltage gated potassium channel subtype (hKv1.5) (Holmes et al., 1996b), it is phosphorylated. It was found that hKv1.5 contains two SH3 binding motifs (RPLPPLP) between amino acid residues 65 and 82 of the channel protein (Holmes et al., 1996b; Tamkun et al., 1991).

In Nav1.2 the SH3 binding motif for Fyn is present in L_{DII-DII} (Figure 17) (Beacham et al., 2007). Insertion of a glycine residue in this motif (-PTLP- to -PTGLP-) nullifies the modulation of Nav1.2 by Fyn (Beacham et al., 2007). In Figure 17, the other

putative SH3 binding motifs are also shown; there is no proline-rich motif present in L_{DII-DIII}, but two putative SH3 binding proline-rich motifs are present in the N-terminal region. In the cardiac sodium channel there are five -PXXP- motifs in L_{DII-DIII}. The cardiac sodium channel has one -PXXP- motif in the loop L_{D1-DII}, which is different from that of Nav1.2. Two of the -PXXP- motifs in L_{DII-DIII} of the cardiac sodium channel are present in the unique sequence found when aligned with other sodium channel isoforms (Figure 16). This suggests that the putative SH3 domain binding motif of the cardiac sodium channel is present in loop L_{DII-DIII}. These studies reveal that the SH3 domain binding domain of the Nav1.2 and Nav1.5 is different. Thus, this could contribute to the difference observed in the modulation by Fyn tyrosine kinase.

Cardiac sodium channel sequence analysis reveals five putative SH3 binding domains in loop L_{DII-DIII} (Figure 16), but there is no proline-rich motif in L_{DII-DIII} of the Nav1.2 sodium channel (Figure 17). Whereas, for the Nav1.2 channel it is proven that there is one SH3 binding motif present in the L_{D1-DII}. However, the same motif is not present in Nav1.5. Inserting a residue in the SH3 motif of Nav1.2 alters the modulation of inactivation kinetics by Fyn. According to suggested proline-rich motifs binding the SH3 domain of Src tyrosine kinases (Yu et al., 1994), in the cardiac sodium channel out of five putative motifs, the sequences 986-RQRPQKP-992, 1120-KAEPQAP-1126 and 1008-PYSPPPP-1014 in L_{DII-DIII} are most likely to form the SH3 binding site for Fyn kinase (Figure 16). The first two putative motifs have a charged amino acid residue (R and K) two residues (any amino acid) before the first proline of the proline-rich motif which is responsible for the SH3 domain binding groove (Brändén and Tooze, 1999; Yu et al., 1994). The third, above mentioned, proline rich motif contains four continuous proline residues making it an ideal candidate for SH3 domain binding. Apart from the previously mentioned proline-rich motifs there are two other SH3 binding -PXXP- motifs present in L_{DII-DIII}. The two proline-rich motifs in L_{DII-DIII} are 1039-PGDPEP-1044 and 1086-PEAPP-1090; these can also form the SH3 domain binding motif, but it lacks the charged R/K residue, two residues before the first proline of the -PXXP- motif. But the 1086-PEAPP-1090 is in very close proximity to the glutamine residue at position 1077. Hence, the consideration of this motif for SH3 binding should not be left out. Apart from L_{DII-DIII}, there is one weak SH3 binding, proline-rich motif (PLAP) in loop L_{D1-DII} (Figure 16). Insertion mutation

or removing the entire motifs will give an insight view on the SH3 binding site of the cardiac sodium channel.

N-Terminal
1 MANFILLPRGT SSFRRTFTRES LAAIEKRMAE KQARGSTTLQ E SREGLPEEE APRPQLDLQA SKKLPDIYGN PPQELIGEPL EDLDPFYSTQ KTFIVLNKGKTIERFSATNA LYVLSPFHPI RRAAVKILVH SLFNMLIMCT I LTNCVFMAQ HDPPWTKYV EYTFTAITYF ESLVKILARG FCLHAFTFLR D PWNWLDFSV I I MAYTTEFV DLGNVSALRT FRVLRALAKTI SVISGLKTIV GALIQSVKKL ADVMVLTVFC LSVFALIGLQ LFMGNLRHKC VRNFTALNGT NGSVEADGLV WESLDLYLSD PENYLLKNGT SDVILLCGNSS DAGTCPEGYR CLKAGENPDH GYTSFDSFAW AFLALFRIMT QDCWERLYQQ TLRSAGKIYM I FFMLVI FLG SFYLVNLILA VVAMAYEEQN QATIAETEEK EKRFQEAMEM LKKEHEALTI RGVDTVSRSS LEMSPLAPVN SHERRSKRRK RMSSGTEECG EDRLPKSDSE DGPRAMNHLS LTRGLSRTSM KPRSSRGSIF TFRRRDLGSE ADFADDENST AGESESHHTS LLVPWPRLRT SAQGQPSPGT SAPGHALHGK KNSTVDCNGV VSILLGAGDPE ATSPGSHLLR PVMLEHPPDT TTPSEEPGGP QMLTSQAPCV DGFEPEPGARQ RALSASVSLT SALEEELESR HKCPCWNRL AQRVYLIWECC PLWMSIKQGV KLVVMDPFTD LTITMCIVLN TL FMALEHYN MTSEFEEMLQ VGNLVFTGIF TAEATFKIIA LDYYYFQQG WNIFDSIIVI LSLMELGLSR MSNLSVLRSF RLLRVFKLAK SWPTLNTLIK IIGNSVGALG NLTVLIAIV FIFAVVGMQL FGKNYSELRD SDSGLLPRWH MMDFFHAFLI I FRILCGEWI ETMWDCMEVS GQSICLLVFL LVMVIGNLUV LNLFALLLS SFSADNLTAP DEDREMNNIQ LALARIQRGL RFVKRTTWDF CCGLLRQRPO KPAALAAQGQ LPSCIATPYS PPPPETEKVP PTRKETRFEE GEQPGQGTPG DPE PVCVPIA VAESTDDEDQE EDEENS LGTE EESSKQQESQ PVSGGPEAPP DSRTWSQVSA TASSEEAASA SQADWRQWK AEPQAPGCGE TPEDSCSEGS TADMTNTAEL LEQIPDLGQD VKDPEDCFTE GCVRRCPCCA VDTTQAPGKV WWRLRKTCYH IVEHSWFETF IIFMILLSSG ALAFEDIYLE ERKTIKVLLE YADKMFTYVF VLEMILLKWVA YGFKKYFTNA WCWLDFLIVD VS LVS LVANT LGFAEMGPIK SLRTLRLALRP LRALSRFEGM RVVVNALVGA IPSIMNVLLV CLIFWLIFI MGVLNFAGKF GRCINQTEGD LPLNYTIVNN KSQCESLNLT GELYWTKVKV NFDNVGAGYL ALLQVATFKG WMDIMYAAVD SRGYEEQFW EYNLYMYIYF VIFIIFGSFF TLNLFIGVII DNFnQQKKL GGQDI FMTEE QKKYYNAMKK LGSKKPQKPI PRPLNKYQGF IFDIVTKQAF DVTIMFLICL NMVTMMVETD DQSPEKINIL AKINLLFVAI FTGECIVKLA ALRHYYFTNS WNI FDFVVVI LSIVGTVLSD IIQKYFFSPT LFRVIRLARI GRILRLIRGA KGIRTLFFAL MMSLPALFNI GLLLFLVMFI YSIFGMANFA YVKWEAGIDD MFNFQTFANS MLCLFQITTS AGWDGLLSPI LNTGPPYCDP TLPNSNGSRG DCGSPAVGIL FFTTYIIISF LIVVNMYIAI ILEENFSVATE ESTEPLSED FDMFYEIWEK FDPEATQFIE YSVLSDFADA LSEPLRIAKP NQISLNLMDL PMVSGDRIH MDILFAFTKR VLGE SGEMDA LKIQMEEKFM AANPSKISYE PITTTLRRKH EEVSAMVIQR AFRRHLLQRS LKHASFLLFRQ QAGSGLSEED APEREGLIAY VMSENFSRPL GPPSSSSISS TSEPPSYDSV TRATSDNLQV RGSDYSHSED LADFPSPSPDR DRES IV 2016
Domain I
L_{DII-DIII}
Domain II
L_{DIII-DIV}
Domain III
Domain IV
C-Terminal

Figure 16: Amino acid sequence of the Q1077 (Accession Number AC137587) cardiac sodium channel.

The cardiac sodium channel numbering and the proposed structure (George et al., 1992) forms the base of different structural parts. The membrane embedded parts and the extracellular loops of domains I-IV are not highlighted. The intracellular parts of the sodium channel are highlighted in grey. The unique sequences in L_{DII-DIII} are highlighted in red. The possible SH3 domain binding motifs (proline-rich) are highlighted in yellow. The intracellular tyrosine residues are marked in green.

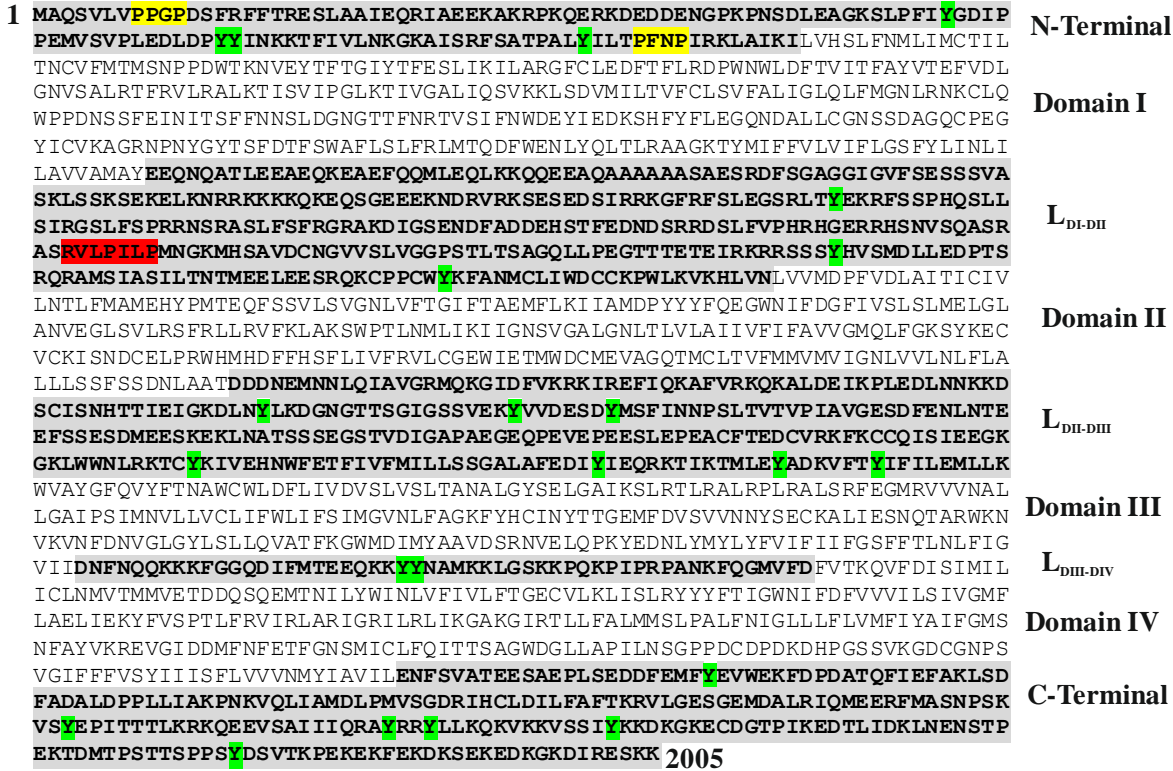


Figure 17: Amino acid sequence of the Nav1.2 (Accession Number NP_001035232) neuronal sodium channel.

The membrane embedded parts and the extracellular loops of domains I-IV are not highlighted. The intracellular parts of the sodium channel are highlighted in grey. The SH3 binding site in Nav1.2 loop L_{DI-DII} is highlighted in red. The other possible SH3 domain binding motifs (proline-rich) are highlighted in yellow. The tyrosine residues are marked in green.

5.6 Importance of the tyrosine residues in sodium channel for Fyn tyrosine kinase

In both Nav1.5 and Nav1.2, the tyrosine residue in the inactivation loop is essential for the modulation of the sodium channel by Fyn (Ahern et al., 2005; Beacham et al., 2007). In the neuronal sodium channel isoform Nav1.2, tyrosine residues Y1497 and Y1498 in the inactivation loop (L_{DIII-DIV}) play an important role in the regulation by Fyn, whereas in the cardiac sodium channel Nav1.5, tyrosine at position Y1495 in L_{DIII-DIV} is the residue responsible for the modulation. When Y1495 is substituted to phenylalanine (Y1495F), the shift caused by Fyn is abolished in cardiac sodium channel (hH1). Mutation in Nav1.2 tyrosine residue Y1498F annuls

Discussion

the effect of Fyn. Our analysis on L_{DIII-DIV} of the sodium channel isoforms reveal that 95% of the amino acids were conserved in L_{DIII-DIV}. The tyrosine residue, which is present in L_{DIII-DIV}, is conserved in all sodium channel isoforms (Fig. 14 and 15, Appendix alignment). It plays an important role in the modulation of sodium channels by Fyn. Although the tyrosine residue is conserved in the inactivation loop, Fyn modulates the sodium channel isoforms differently.

Nav1.1 is not modulated by Fyn (Beacham et al., 2007), whereas in Nav1.2 Fyn shifts the inactivation curve to more hyperpolarizing potentials (Beacham et al., 2007). In hH1 (Ahern et al., 2005) and Q1077Present (Figure 9 and Table 9) cardiac sodium channel variants, Fyn shifts the inactivation curves to more depolarizing potentials. In the ΔQ1077 (Figure 9 and Table 9) cardiac sodium channel variant and the Q1077A, Q1077Y, Q1077P and Q1077K mutants, the inactivation curves are shifted to more hyperpolarizing potentials. Thus, although all sodium channels have a conserved tyrosine residue in L_{DIII-DIV}, which is responsible for the modulation, different sodium channels are modulated differently by Fyn.

In loop L_{DII-DIII}, there are two tyrosine residues, one at the distal end and one embedded in the proline-rich motif -PYSPPPP-. In Nav1.2, there is Y730 in L_{DII-DIII}, which is in close proximity to the SH3 binding domain that is involved in the regulation of Fyn (Beacham et al., 2007). In the cardiac sodium channel five putative SH3 binding sites are present in L_{DII-DIII}. The tyrosine residues at position 1008 and 1118 in L_{DII-DIII} could contribute to the regulation of Fyn tyrosine kinase. Y1008 is unique in Nav1.5 compared to other sodium channel isoforms. The distal end tyrosine residue Y1118 in L_{DII-DIII} is conserved in Nav1.2, Nav1.7, Nav1.3 and cardiac sodium channel Nav1.5. Hence, these two tyrosine residues in L_{DII-DIII} of the cardiac sodium channel might also be involved in the regulation of the sodium channel by Fyn.

Conclusion

Results from the thesis proclaim that Q1077Present and Δ Q1077 encoding for cardiac sodium channel (Nav1.5) variants are differently regulated by Fyn tyrosine kinase. In Q1077Present, Fyn shifted the inactivation curve to more depolarizing potentials, whereas in Δ Q1077 it was shifted to more hyperpolarizing potentials. Mutational analysis at position 1077 revealed the role of glutamine at this position, which is important for the modulation by Fyn. Fyn shifted the inactivation curves of all mutants (Q1077A, Q1077K, Q1077P and Q1077Y) to more hyperpolarizing potentials. Hydrophobicity of the substituted amino acid is one of the prominent factors in the extent of the shift. Sequence alignment showed that the region around L_{DII-DIII} is unique and the glutamine residue at position 1077 is present in one of the unique segments of L_{DII-DIII}. Results from this thesis speculate that the putative SH3 binding site should be situated in L_{DII-DIII}, and the SH2 binding site in the C-terminal. These data will be pertinent in understanding the role of Q1077 and its surrounding amino acids, which are present in the transport associated region (L_{DII-DIII}). Results show that L_{DII-DIII} of the cardiac sodium channel is pivotal in Fyn binding and regulation of function.

Abbreviations

AF	Atrial Fibrillation
BrS	Brugada syndrome
Ca _v	Voltage-gated calcium channel
CK2	Casein Kinase 2
CNS	Central Nervous System
DI-DIV	Voltage-gated sodium channel domain (I-IV)
DRG	Dorsal Root Ganglion
GoF	Gain-of-function
hNa _v	Human voltage gated sodium channel
I _{Na}	Sodium Current
K _v	Voltage gated potassium channel
LB	Lysogeny broth
LQT	Long QT syndrome
LoF	Loss-of-function
mRNA	Messenger ribonucleic acid
Na ⁺	Sodium ion
Na _v	Voltage gated sodium channel
Na _v 1.5 _X	cardiac sodium channel splice variants
PTK	Protein tyrosine kinase
rNa _v	Rat voltage gated sodium channel
S1-S6	Trans-membrane helices (1-6)
SA	Sinoatrial
SCNXA	Voltage gated sodium channel (X- Subtype)
SH2	Src Homology 2
SH3	Src Homology 3
SIDS	Sudden infant death syndrome
SOC	Super optimal broth (modified)
Src tyrosine kinase	Sarcoma tyrosine kinase
SSS	Sick Sinus Syndrome
TTX	Tetrodotoxin
WT	Wild type

References

- Abe, M., Kurihara, T., Han, W., Shinomiya, K., and Tanabe, T., 2002, Changes in expression of voltage-dependent ion channel subunits in dorsal root ganglia of rats with radicular injury and pain, *Spine (Phila Pa 1976)* **27**(14):1517-24; discussion 1525.
- Abriel, H., and Kass, R. S., 2005, Regulation of the voltage-gated cardiac sodium channel Nav1.5 by interacting proteins, *Trends Cardiovasc Med* **15**(1):35-40.
- Agnew, W. S., Levinson, S. R., Brabson, J. S., and Raftery, M. A., 1978, Purification of the tetrodotoxin-binding component associated with the voltage-sensitive sodium channel from Electrophorus electricus electroplax membranes, *Proc Natl Acad Sci U S A* **75**(6):2606-10.
- Ahern, C. A., Zhang, J. F., Wookalis, M. J., and Horn, R., 2005, Modulation of the cardiac sodium channel NaV1.5 by Fyn, a Src family tyrosine kinase, *Circ Res* **96**(9):991-8.
- Ahn, M., Beacham, D., Westenbroek, R. E., Scheuer, T., and Catterall, W. A., 2007, Regulation of Na(v)1.2 channels by brain-derived neurotrophic factor, TrkB, and associated Fyn kinase, *J Neurosci* **27**(43):11533-42.
- Beacham, D., Ahn, M., Catterall, W. A., and Scheuer, T., 2007, Sites and molecular mechanisms of modulation of Na(v)1.2 channels by Fyn tyrosine kinase, *J Neurosci* **27**(43):11543-51.
- Bendahhou, S., Cummins, T. R., Hahn, A. F., Langlois, S., Waxman, S. G., and Ptacek, L. J., 2000, A double mutation in families with periodic paralysis defines new aspects of sodium channel slow inactivation, *J Clin Invest* **106**(3):431-8.
- Bendahhou, S., Cummins, T. R., Tawil, R., Waxman, S. G., and Ptacek, L. J., 1999, Activation and inactivation of the voltage-gated sodium channel: role of segment S5 revealed by a novel hyperkalaemic periodic paralysis mutation, *J Neurosci* **19**(12):4762-71.
- Benito, B., Brugada, J., Brugada, R., and Brugada, P., 2009, Brugada syndrome, *Rev Esp Cardiol* **62**(11):1297-315.
- Bennett, P. B., Yazawa, K., Makita, N., and George, A. L., Jr., 1995, Molecular mechanism for an inherited cardiac arrhythmia, *Nature* **376**(6542):683-5.
- Benson, D. W., Wang, D. W., Dyment, M., Knilans, T. K., Fish, F. A., Strieper, M. J., Rhodes, T. H., and George, A. L., Jr., 2003, Congenital sick sinus syndrome caused by recessive mutations in the cardiac sodium channel gene (SCN5A), *J Clin Invest* **112**(7):1019-28.
- Blechschmidt, S., Haufe, V., Benndorf, K., and Zimmer, T., 2008, Voltage-gated Na⁺ channel transcript patterns in the mammalian heart are species-dependent, *Prog Biophys Mol Biol* **98**(2-3):309-18.
- Boggon, T. J., and Eck, M. J., 2004, Structure and regulation of Src family kinases, *Oncogene* **23**(48):7918-27.
- Bolen, J. B., and Brugge, J. S., 1997, Leukocyte protein tyrosine kinases: potential targets for drug discovery, *Annu Rev Immunol* **15**:371-404.

References

- Boucher, T. J., Okuse, K., Bennett, D. L., Munson, J. B., Wood, J. N., and McMahon, S. B., 2000, Potent analgesic effects of GDNF in neuropathic pain states, *Science* **290**(5489):124-7.
- Brackenbury, W. J., Chioni, A. M., Diss, J. K., and Djamgoz, M. B., 2007, The neonatal splice variant of Nav1.5 potentiates in vitro invasive behaviour of MDA-MB-231 human breast cancer cells, *Breast Cancer Res Treat* **101**(2):149-60.
- Brackenbury, W. J., Djamgoz, M. B., and Isom, L. L., 2008, An emerging role for voltage-gated Na⁺ channels in cellular migration: regulation of central nervous system development and potentiation of invasive cancers, *Neuroscientist* **14**(6):571-83.
- Brändén, C.-I., and Tooze, J., 1999, Introduction to protein structure, Garland Pub., New York, pp. xiv, 410 p.
- Brown, M. T., and Cooper, J. A., 1996, Regulation, substrates and functions of src, *Biochim Biophys Acta* **1287**(2-3):121-49.
- Brugada, P., Benito, B., Brugada, R., and Brugada, J., 2009, Brugada syndrome: update 2009, *Hellenic J Cardiol* **50**(5):352-72.
- Brugge, J. S., and Erikson, R. L., 1977, Identification of a transformation-specific antigen induced by an avian sarcoma virus, *Nature* **269**(5626):346-8.
- Bulman, D. E., Scoggan, K. A., van Oene, M. D., Nicolle, M. W., Hahn, A. F., Tollar, L. L., and Ebers, G. C., 1999, A novel sodium channel mutation in a family with hypokalemic periodic paralysis, *Neurology* **53**(9):1932-6.
- Camacho, J. A., Hensellek, S., Rougier, J. S., Blechschmidt, S., Abriel, H., Benndorf, K., and Zimmer, T., 2006, Modulation of Nav1.5 channel function by an alternatively spliced sequence in the DII/DIII linker region, *J Biol Chem* **281**(14):9498-506.
- Cance, W. G., Craven, R. J., Bergman, M., Xu, L., Alitalo, K., and Liu, E. T., 1994, Rak, a novel nuclear tyrosine kinase expressed in epithelial cells, *Cell Growth Differ* **5**(12):1347-55.
- Cantrell, A. R., and Catterall, W. A., 2001, Neuromodulation of Na⁺ channels: an unexpected form of cellular plasticity, *Nat Rev Neurosci* **2**(6):397-407.
- Carr, D. B., Day, M., Cantrell, A. R., Held, J., Scheuer, T., Catterall, W. A., and Surmeier, D. J., 2003, Transmitter modulation of slow, activity-dependent alterations in sodium channel availability endows neurons with a novel form of cellular plasticity, *Neuron* **39**(5):793-806.
- Cascio, W. E., 2001, Myocardial ischemia: what factors determine arrhythmogenesis?, *J Cardiovasc Electrophysiol* **12**(6):726-9.
- Catterall, W. A., 1991, Structure and function of voltage-gated sodium and calcium channels, *Curr Opin Neurobiol* **1**(1):5-13.
- Catterall, W. A., 2000, From ionic currents to molecular mechanisms: the structure and function of voltage-gated sodium channels, *Neuron* **26**(1):13-25.
- Catterall, W. A., Goldin, A. L., and Waxman, S. G., 2005, International Union of Pharmacology. XLVII. Nomenclature and structure-function relationships of voltage-gated sodium channels, *Pharmacol Rev* **57**(4):397-409.
- Chen, Q., Kirsch, G. E., Zhang, D., Brugada, R., Brugada, J., Brugada, P., Potenza, D., Moya, A., Borggrefe, M., Breithardt, G., Ortiz-Lopez, R., Wang, Z., Antzelevitch, C., O'Brien, R. E., Schulze-Bahr, E., Keating, M. T., Towbin, J. A., and Wang, Q., 1998, Genetic basis and molecular mechanism for idiopathic ventricular fibrillation, *Nature* **392**(6673):293-6.

- Chen, Y., Yu, F. H., Surmeier, D. J., Scheuer, T., and Catterall, W. A., 2006, Neuromodulation of Na⁺ channel slow inactivation via cAMP-dependent protein kinase and protein kinase C, *Neuron* **49**(3):409-20.
- Chen, Y. H., Dale, T. J., Romanos, M. A., Whitaker, W. R., Xie, X. M., and Clare, J. J., 2000, Cloning, distribution and functional analysis of the type III sodium channel from human brain, *Eur J Neurosci* **12**(12):4281-9.
- Choi, J. S., Cheng, X., Foster, E., Leffler, A., Tyrrell, L., Te Morsche, R. H., Eastman, E. M., Jansen, H. J., Huehne, K., Nau, C., Dib-Hajj, S. D., Drenth, J. P., and Waxman, S. G., 2010, Alternative splicing may contribute to time-dependent manifestation of inherited erythromelalgia, *Brain* **133**(Pt 6):1823-35.
- Cocquet, J., Chong, A., Zhang, G., and Veitia, R. A., 2006, Reverse transcriptase template switching and false alternative transcripts, *Genomics* **88**(1):127-31.
- Cohen, G. B., Ren, R., and Baltimore, D., 1995, Modular binding domains in signal transduction proteins, *Cell* **80**(2):237-48.
- Collett, M. S., and Erikson, R. L., 1978, Protein kinase activity associated with the avian sarcoma virus src gene product, *Proc Natl Acad Sci U S A* **75**(4):2021-4.
- Coward, K., Plumpton, C., Facer, P., Birch, R., Carlstedt, T., Tate, S., Bountra, C., and Anand, P., 2000, Immunolocalization of SNS/PN3 and NaN/SNS2 sodium channels in human pain states, *Pain* **85**(1-2):41-50.
- Cox, J. J., Reimann, F., Nicholas, A. K., Thornton, G., Roberts, E., Springell, K., Karbani, G., Jafri, H., Mannan, J., Raashid, Y., Al-Gazali, L., Hamamy, H., Valente, E. M., Gorman, S., Williams, R., McHale, D. P., Wood, J. N., Gribble, F. M., and Woods, C. G., 2006, An SCN9A channelopathy causes congenital inability to experience pain, *Nature* **444**(7121):894-8.
- Cummins, T. R., and Waxman, S. G., 1997, Downregulation of tetrodotoxin-resistant sodium currents and upregulation of a rapidly repriming tetrodotoxin-sensitive sodium current in small spinal sensory neurons after nerve injury, *J Neurosci* **17**(10):3503-14.
- Cunha, S. R., and Mohler, P. J., 2006, Cardiac ankyrins: Essential components for development and maintenance of excitable membrane domains in heart, *Cardiovasc Res* **71**(1):22-9.
- Davies, N. P., Eunson, L. H., Samuel, M., and Hanna, M. G., 2001, Sodium channel gene mutations in hypokalemic periodic paralysis: an uncommon cause in the UK, *Neurology* **57**(7):1323-5.
- Denac, H., Mevissen, M., and Scholtysik, G., 2000, Structure, function and pharmacology of voltage-gated sodium channels, *Naunyn Schmiedebergs Arch Pharmacol* **362**(6):453-79.
- Dib-Hajj, S. D., Tyrrell, L., Black, J. A., and Waxman, S. G., 1998, NaN, a novel voltage-gated Na channel, is expressed preferentially in peripheral sensory neurons and down-regulated after axotomy, *Proc Natl Acad Sci U S A* **95**(15):8963-8.
- Drenth, J. P., te Morsche, R. H., Guillet, G., Taieb, A., Kirby, R. L., and Jansen, J. B., 2005, SCN9A mutations define primary erythermalgia as a neuropathic disorder of voltage gated sodium channels, *J Invest Dermatol* **124**(6):1333-8.
- Ellinor, P. T., Nam, E. G., Shea, M. A., Milan, D. J., Ruskin, J. N., and MacRae, C. A., 2008, Cardiac sodium channel mutation in atrial fibrillation, *Heart Rhythm* **5**(1):99-105.
- Eriksson, J., Jablonski, A., Persson, A. K., Hao, J. X., Kouya, P. F., Wiesenfeld-Hallin, Z., Xu, X. J., and Fried, K., 2005, Behavioral changes and trigeminal

- ganglion sodium channel regulation in an orofacial neuropathic pain model, *Pain* **119**(1-3):82-94.
- Fahmi, A. I., Patel, M., Stevens, E. B., Fowden, A. L., John, J. E., 3rd, Lee, K., Pinnock, R., Morgan, K., Jackson, A. P., and Vandenberg, J. I., 2001, The sodium channel beta-subunit SCN3b modulates the kinetics of SCN5a and is expressed heterogeneously in sheep heart, *J Physiol* **537**(Pt 3):693-700.
- Feng, S., Chen, J. K., Yu, H., Simon, J. A., and Schreiber, S. L., 1994, Two binding orientations for peptides to the Src SH3 domain: development of a general model for SH3-ligand interactions, *Science* **266**(5188):1241-7.
- Fertleman, C. R., Baker, M. D., Parker, K. A., Moffatt, S., Elmslie, F. V., Abrahamsen, B., Ostman, J., Klugbauer, N., Wood, J. N., Gardiner, R. M., and Rees, M., 2006, SCN9A mutations in paroxysmal extreme pain disorder: allelic variants underlie distinct channel defects and phenotypes, *Neuron* **52**(5):767-74.
- Finn, R. D., Mistry, J., Tate, J., Coggill, P., Heger, A., Pollington, J. E., Gavin, O. L., Gunasekaran, P., Ceric, G., Forslund, K., Holm, L., Sonnhammer, E. L., Eddy, S. R., and Bateman, A., 2010, The Pfam protein families database, *Nucleic Acids Res* **38**(Database issue):D211-22.
- Fraser, S. P., Diss, J. K., Chioni, A. M., Mycielska, M. E., Pan, H., Yamaci, R. F., Pani, F., Siwy, Z., Krasowska, M., Grzywna, Z., Brackenbury, W. J., Theodorou, D., Koyuturk, M., Kaya, H., Battaloglu, E., De Bella, M. T., Slade, M. J., Tolhurst, R., Palmieri, C., Jiang, J., Latchman, D. S., Coombes, R. C., and Djamgoz, M. B., 2005, Voltage-gated sodium channel expression and potentiation of human breast cancer metastasis, *Clin Cancer Res* **11**(15):5381-9.
- French, R. J., and Horn, R., 1983, Sodium channel gating: models, mimics, and modifiers, *Annu Rev Biophys Bioeng* **12**:319-56.
- Gabashvili, I. S., Sokolowski, B. H., Morton, C. C., and Giersch, A. B., 2007, Ion channel gene expression in the inner ear, *J Assoc Res Otolaryngol* **8**(3):305-28.
- Gazina, E. V., Richards, K. L., Mokhtar, M. B., Thomas, E. A., Reid, C. A., and Petrou, S., 2010, Differential expression of exon 5 splice variants of sodium channel alpha subunit mRNAs in the developing mouse brain, *Neuroscience* **166**(1):195-200.
- Gellens, M. E., George, A. L., Jr., Chen, L. Q., Chahine, M., Horn, R., Barchi, R. L., and Kallen, R. G., 1992, Primary structure and functional expression of the human cardiac tetrodotoxin-insensitive voltage-dependent sodium channel, *Proc Natl Acad Sci U S A* **89**(2):554-8.
- George, A. L., Jr., 2005, Inherited disorders of voltage-gated sodium channels, *J Clin Invest* **115**(8):1990-9.
- George, A. L., Jr., Knittle, T. J., and Tamkun, M. M., 1992, Molecular cloning of an atypical voltage-gated sodium channel expressed in human heart and uterus: evidence for a distinct gene family, *Proc Natl Acad Sci U S A* **89**(11):4893-7.
- Glass, C. K., Rosenfeld, M. G., Rose, D. W., Kurokawa, R., Kamei, Y., Xu, L., Torchia, J., Ogliastro, M. H., and Westin, S., 1997, Mechanisms of transcriptional activation by retinoic acid receptors, *Biochem Soc Trans* **25**(2):602-5.
- Goldenberg, I., and Moss, A. J., 2008, Long QT syndrome, *J Am Coll Cardiol* **51**(24):2291-300.

- Goldin, A. L., 2001, Resurgence of sodium channel research, *Annu Rev Physiol* **63**:871-94.
- Grant, A. O., Starmer, C. F., and Strauss, H. C., 1984, Antiarrhythmic drug action. Blockade of the inward sodium current, *Circ Res* **55**(4):427-39.
- Han, C., Rush, A. M., Dib-Hajj, S. D., Li, S., Xu, Z., Wang, Y., Tyrrell, L., Wang, X., Yang, Y., and Waxman, S. G., 2006, Sporadic onset of erythermalgia: a gain-of-function mutation in Nav1.7, *Ann Neurol* **59**(3):553-8.
- Harrison, S. C., 2003, Variation on an Src-like theme, *Cell* **112**(6):737-40.
- Harty, T. P., Dib-Hajj, S. D., Tyrrell, L., Blackman, R., Hisama, F. M., Rose, J. B., and Waxman, S. G., 2006, Na(V)1.7 mutant A863P in erythromelalgia: effects of altered activation and steady-state inactivation on excitability of nociceptive dorsal root ganglion neurons, *J Neurosci* **26**(48):12566-75.
- Heine, R., Pika, U., and Lehmann-Horn, F., 1993, A novel SCN4A mutation causing myotonia aggravated by cold and potassium, *Hum Mol Genet* **2**(9):1349-53.
- Heinemann, S. H., Terlau, H., Stuhmer, W., Imoto, K., and Numa, S., 1992, Calcium channel characteristics conferred on the sodium channel by single mutations, *Nature* **356**(6368):441-3.
- Herlenius, E., Heron, S. E., Grinton, B. E., Keay, D., Scheffer, I. E., Mulley, J. C., and Berkovic, S. F., 2007, SCN2A mutations and benign familial neonatal-infantile seizures: the phenotypic spectrum, *Epilepsia* **48**(6):1138-42.
- Heron, S. E., Hernandez, M., Edwards, C., Edkins, E., Jansen, F. E., Scheffer, I. E., Berkovic, S. F., and Mulley, J. C., 2009, Neonatal seizures and Long QT Syndrome: A cardiocerebral channelopathy?, *Epilepsia*.
- Heron, S. E., Scheffer, I. E., Berkovic, S. F., Dibbens, L. M., and Mulley, J. C., 2007, Channelopathies in idiopathic epilepsy, *Neurotherapeutics* **4**(2):295-304.
- Hilborn, M. D., Vaillancourt, R. R., and Rane, S. G., 1998, Growth factor receptor tyrosine kinases acutely regulate neuronal sodium channels through the src signaling pathway, *J Neurosci* **18**(2):590-600.
- Hodgkin, A. L., and Huxley, A. F., 1952a, Currents carried by sodium and potassium ions through the membrane of the giant axon of Loligo, *J Physiol* **116**(4):449-72.
- Hodgkin, A. L., and Huxley, A. F., 1952b, A quantitative description of membrane current and its application to conduction and excitation in nerve, *J Physiol* **117**(4):500-44.
- Hoffman, B. F., and Cranefield, P. F., 1960, Electrophysiology of the heart [by] Brian F. Hoffman [and] Paul F. Cranefield. With a foreword by Franklin D. Johnston, McGraw-Hill, New York, pp. 323p.
- Holmes, T. C., Fadool, D. A., and Levitan, I. B., 1996a, Tyrosine phosphorylation of the Kv1.3 potassium channel, *J Neurosci* **16**(5):1581-90.
- Holmes, T. C., Fadool, D. A., Ren, R., and Levitan, I. B., 1996b, Association of Src tyrosine kinase with a human potassium channel mediated by SH3 domain, *Science* **274**(5295):2089-91.
- Hondeghem, L. M., and Katzung, B. G., 1977, Time- and voltage-dependent interactions of antiarrhythmic drugs with cardiac sodium channels, *Biochim Biophys Acta* **472**(3-4):373-98.
- Hou, X. Y., Zhang, G. Y., Yan, J. Z., and Liu, Y., 2003, Increased tyrosine phosphorylation of alpha(1C) subunits of L-type voltage-gated calcium channels and interactions among Src/Fyn, PSD-95 and alpha(1C) in rat hippocampus after transient brain ischemia, *Brain Res* **979**(1-2):43-50.

References

- Hubbard, S. R., Wei, L., Ellis, L., and Hendrickson, W. A., 1994, Crystal structure of the tyrosine kinase domain of the human insulin receptor, *Nature* **372**(6508):746-54.
- Imamoto, A., and Soriano, P., 1993, Disruption of the csk gene, encoding a negative regulator of Src family tyrosine kinases, leads to neural tube defects and embryonic lethality in mice, *Cell* **73**(6):1117-24.
- Isom, L. L., 2001, Sodium channel beta subunits: anything but auxiliary, *Neuroscientist* **7**(1):42-54.
- Isom, L. L., De Jongh, K. S., and Catterall, W. A., 1994, Auxiliary subunits of voltage-gated ion channels, *Neuron* **12**(6):1183-94.
- Isom, L. L., De Jongh, K. S., Patton, D. E., Reber, B. F., Offord, J., Charbonneau, H., Walsh, K., Goldin, A. L., and Catterall, W. A., 1992, Primary structure and functional expression of the beta 1 subunit of the rat brain sodium channel, *Science* **256**(5058):839-42.
- Isom, L. L., Ragsdale, D. S., De Jongh, K. S., Westenbroek, R. E., Reber, B. F., Scheuer, T., and Catterall, W. A., 1995, Structure and function of the beta 2 subunit of brain sodium channels, a transmembrane glycoprotein with a CAM motif, *Cell* **83**(3):433-42.
- Ji, Q. S., Chattopadhyay, A., Vecchi, M., and Carpenter, G., 1999, Physiological requirement for both SH2 domains for phospholipase C-gamma1 function and interaction with platelet-derived growth factor receptors, *Mol Cell Biol* **19**(7):4961-70.
- Jiang, Y., Lee, A., Chen, J., Ruta, V., Cadene, M., Chait, B. T., and MacKinnon, R., 2003, X-ray structure of a voltage-dependent K⁺ channel, *Nature* **423**(6935):33-41.
- Johnson, J. A., Gray, M. O., Chen, C. H., and Mochly-Rosen, D., 1996, A protein kinase C translocation inhibitor as an isozyme-selective antagonist of cardiac function, *J Biol Chem* **271**(40):24962-6.
- Jurman, M. E., Boland, L. M., Liu, Y., and Yellen, G., 1994, Visual identification of individual transfected cells for electrophysiology using antibody-coated beads, *Biotechniques* **17**(5):876-81.
- Kass, R. S., 2006, Sodium channel inactivation in heart: a novel role of the carboxy-terminal domain, *J Cardiovasc Electrophysiol* **17 Suppl 1**:S21-S25.
- Kerr, N. C., Holmes, F. E., and Wynick, D., 2004, Novel isoforms of the sodium channels Nav1.8 and Nav1.5 are produced by a conserved mechanism in mouse and rat, *J Biol Chem* **279**(23):24826-33.
- Kerr, N. C., Holmes, F. E., and Wynick, D., 2008, Novel mRNA isoforms of the sodium channels Na(v)1.2, Na(v)1.3 and Na(v)1.7 encode predicted two-domain, truncated proteins, *Neuroscience* **155**(3):797-808.
- Kmiecik, T. E., and Shalloway, D., 1987, Activation and suppression of pp60c-src transforming ability by mutation of its primary sites of tyrosine phosphorylation, *Cell* **49**(1):65-73.
- Knighton, D. R., Zheng, J. H., Ten Eyck, L. F., Ashford, V. A., Xuong, N. H., Taylor, S. S., and Sowadski, J. M., 1991a, Crystal structure of the catalytic subunit of cyclic adenosine monophosphate-dependent protein kinase, *Science* **253**(5018):407-14.
- Knighton, D. R., Zheng, J. H., Ten Eyck, L. F., Xuong, N. H., Taylor, S. S., and Sowadski, J. M., 1991b, Structure of a peptide inhibitor bound to the catalytic subunit of cyclic adenosine monophosphate-dependent protein kinase, *Science* **253**(5018):414-20.

References

- Koch, M. C., Baumbach, K., George, A. L., and Ricker, K., 1995, Paramyotonia congenita without paralysis on exposure to cold: a novel mutation in the SCN4A gene (Val1293Ile), *Neuroreport* **6**(15):2001-4.
- Kohrman, D. C., Smith, M. R., Goldin, A. L., Harris, J., and Meisler, M. H., 1996, A missense mutation in the sodium channel Scn8a is responsible for cerebellar ataxia in the mouse mutant jolting, *J Neurosci* **16**(19):5993-9.
- Kuhn, F. J., and Greeff, N. G., 1999, Movement of voltage sensor S4 in domain 4 is tightly coupled to sodium channel fast inactivation and gating charge immobilization, *J Gen Physiol* **114**(2):167-83.
- Larkin, M. A., Blackshields, G., Brown, N. P., Chenna, R., McGgettigan, P. A., McWilliam, H., Valentin, F., Wallace, I. M., Wilm, A., Lopez, R., Thompson, J. D., Gibson, T. J., and Higgins, D. G., 2007, Clustal W and Clustal X version 2.0, *Bioinformatics* **23**(21):2947-8.
- Lee, J., Wang, Z., Luoh, S. M., Wood, W. I., and Scadden, D. T., 1994, Cloning of FRK, a novel human intracellular SRC-like tyrosine kinase-encoding gene, *Gene* **138**(1-2):247-51.
- Lei, M., Huang, C. L., and Zhang, Y., 2008, Genetic Na⁺ channelopathies and sinus node dysfunction, *Prog Biophys Mol Biol* **98**(2-3):171-8.
- Levinson, A. D., Oppermann, H., Levintow, L., Varmus, H. E., and Bishop, J. M., 1978, Evidence that the transforming gene of avian sarcoma virus encodes a protein kinase associated with a phosphoprotein, *Cell* **15**(2):561-72.
- Levitan, I. B., 1994, Modulation of ion channels by protein phosphorylation and dephosphorylation, *Annu Rev Physiol* **56**:193-212.
- Lim, W. A., 1996, Reading between the lines: SH3 recognition of an intact protein, *Structure* **4**(6):657-9.
- Lossin, C., 2009, A catalog of SCN1A variants, *Brain Dev* **31**(2):114-30.
- Ma, Y. C., and Huang, X. Y., 2002, Novel signaling pathway through the beta-adrenergic receptor, *Trends Cardiovasc Med* **12**(1):46-9.
- Maier, S. K., Westenbroek, R. E., Schenkman, K. A., Feigl, E. O., Scheuer, T., and Catterall, W. A., 2002, An unexpected role for brain-type sodium channels in coupling of cell surface depolarization to contraction in the heart, *Proc Natl Acad Sci U S A* **99**(6):4073-8.
- Makielski, J. C., 2006, SIDS: genetic and environmental influences may cause arrhythmia in this silent killer, *J Clin Invest* **116**(2):297-9.
- Makielski, J. C., Ye, B., Valdivia, C. R., Pagel, M. D., Pu, J., Tester, D. J., and Ackerman, M. J., 2003, A ubiquitous splice variant and a common polymorphism affect heterologous expression of recombinant human SCN5A heart sodium channels, *Circ Res* **93**(9):821-8.
- Malo, M. S., Blanchard, B. J., Andresen, J. M., Srivastava, K., Chen, X. N., Li, X., Jabs, E. W., Korenberg, J. R., and Ingram, V. M., 1994, Localization of a putative human brain sodium channel gene (SCN1A) to chromosome band 2q24, *Cytogenet Cell Genet* **67**(3):178-86.
- Mandel, G., 1992, Tissue-specific expression of the voltage-sensitive sodium channel, *J Membr Biol* **125**(3):193-205.
- Marban, E., Yamagishi, T., and Tomaselli, G. F., 1998, Structure and function of voltage-gated sodium channels, *J Physiol* **508** (Pt 3):647-57.
- Marchler-Bauer, A., Lu, S., Anderson, J. B., Chitsaz, F., Derbyshire, M. K., DeWeese-Scott, C., Fong, J. H., Geer, L. Y., Geer, R. C., Gonzales, N. R., Gwadz, M., Hurwitz, D. I., Jackson, J. D., Ke, Z., Lanczycki, C. J., Lu, F., Marchler, G. H., Mullokandov, M., Omelchenko, M. V., Robertson, C. L.,

References

- Song, J. S., Thanki, N., Yamashita, R. A., Zhang, D., Zhang, N., Zheng, C., and Bryant, S. H., 2011, CDD: a Conserved Domain Database for the functional annotation of proteins, *Nucleic Acids Res* **39**(Database issue):D225-9.
- Marfatia, K. A., Harreman, M. T., Fanara, P., Vertino, P. M., and Corbett, A. H., 2001, Identification and characterization of the human MOG1 gene, *Gene* **266**(1-2):45-56.
- McNair, W. P., Ku, L., Taylor, M. R., Fain, P. R., Dao, D., Wolfel, E., and Mestroni, L., 2004, SCN5A mutation associated with dilated cardiomyopathy, conduction disorder, and arrhythmia, *Circulation* **110**(15):2163-7.
- Meggio, F., and Pinna, L. A., 2003, One-thousand-and-one substrates of protein kinase CK2?, *FASEB J* **17**(3):349-68.
- Misra, S. N., Kahlig, K. M., and George, A. L., Jr., 2008, Impaired NaV1.2 function and reduced cell surface expression in benign familial neonatal-infantile seizures, *Epilepsia* **49**(9):1535-45.
- Mitrovic, N., George, A. L., Jr., Lerche, H., Wagner, S., Fahlke, C., and Lehmann-Horn, F., 1995, Different effects on gating of three myotonia-causing mutations in the inactivation gate of the human muscle sodium channel, *J Physiol* **487** (Pt 1):107-14.
- Mohler, P. J., Rivolta, I., Napolitano, C., LeMaillet, G., Lambert, S., Priori, S. G., and Bennett, V., 2004, Nav1.5 E1053K mutation causing Brugada syndrome blocks binding to ankyrin-G and expression of Nav1.5 on the surface of cardiomyocytes, *Proc Natl Acad Sci U S A* **101**(50):17533-8.
- Morgan, D. O., Kaplan, J. M., Bishop, J. M., and Varmus, H. E., 1989, Mitosis-specific phosphorylation of p60c-src by p34cdc2-associated protein kinase, *Cell* **57**(5):775-86.
- Morgan, K., Stevens, E. B., Shah, B., Cox, P. J., Dixon, A. K., Lee, K., Pinnock, R. D., Hughes, J., Richardson, P. J., Mizuguchi, K., and Jackson, A. P., 2000, beta 3: an additional auxiliary subunit of the voltage-sensitive sodium channel that modulates channel gating with distinct kinetics, *Proc Natl Acad Sci U S A* **97**(5):2308-13.
- Nada, S., Okada, M., MacAuley, A., Cooper, J. A., and Nakagawa, H., 1991, Cloning of a complementary DNA for a protein-tyrosine kinase that specifically phosphorylates a negative regulatory site of p60c-src, *Nature* **351**(6321):69-72.
- Nitabach, M. N., Llamas, D. A., Araneda, R. C., Intile, J. L., Thompson, I. J., Zhou, Y. I., and Holmes, T. C., 2001, A mechanism for combinatorial regulation of electrical activity: Potassium channel subunits capable of functioning as Src homology 3-dependent adaptors, *Proc Natl Acad Sci U S A* **98**(2):705-10.
- Noda, M., Shimizu, S., Tanabe, T., Takai, T., Kayano, T., Ikeda, T., Takahashi, H., Nakayama, H., Kanaoka, Y., Minamino, N., and et al., 1984, Primary structure of Electrophorus electricus sodium channel deduced from cDNA sequence, *Nature* **312**(5990):121-7.
- Oberg-Welsh, C., and Welsh, M., 1995, Cloning of BSK, a murine FRK homologue with a specific pattern of tissue distribution, *Gene* **152**(2):239-42.
- Olson, T. M., Michels, V. V., Ballew, J. D., Reyna, S. P., Karst, M. L., Herron, K. J., Horton, S. C., Rodeheffer, R. J., and Anderson, J. L., 2005, Sodium channel mutations and susceptibility to heart failure and atrial fibrillation, *JAMA* **293**(4):447-54.

References

- Onkal, R., Mattis, J. H., Fraser, S. P., Diss, J. K., Shao, D., Okuse, K., and Djamgoz, M. B., 2008, Alternative splicing of Nav1.5: an electrophysiological comparison of 'neonatal' and 'adult' isoforms and critical involvement of a lysine residue, *J Cell Physiol* **216**(3):716-26.
- Orrell, R. W., Jurkat-Rott, K., Lehmann-Horn, F., and Lane, R. J., 1998, Familial cramp due to potassium-aggravated myotonia, *J Neurol Neurosurg Psychiatry* **65**(4):569-72.
- Ou, S. W., Kameyama, A., Hao, L. Y., Horiuchi, M., Minobe, E., Wang, W. Y., Makita, N., and Kameyama, M., 2005, Tetrodotoxin-resistant Na⁺ channels in human neuroblastoma cells are encoded by new variants of Nav1.5/SCN5A, *Eur J Neurosci* **22**(4):793-801.
- Pawson, T., 1995, Protein modules and signalling networks, *Nature* **373**(6515):573-80.
- Peretz, A., Gil-Henn, H., Sobko, A., Shinder, V., Attali, B., and Elson, A., 2000, Hypomyelination and increased activity of voltage-gated K(+) channels in mice lacking protein tyrosine phosphatase epsilon, *EMBO J* **19**(15):4036-45.
- Ptacek, L. J., George, A. L., Jr., Barchi, R. L., Griggs, R. C., Riggs, J. E., Robertson, M., and Leppert, M. F., 1992, Mutations in an S4 segment of the adult skeletal muscle sodium channel cause paramyotonia congenita, *Neuron* **8**(5):891-7.
- Ptacek, L. J., Gouw, L., Kwiecinski, H., McManis, P., Mendell, J. R., Barohn, R. J., George, A. L., Jr., Barchi, R. L., Robertson, M., and Leppert, M. F., 1993, Sodium channel mutations in paramyotonia congenita and hyperkalemic periodic paralysis, *Ann Neurol* **33**(3):300-7.
- Rahuel, J., Gay, B., Erdmann, D., Strauss, A., Garcia-Echeverria, C., Furet, P., Caravatti, G., Fretz, H., Schoepfer, J., and Grutter, M. G., 1996, Structural basis for specificity of Grb2-SH2 revealed by a novel ligand binding mode, *Nat Struct Biol* **3**(7):586-9.
- Ratcliffe, C. F., Qu, Y., McCormick, K. A., Tibbs, V. C., Dixon, J. E., Scheuer, T., and Catterall, W. A., 2000, A sodium channel signaling complex: modulation by associated receptor protein tyrosine phosphatase beta, *Nat Neurosci* **3**(5):437-44.
- Ren, D., Navarro, B., Xu, H., Yue, L., Shi, Q., and Clapham, D. E., 2001, A prokaryotic voltage-gated sodium channel, *Science* **294**(5550):2372-5.
- Resh, M. D., 1993, Interaction of tyrosine kinase oncoproteins with cellular membranes, *Biochim Biophys Acta* **1155**(3):307-22.
- Richards, F. M., 1977, Areas, volumes, packing and protein structure, *Annu Rev Biophys Bioeng* **6**:151-76.
- Rickles, R. J., Botfield, M. C., Zhou, X. M., Henry, P. A., Brugge, J. S., and Zoller, M. J., 1995, Phage display selection of ligand residues important for Src homology 3 domain binding specificity, *Proc Natl Acad Sci U S A* **92**(24):10909-13.
- Rodriguez, F. A., Contreras, C., Bolanos-Garcia, V., and Allende, J. E., 2008, Protein kinase CK2 as an ectokinase: the role of the regulatory CK2beta subunit, *Proc Natl Acad Sci U S A* **105**(15):5693-8.
- Rogers, M., Tang, L., Madge, D. J., and Stevens, E. B., 2006, The role of sodium channels in neuropathic pain, *Semin Cell Dev Biol* **17**(5):571-81.
- Romine, W. O., Jr., Schoepfle, G. M., Smythies, J. R., Al-Zahid, G., and Bradley, R. J., 1974, Pharmacological evidence related to the existence of two sodium channel gating mechanisms, *Nature* **248**(5451):797-9.

References

- Roskoski, R., Jr., 2004, Src protein-tyrosine kinase structure and regulation, *Biochem Biophys Res Commun* **324**(4):1155-64.
- Sadoshima, J., Qiu, Z., Morgan, J. P., and Izumo, S., 1995, Angiotensin II and other hypertrophic stimuli mediated by G protein-coupled receptors activate tyrosine kinase, mitogen-activated protein kinase, and 90-kD S6 kinase in cardiac myocytes. The critical role of Ca(2+)-dependent signaling, *Circ Res* **76**(1):1-15.
- Satin, J., Kyle, J. W., Chen, M., Bell, P., Cribbs, L. L., Fozzard, H. A., and Rogart, R. B., 1992, A mutant of TTX-resistant cardiac sodium channels with TTX-sensitive properties, *Science* **256**(5060):1202-5.
- Schirmeyer, J., Szafranski, K., Leipold, E., Mawrin, C., Platzer, M., and Heinemann, S. H., 2010, A subtle alternative splicing event of the Na(V)1.8 voltage-gated sodium channel is conserved in human, rat, and mouse, *J Mol Neurosci* **41**(2):310-4.
- Schott, J. J., Alshinawi, C., Kyndt, F., Probst, V., Hoornje, T. M., Hulsbeek, M., Wilde, A. A., Escande, D., Mannens, M. M., and Le Marec, H., 1999, Cardiac conduction defects associate with mutations in SCN5A, *Nat Genet* **23**(1):20-1.
- Schroeter, A., Walzik, S., Blechschmidt, S., Haufe, V., Benndorf, K., and Zimmer, T., 2010, Structure and function of splice variants of the cardiac voltage-gated sodium channel Na(v)1.5, *J Mol Cell Cardiol* **49**(1):16-24.
- Shang, L. L., Gao, G., and Dudley, S. C., Jr., 2008, The tail of the cardiac sodium channel, *Channels (Austin)* **2**(3):161-2.
- Shang, L. L., Pfahl, A. E., Sanyal, S., Jiao, Z., Allen, J., Banach, K., Fahrenbach, J., Weiss, D., Taylor, W. R., Zafari, A. M., and Dudley, S. C., Jr., 2007, Human heart failure is associated with abnormal C-terminal splicing variants in the cardiac sodium channel, *Circ Res* **101**(11):1146-54.
- Sicheri, F., Moarefi, I., and Kuriyan, J., 1997, Crystal structure of the Src family tyrosine kinase Hck, *Nature* **385**(6617):602-9.
- Siegelbaum, S. A., 1994, Channel regulation. Ion channel control by tyrosine phosphorylation, *Curr Biol* **4**(3):242-5.
- Sivilotti, L., Okuse, K., Akopian, A. N., Moss, S., and Wood, J. N., 1997, A single serine residue confers tetrodotoxin insensitivity on the rat sensory-neuron-specific sodium channel SNS, *FEBS Lett* **409**(1):49-52.
- Skinner, J. R., Chung, S. K., Montgomery, D., McCulley, C. H., Crawford, J., French, J., and Rees, M. I., 2005, Near-miss SIDS due to Brugada syndrome, *Arch Dis Child* **90**(5):528-9.
- Sobko, A., Peretz, A., and Attali, B., 1998, Constitutive activation of delayed-rectifier potassium channels by a src family tyrosine kinase in Schwann cells, *EMBO J* **17**(16):4723-34.
- Songyang, Z., Shoelson, S. E., Chaudhuri, M., Gish, G., Pawson, T., Haser, W. G., King, F., Roberts, T., Ratnofsky, S., Lechleider, R. J., and et al., 1993, SH2 domains recognize specific phosphopeptide sequences, *Cell* **72**(5):767-78.
- Sugawara, T., Tsurubuchi, Y., Agarwala, K. L., Ito, M., Fukuma, G., Mazaki-Miyazaki, E., Nagafuji, H., Noda, M., Imoto, K., Wada, K., Mitsudome, A., Kaneko, S., Montal, M., Nagata, K., Hirose, S., and Yamakawa, K., 2001, A missense mutation of the Na⁺ channel alpha II subunit gene Na(v)1.2 in a patient with febrile and afebrile seizures causes channel dysfunction, *Proc Natl Acad Sci U S A* **98**(11):6384-9.

- Tamkun, M. M., Knoth, K. M., Walbridge, J. A., Kroemer, H., Roden, D. M., and Glover, D. M., 1991, Molecular cloning and characterization of two voltage-gated K⁺ channel cDNAs from human ventricle, *FASEB J* **5**(3):331-7.
- Tan, B. H., Valdivia, C. R., Rok, B. A., Ye, B., Ruwaldt, K. M., Tester, D. J., Ackerman, M. J., and Makielinski, J. C., 2005, Common human SCN5A polymorphisms have altered electrophysiology when expressed in Q1077 splice variants, *Heart Rhythm* **2**(7):741-7.
- Tan, B. H., Valdivia, C. R., Song, C., and Makielinski, J. C., 2006, Partial expression defect for the SCN5A missense mutation G1406R depends on splice variant background Q1077 and rescue by mexiletine, *Am J Physiol Heart Circ Physiol* **291**(4):H1822-8.
- Thomas, S. M., and Brugge, J. S., 1997, Cellular functions regulated by Src family kinases, *Annu Rev Cell Dev Biol* **13**:513-609.
- Thompson, J. D., Higgins, D. G., and Gibson, T. J., 1994, CLUSTAL W: improving the sensitivity of progressive multiple sequence alignment through sequence weighting, position-specific gap penalties and weight matrix choice, *Nucleic Acids Res* **22**(22):4673-80.
- Thuvesson, M., Albrecht, D., Zurcher, G., Andres, A. C., and Ziernicki, A., 1995, iyk, a novel intracellular protein tyrosine kinase differentially expressed in the mouse mammary gland and intestine, *Biochem Biophys Res Commun* **209**(2):582-9.
- Tomaselli, G. F., Chiamvimonvat, N., Nuss, H. B., Balser, J. R., Perez-Garcia, M. T., Xu, R. H., Orias, D. W., Backx, P. H., and Marban, E., 1995, A mutation in the pore of the sodium channel alters gating, *Biophys J* **68**(5):1814-27.
- Tomaselli, G. F., and Zipes, D. P., 2004, What causes sudden death in heart failure?, *Circ Res* **95**(8):754-63.
- Toyofuku, T., Akamatsu, Y., Zhang, H., Kuzuya, T., Tada, M., and Hori, M., 2001, c-Src regulates the interaction between connexin-43 and ZO-1 in cardiac myocytes, *J Biol Chem* **276**(3):1780-8.
- Tsai, W., Morielli, A. D., Cachero, T. G., and Peralta, E. G., 1999, Receptor protein tyrosine phosphatase alpha participates in the m1 muscarinic acetylcholine receptor-dependent regulation of Kv1.2 channel activity, *EMBO J* **18**(1):109-18.
- Vilin, Y. Y., and Ruben, P. C., 2001, Slow inactivation in voltage-gated sodium channels: molecular substrates and contributions to channelopathies, *Cell Biochem Biophys* **35**(2):171-90.
- Wang, D. W., Desai, R. R., Crotti, L., Arnestad, M., Insolia, R., Pedrazzini, M., Ferrandi, C., Vege, A., Rognum, T., Schwartz, P. J., and George, A. L., Jr., 2007, Cardiac sodium channel dysfunction in sudden infant death syndrome, *Circulation* **115**(3):368-76.
- Wang, J., Ou, S. W., Wang, Y. J., Kameyama, M., Kameyama, A., and Zong, Z. H., 2009, Analysis of four novel variants of Nav1.5/SCN5A cloned from the brain, *Neurosci Res* **64**(4):339-47.
- Wang, J., Ou, S. W., Wang, Y. J., Zong, Z. H., Lin, L., Kameyama, M., and Kameyama, A., 2008, New variants of Nav1.5/SCN5A encode Na⁺ channels in the brain, *J Neurogenet* **22**(1):57-75.
- Wang, Y., Wagner, M. B., Kumar, R., Cheng, J., and Joyner, R. W., 2003, Inhibition of fast sodium current in rabbit ventricular myocytes by protein tyrosine kinase inhibitors, *Pflugers Arch* **446**(4):485-91.

- Wedeck, H., Bajanowski, T., Friederich, P., Breithardt, G., Wulffing, T., Siebrands, C., Engeland, B., Monnig, G., Haverkamp, W., Brinkmann, B., and Schulze-Bahr, E., 2006, Sudden infant death syndrome and long QT syndrome: an epidemiological and genetic study, *Int J Legal Med* **120**(3):129-37.
- Winkler, D. G., Park, I., Kim, T., Payne, N. S., Walsh, C. T., Strominger, J. L., and Shin, J., 1993, Phosphorylation of Ser-42 and Ser-59 in the N-terminal region of the tyrosine kinase p56lck, *Proc Natl Acad Sci U S A* **90**(11):5176-80.
- Wischmeyer, E., Doring, F., and Karschin, A., 1998, Acute suppression of inwardly rectifying Kir2.1 channels by direct tyrosine kinase phosphorylation, *J Biol Chem* **273**(51):34063-8.
- Wu, F. F., Takahashi, M. P., Pegoraro, E., Angelini, C., Colleselli, P., Cannon, S. C., and Hoffman, E. P., 2001, A new mutation in a family with cold-aggravated myotonia disrupts Na⁺ channel inactivation, *Neurology* **56**(7):878-84.
- Wu, J. Y., Yu, H., and Cohen, I. S., 2000, Epidermal growth factor increases i(f) in rabbit SA node cells by activating a tyrosine kinase, *Biochim Biophys Acta* **1463**(1):15-9.
- Wu, L., Yong, S. L., Fan, C., Ni, Y., Yoo, S., Zhang, T., Zhang, X., Obejero-Paz, C. A., Rho, H. J., Ke, T., Szafranski, P., Jones, S. W., Chen, Q., and Wang, Q. K., 2008, Identification of a new co-factor, MOG1, required for the full function of cardiac sodium channel Nav 1.5, *J Biol Chem* **283**(11):6968-78.
- Xu, W., Doshi, A., Lei, M., Eck, M. J., and Harrison, S. C., 1999, Crystal structures of c-Src reveal features of its autoinhibitory mechanism, *Mol Cell* **3**(5):629-38.
- Xu, W., Harrison, S. C., and Eck, M. J., 1997, Three-dimensional structure of the tyrosine kinase c-Src, *Nature* **385**(6617):595-602.
- Yang, N., George, A. L., Jr., and Horn, R., 1996, Molecular basis of charge movement in voltage-gated sodium channels, *Neuron* **16**(1):113-22.
- Yang, Y., Wang, Y., Li, S., Xu, Z., Li, H., Ma, L., Fan, J., Bu, D., Liu, B., Fan, Z., Wu, G., Jin, J., Ding, B., Zhu, X., and Shen, Y., 2004, Mutations in SCN9A, encoding a sodium channel alpha subunit, in patients with primary erythermalgia, *J Med Genet* **41**(3):171-4.
- Yu, F. H., and Catterall, W. A., 2003, Overview of the voltage-gated sodium channel family, *Genome Biol* **4**(3):207.
- Yu, H., Chen, J. K., Feng, S., Dalgarno, D. C., Brauer, A. W., and Schreiber, S. L., 1994, Structural basis for the binding of proline-rich peptides to SH3 domains, *Cell* **76**(5):933-45.
- Zhang, Y. H., and Hancox, J. C., 2003, A novel, voltage-dependent nonselective cation current activated by insulin in guinea pig isolated ventricular myocytes, *Circ Res* **92**(7):765-8.
- Zhou, J., Yi, J., Hu, N., George, A. L., Jr., and Murray, K. T., 2000, Activation of protein kinase A modulates trafficking of the human cardiac sodium channel in Xenopus oocytes, *Circ Res* **87**(1):33-8.
- Zimmer, T., Bollensdorff, C., Haufe, V., Birch-Hirschfeld, E., and Benndorf, K., 2002, Mouse heart Na⁺ channels: primary structure and function of two isoforms and alternatively spliced variants, *Am J Physiol Heart Circ Physiol* **282**(3):H1007-17.

Appendix

9.1 Abstract

Voltage-gated sodium channels are very large membrane proteins. They are encoded by ten genes in mammals. Sodium channels are a crucial component of excitable tissues; hence, they are a target for various drugs and toxins. Nav1.5 is the cardiac voltage-gated sodium channel involved in the rapid depolarizing phase of the cardiac action potential. This isoform is also involved in the propagation of electrical impulses in the heart. Out of nine Na_v1.5 splice variants, four of them were functional. The splice variant ΔQ1077 and Q1077Present variant of Nav1.5 are present in 45% and 25 % of human population, respectively. Cardiac sodium channels are modulated by different intracellular proteins. Tyrosine kinases are one of the potent intracellular modulators of ion channels. Fyn, a member of the Src tyrosine kinase family, modulates sodium channel isoforms distinctly.

Results on the Q1077Present and the ΔQ1077 variants show different steady-state inactivation in presence of catalytic active Fyn^{CA}. While the Q1077Present variant shifted the inactivation curve to more depolarizing potentials, the ΔQ1077 variant shifted the inactivation curve to more hyperpolarizing potentials, similar to neuronal sodium channel Nav1.2. The Fyn-induced shift in inactivation of Q1077Present was similar to the modulation observed in the hH1 polymorphic cardiac sodium channel variant with Fyn. The Src tyrosine kinase inhibitor PP2 reversed back the shifts caused by Fyn^{CA} in both Q1077Present and ΔQ1077 cardiac sodium channel variants. Moreover, the kinase dead mutant Fyn^{KD} did not shift both the ΔQ1077 and Q1077Present inactivation curves. The activation curves of both Q1077Present and ΔQ1077 were not affected by active Fyn. Sequence analysis of all the sodium channel isoforms reveal that the Q1077glutamine is present in one the three unique sequences in the intracellular loop connecting the domain DII and DIII, which forms the ‘sodium ion transport associated’ region. Point mutation at position 1077 from glutamine to alanine, lysine, tyrosine and proline shifted the inactivation curves to more hyperpolarizing potentials with Fyn^{CA}. Linear correlation was observed between the

Appendix

hyperpolarizing shift caused by Fyn^{CA} and the hydrophobicity of the amino acids' side chains. Putative SH2 and SH3 binding sites for Fyn in the cardiac sodium channel were also determined. Five unique proline-rich motifs were identified, which are potential SH3 binding sites for Fyn in the cardiac sodium channel. Putative SH2 binding motifs for Fyn were found in the C-terminal of Na_v1.5.

These data will be pertinent in understanding the role of Q1077 and its surrounding amino acids. The intracellular loop L_{DII-DIII}, which is distinct in cardiac sodium channels from other sodium channel isoforms, forms one of the 'sodium ion transport associated' regions. Thus, L_{DII-DIII} plays a pivotal role in regulating cardiac sodium channel binding to various intracellular signaling molecules.

9.2 Zusammenfassung

Spannungabhängige Natriumkanäle sind sehr große Membranproteine. In Säugetieren werden sie von zehn Genen kodiert. Natriumkanäle spielen eine wichtige Rolle in erregbaren Zellen und sie sind deshalb ein wichtiger Angriffspunkt für Arzneistoffe und Toxine. Nav1.5 ist der spannungsabhängige Natriumkanal im Herzen, wo er für die rasche Depolarisationsphase im Aktionspotential verantwortlich ist und auch an der Reizweiterleitung beteiligt ist. Von den neun Spleißvarianten von Nav1.5 sind vier funktionell. Die Spleißvariante $\Delta Q1077$ und die Q1077Present Variante des kardialen Natriumkanals sind in 45% bzw. 25% der Bevölkerung anzutreffen. Kardiale Natriumkanäle werden durch unterschiedliche intrazelluläre Proteine moduliert. Tyrosinkinasen sind eine der potennten Modulatoren verschiedener Ionenkanäle. Fyn, das zur Src Tyrosinkinase-Familie gehört, moduliert verschiedene Natriumkanal-Isoformen auf unterschiedliche Weise. Die mit den Q1077Present und $\Delta Q1077$ Varianten erhaltenen Ergebnisse zeigten unterschiedliche Inaktivierung in Gegenwart katalytisch aktiver Fyn^{CA}. Während die Q1077Present Variante die Inaktivierungskurve in die depolarisierende Richtung verschob, trat die halbmaximale Inaktivierung bei $\Delta Q1077$ bei negativeren Potentialen auf, ähnlich wie beim neuronalen Natriumkanal Nav1.2. Die durch Fyn^{CA} bedingte Verschiebung der Inaktivierungskurve in der Q1077Present Variante war vergleichbar mit der durch Fyn^{CA} hervorgerufenen Modulation in der hH1 polymorphen kardialen Natriumkanal-Variante. Mit der Kinase-toten Mutante Fyn^{KD} kam es weder bei $\Delta Q1077$ noch bei Q1077Present zu einer Verschiebung der Inaktivierungskurven. Weiters konnte in beiden Varianten die durch Fyn^{CA} bedingte Verschiebung der Inaktivierungskurven durch den Src Tyrosinkinase-Hemmer PP2 aufgehoben werden. Die Aktivierungskurven beider Varianten, Q1077Present und $\Delta Q1077$, wurden durch Fyn^{CA} nicht beeinflusst. Eine Sequenzanalyse aller Natriumkanal-Isoformen zeigte, dass Glutamin in Position 1077 in einer der drei für Nav1.5 einzigartigen Sequenzen in der intrazellulären Schleife liegt, die die Domänen DII und DIII verbindet und die "Natriumionentransport-assoziierte" Region bildet. Eine Punktmutation in Position 1077 von Glutamin zu Alanin, Lysin, Tyrosin oder Prolin verschob die Inaktivierungskurven in Gegenwart von Fyn^{CA} zu negativeren Potentialen. Es konnte

Appendix

eine lineare Korrelation zwischen dem Ausmaß der Verschiebung der Inaktivierungskurven durch Fyn^{CA} und der hydrophoben Eigenschaft der Aminosäuren-Seitenketten beobachtet werden. Mögliche SH2 und SH3 Bindungsstellen für Fyn im kardialen Natriumkanal wurden ebenfalls identifiziert. Fünf spezifische, prolinreiche Motive, die als SH3 Bindungsstelle für Fyn im kardialen Natriumkanal fungieren könnten, wurden aufgefunden. Mögliche SH2 Bindungsmotive für Fyn wurden im C-Terminus von Nav1.5 identifiziert.

Diese Daten tragen zum Verständnis der Rolle des Q1077 und den angrenzenden Aminosäuren bei. Die intrazelluläre Schleife L_{DII-DIII} des kardialen Natriumkanals, die sich wesentlich von der anderer Natriumkanal-Isoformen unterscheidet, bildet eine der "Natriumionentransport-assoziierten" Regionen. Deshalb spielt L_{DII-DIII} eine wichtige Rolle bei der Bindung intrazellulärer Signalmoleküle an den Natriumkanal.

9.3 Alignment

Nav1.1	---MEQTVLVPPGPDSFNFFTRESLAAIERRIAEEKAKNPKD---	KKDDDENGPKPNS
Nav1.8	---MEQTVLVPPGPDSFNFFTRESLAAIERRIAEEKAKNPKD---	KKDDDENGPKPNS
Nav1.9	---MEQTVLVPPGPDSFNFFTRESLAAIERRIAEEKAKNPKD---	KKDDDENGPKPNS
Nav1.2	---MAQSVLVPPGPDSFRFFTRESLAAIEQRIAEEKAKRKPQER---	KDEDDENGPKPNS
Nav1.3	---MAQALLVPPGPESFRLFTRESLAAIEKRAAEEKAKKPKKE---	QDNDDENPKPNS
Nav1.7	-----MAMLPPPQSFVFHFTQSLALIEQRIAERKSKEPKEE---	KKDDDEEAPKPSS
Nav1.6	---MAARLLAPPGPDSFKPFTPESLANIERRIAESKLKPKADGSHREDEDSKPKPNS	
Nav1.4	MARPSLCTLVPLGPECLRPFTRESLAAIEQRAVEEEARLQRNK---	QMEIEEPPERKPRS
Nav1.5	----MANFLLPRGTSSRRFTRESLAAIEKRMAEQARGSTTLQESREGLPEEEAPRQL * * *...: ** :*** *;*: . * : : . :: :* :	
Nav1.1	DLEAGKNLPFIYGDIPPEMVSEPLEDLDPYYINKKTFIVLNKGKAIFRFSATSALYILTP	
Nav1.8	DLEAGKNLPFIYGDIPPEMVSEPLEDLDPYYINKKTFIVLNKGKAIFRFSATSALYILTP	
Nav1.9	DLEAGKNLPFIYGDIPPEMVSEPLEDLDPYYINKKTFIVLNKGKAISRFSATPALYILTP	
Nav1.2	DLEAGKSLPFIYGDIPPEMVSEPLEDLDPYYINKKTFIVLNKGKAIFRFSATSALYILTP	
Nav1.3	DLEAGKNLPFIYGDIPPEMVSEPLEDLDPYYINKKTFIVMNKGKAIFRFSATSALYILTP	
Nav1.7	DLEAGKQLPFIYGDIPPGMVSEPLEDLDPYYADKKTTFIVLNKGKTIFRFNATPALYMLSP	
Nav1.6	DLEAGKSLPFIYGDIPQGLAVAPLEDFDPYYLTQKTFVVLNRGKTLFRFSATPALYILSP	
Nav1.4	DLEAGKNLPIMIYGDPPPEVIGIPLEDLDPYYSNKKTFIVLNKGKAIFRFSATPALYLLSP	
Nav1.5	DLQASKKLPLDLYGNPPQELIGEPLEDLDPFYSTQKTFIVLNKGKTIFRFSATNALYVLSP **:.*.*.* : * : . ***:***: * :***:***:***: ***.*** ***:*	
Nav1.1	FNPLRKIAIKILVHSLFSMLIMCTILTNCVFMTMSNPPDWTKNVEYTFTGIYTFESLIKI	
Nav1.8	FNPLRKIAIKILVHSLFSMLIMCTILTNCVFMTMSNPPDWTKNVEYTFTGIYTFESLIKI	
Nav1.9	FNPLRKIAIKILVHSLFSMLIMCTILTNCVFMTMSNPPDWTKNVEYTFTGIYTFESLIKI	
Nav1.2	FNPIRKLAIKILVHSLFNMNLMIMCTILTNCVFMTMSNPPDWTKNVEYTFTGIYTFESLIKI	
Nav1.3	LNPVRKIAIKILVHSLFSMLIMCTILTNCVFMTLSNPPDWTKNVEYTFTGIYTFESLIKI	
Nav1.7	FSPLRRISIKILVHSLFSMLIMCTILTNCIFMTMNNPPDWTKNVEYTFTGIYTFESLVKI	
Nav1.6	FNLIRRIAIKILIHSVFSMIIMCTILTNCVFMTFSNPPDWSKNVEYTFTGIYTFESLVKI	
Nav1.4	FSVVRGAIKVLIHALFSMFIMITILTNCVFMTMSDPPPWSKNVEYTFTGIYTFESLIKI	
Nav1.5	FHIPRRAAVKILVHSLFNMNLMIMCTILTNCVFMAQHDPPPWTKYVEYTFTAIYTFESLVKI : :*: :*:***:***:*.** *****:***: :** *: * *****.*****:***	
Nav1.1	IARGFCLEDFTFLRDPWNWLDFTVITFAYVTEFVLDGNVSALRTFRVLRAALKTISVIPGL	
Nav1.8	IARGFCLEDFTFLRDPWNWLDFTVITFAYVTEFVLDGNVSALRTFRVLRAALKTISVIPGL	
Nav1.9	IARGFCLEDFTFLRDPWNWLDFTVITFAYVTEFVLDGNVSALRTFRVLRAALKTISVIPGL	
Nav1.2	LARGFCLEDFTFLRDPWNWLDFTVITFAYVTEFVLDGNVSALRTFRVLRAALKTISVIPGL	
Nav1.3	LARGFCLEDFTFLRDPWNWLDFTVITFAYVTEFVLDGNVSALRTFRVLRAALKTISVIPGL	
Nav1.7	LARGFCVGEFTFLRDPWNWLDFTVVIVFAYLTEFVNGLGNVSALRTFRVLRAALKTISVIPGL	
Nav1.6	IARGFCIDGFTFLRDPWNWLDFTVIMMAYITEFVNGLGNVSALRTFRVLRAALKTISVIPGL	
Nav1.4	LARGFCVDDFTFLRDPWNWLDFTVIMMAYLTETFDLGNNISALRTFRVLRAALKTITVIPGL	
Nav1.5	LARGFCFLHAFTFLRDPWNWLDFTVIIMAYTTEFVLDGNVSALRTFRVLRAALKTISVISGL *****: *****:*****:***: * :** *: *:*****:*****:***:***	
Nav1.1	KTIVGALIQSVKKLSDVMILTVFCLSVFALIGLQLFMGNLRNKCQWPP-----T	
Nav1.8	KTIVGALIQSVKKLSDVMILTVFCLSVFALIGLQLFMGNLRNKCQWPP-----T	
Nav1.9	KTIVGALIQSVKKLSDVMILTVFCLSVFALIGLQLFMGNLRNKCQWPP-----T	
Nav1.2	KTIVGALIQSVKKLSDVMILTVFCLSVFALIGLQLFMGNLRNKCQWPP-----D	
Nav1.3	KTIVGALIQSVKKLSDVMILTVFCLSVFALIGLQLFMGNLRNKCQWPP-----S	
Nav1.7	KTIVGALIQSVKKLSDVMILTVFCLSVFALIGLQLFMGNLKHKCFRN-----	
Nav1.6	KTIVGALIQSVKKLSDVMILTVFCLSVFALIGLQLFMGNLRNKCVRWPPPNDNTTWYS	
Nav1.4	KTIVGALIQSVKKLADVMVLTVFCLSVFALIGLQLFMGNLRHKCVRNFT-----	
Nav1.5	*****:*****:*****:*****:*****:*****:***.	

Appendix

Nav1.1 NASLEEHsiekn-ITVNYNGTLINETVF-----EFDWKSYIQDSRYHYFLEGFLD
 Nav1.8 NASLEEHsiekn-ITVNYNGTLINETVF-----EFDWKSYIQDSRYHYFLEGFLD
 Nav1.9 NASLEEHsiekn-ITVNYNGTLINETVF-----EFDWKSYIQDSRYHYFLEGFLD
 Nav1.2 NSSFEINITSFFNNSLDGNGTTFNRTVS-----IFNwDEYIEDKSHFYFLEGQND
 Nav1.3 DSAFETNTTSYFNGTMDSNGTFVNVTMS-----TFNWKDYIGDDSHFYVLGQKD
 Nav1.7 --SLENNETLES-----IMNTLES-----EEDFR-----KYFYYLEGSKD
 Nav1.6 -----INFNESYLENGTK-----GFDWEELYINNKTNFYTVPGMLE
 Nav1.4 NDTWYGNDTWYGNEMWYGNDSWYANDTWSHASWATNTFDWDAYISDEGNFYFLEG SND
 Nav1.5 -----ALNGTNGSVEADGLV-----WESLDLYLSDPENYLLKNGTSD
 . . * :

 Nav1.1 ALLCGNSSDAGQCPEGYMCVKAGRNPNYGYTSFDTFSWAFLSLFRLMTQDFWENLYQLTL
 Nav1.8 ALLCGNSSDAGQCPEGYMCVKAGRNPNYGYTSFDTFSWAFLSLFRLMTQDFWENLYQLTL
 Nav1.9 ALLCGNSSDAGQCPEGYMCVKAGRNPNYGYTSFDTFSWAFLSLFRLMTQDFWENLYQLTL
 Nav1.2 ALLCGNSSDAGQCPEGYICVKAGRNPNYGYTSFDTFSWAFLSLFRLMTQDFWENLYQLTL
 Nav1.3 PLLCGNGSDAGQCPEGYICVKAGRNPNYGYTSFDTFSWAFLSLFRLMTQDFWENLYQLTL
 Nav1.7 ALLCGFSTDGSQCPGEGYTCVKIGRNPDPGYTSFDTFSWAFLALFRLMTQDYWENLYQQT L
 Nav1.6 PLLCGNNSDAGQCPEGYQCMKAGRNPNYGYTSFDTFSWAFLALFRLMTQDYWENLYQLTL
 Nav1.4 ALLCGNNSDAGHCPEGYEICKTRNPNPYGYTSYDFTFSWAFLALFRLMTQDYWENLFQLTL
 Nav1.5 VLLCGNNSDAGTCPEGYRCLKAGENPDHGYTSFDSWAFLALFRLMTQDCWERLYQQT L
 **** .::* **** *.*.*;*****:.*.*****:*****:*****:*****:*****:

 Nav1.1 RAAGKTYMIFFVLVIFLGSFYLINLILAVVAMAYEEQNQATLEEAEQKEAEFQQMIEQLK
 Nav1.8 RAAGKTYMIFFVLVIFLGSFYLINLILAVVAMAYEEQNQATLEEAEQKEAEFQQMIEQLK
 Nav1.9 RAAGKTYMIFFVLVIFLGSFYLINLILAVVAMAYEEQNQATLEEAEQKEAEFQQMIEQLK
 Nav1.2 RAAGKTYMIFFVLVIFLGSFYLINLILAVVAMAYEEQNQATLEEAEQKEAEFQQMIEQLK
 Nav1.3 RAAGKTYMIFFVLVIFLGSFYLVNLILAVVAMAYEEQNQATLEEAEQKEAEFQQMIEQLK
 Nav1.7 RAAGKTYMIFFVVVIFLGSFYLINLILAVVAMAYEEQNQANIEAKQKELEFQQMLDRLK
 Nav1.6 RAAGKTYMIFFVVIIFLGSFYLINLILAVVAMAYEEQNQATLEEAEQKEAEFKAMLEQLK
 Nav1.4 RAAGKTYMIFFVVIIFLGSFYLVNLILAVVAMAYEEQNQATLEEAEQKEAEFQQMIEQLK
 Nav1.5 RSAGKIYMIFFMLVIFLGSFYLVNLILAVVAMAYEEQNQATIAETEEKEKRFQEAMEMLK
 *.:*** *****:;:***:*****:*****:*****:*****:*****:*****:

 Nav1.1 KQQEAAQQAAAT---ASEHSREPSA--AGR LSDSSSEASKLSSSAKERRNRRKKRKQ
 Nav1.8 KQQEAAQQAAAT---ASEHSREPSA--AGR LSDSSSEASKLSSSAKERRNRRKKRKQ
 Nav1.9 KQQEAAQQAAAT---ASEHSREPSA--AGR LSDSSSEASKLSSSAKERRNRRKKRKQ
 Nav1.2 KQQEEAQAAAAASA--ESRDFSGAGG--IGVFSESSSVASKLSSKSEKELKNRRKKKQ
 Nav1.3 KQQEEAQAVAAS-A--ASRDFSGIGG--LGELLESSSEASKLSSSAKEWRNRRKKRQ
 Nav1.7 KEQEEAEAIAAA---AEYTSIRR--IMGLSESSSETSKLSSSAKERRNRRKKNQ
 Nav1.6 KQQEEAQAAAMATSAGTVSEDAIEEGEEGGGSPRSSSEISKLSSSAKERRNRRKKRQ
 Nav1.4 KHQEELAKAAQ-----
 Nav1.5 KEHEALTIRGVDT-----VSRSSLEMSPLAPVNSHERRSKRRK-----
 .:

 Nav1.1 KEQSGGEEKDEDE-FQKSEEDSIRRKGRFSIEGNRLTYEKRYSSPHQSLLSIRGSLFS
 Nav1.8 KEQSGGEEKDEDE-FQKSEEDSIRRKGRFSIEGNRLTYEKRYSSPHQSLLSIRGSLFS
 Nav1.9 KEQSGGEEKDEDE-FQKSEEDSIRRKGRFSIEGNRLTYEKRYSSPHQSLLSIRGSLFS
 Nav1.2 KEQSGEEEKNDR--VRKSEEDSIRRKGRFSLEGSRLTYEKRFSSPHQSLLSIRGSLFS
 Nav1.3 REHLEGNNKGGERDSFPKSEEDSVKRSSFLFMSMDGNRLTSDKKFCSPHQSLLSIRGSLFS
 Nav1.7 KKLSSGEEKKGDAEKLKSEEDSIRRKSFHLGVGHRAHEKRLSTPNQSPLSIRGSLFS
 Nav1.6 KELSEGEKGDPKVFKSEEDGMRRKAFLPD--NRIG--RKFSIMNQSLLSIPGPSPFL
 Nav1.4 -ALEGGEADGDP-----A
 Nav1.5 ---MSSGTEECGEDRLPKSDSEDGPR-----AMNHLSLTRGLSRTSM
 .

 Nav1.1 PRRNSRTSLFSFRG--RAKVGSENDFADDEHSTFEDNESRRDSLFPVRRHGERRNSNL -
 Nav1.8 PRRNSRTSLFSFRG--RAKVGSENDFADDEHSTFEDNESRRDSLFPVRRHGERRNSNL -
 Nav1.9 PRRNSRTSLFSFRG--RAKVGSENDFADDEHSTFEDNESRRDSLFPVRRHGERRNSNL -
 Nav1.2 PRRNSRASLFSFRG--RAKDIGSENDFADDEHSTFEDNDSRRDSLFPVPHRGERRHSNV -
 Nav1.3 PRRNSKTSIFSFRG--RAKVGSENDFADDEHSTFEDSESRRDSLFPVPHRGERRNS --
 Nav1.7 ARRSSRTSLFSFKG--RGRDIGSETEFADDEHSIFGDNESRRGSLFPVPHRPQERRSSNI -
 Nav1.6 SRHNSKSSIFSFRGPGRFRDPGSENEFADDEHSTVEESEGRDSLFIPIRARERRSSYSG
 Nav1.4 HGKDCNGSLDTSQG-----
 Nav1.5 KPRSSRGSIFTFRR----RDLGSEADFADDENSTAGESESHHTSLLVPWPLRRTSAQGQ-
 *: : :

Appendix

Appendix

Appendix

Appendix

Nav1.1 RTLLFALMMSLPALFNIGLLLFLVMFIYAIFGMSNFAYVKREVGIDDMFNFETFGNSMIC
 Nav1.8 RTLLFALMMSLPALFNIGLLLFLVMFIYAIFGMSNFAYVKREVGIDDMFNFETFGNSMIC
 Nav1.9 RTLLFALMMSLPALFNIGLLLFLVMFIYAIFGMSNFAYVKREVGIDDMFNFETFGNSMIC
 Nav1.2 RTLLFALMMSLPALFNIGLLLFLVMFIYAIFGMSNFAYVKREVGIDDMFNFETFGNSMIC
 Nav1.3 RTLLFALMMSLPALFNIGLLLFLVMFIYAIFGMSNFAYVKKEAGIDDMFNFETFGNSMIC
 Nav1.7 RTLLFALMMSLPALFNIGLLLFLVMFIYAIFGMSNFAYVKKEAGIDDMFNFETFGNSMIC
 Nav1.6 RTLLFALMMSLPALFNIGLLLFLVMFIFSIFGMSNFAYVKHEAGIDDMFNFETFGNSMIC
 Nav1.4 RTLLFALMMSLPALFNIGLLLFLVMFIYSIFGMSNFAYVKKESGIDDMFNFETFGNSIIC
 Nav1.5 RTLLFALMMSLPALFNIGLLLFLVMFIYSIFGMANFAYVKWEAGIDDMFNFQTFANSMLC
 *****:*****:*****:*****:*****:*****:*****:*****:*****:*****:

 Nav1.1 LFQITTSAGWDGLLAPILNKPPDCPNKVNPONGSSVGKGDCGNPSVGIFFFSYIIISFLV
 Nav1.8 LFQITTSAGWDGLLAPILNKPPDCPNKVNPONGSSVGKGDCGNPSVGIFFFSYIIISFLV
 Nav1.9 LFQITTSAGWDGLLAPILNKPPDCPNKVNPONGSSVGKGDCGNPSVGIFFFSYIIISFLV
 Nav1.2 LFQITTSAGWDGLLAPILNKPPDCPNKVNPONGSSVGKGDCGNPSVGIFFFSYIIISFLV
 Nav1.3 LFQITTSAGWDGLLAPILNKPPDCPNKVNPONGSSVGKGDCGNPSVGIFFFSYIIISFLV
 Nav1.7 LFQITTSAGWDGLLAPILNKPPDCPNKVNPONGSSVGKGDCGNPSVGIFFFSYIIISFLV
 Nav1.6 LFQITTSAGWDGLLAPILNKPPDCPNKVNPONGSSVGKGDCGNPSVGIFFFSYIIISFLV
 Nav1.4 LFQITTSAGWDGLLAPILNKPPDCPNLV-RPPDCSLDKEHPGSGFKGDCGNPSVGIFFFSYIIISFLI
 Nav1.5 LFEITTSAGWDGLLNPILNKPPDCPNLENPGTSVKGDCGNPSV ригическое
 LFQITTSAGWDGLLSPINTGPPYCDPTLPNS-NGSRGDCGSAPAVGILFFTYIIISFLI
 :**:*****:*****:*****:*****:*****:*****:*****:

 Nav1.1 VVNMYIAVILENFSVATEESAEPLEDDFEMFYEVWEKFDPDATQFMEFEKLSQFAAALE
 Nav1.8 VVNMYIAVILENFSVATEESAEPLEDDFEMFYEVWEKFDPDATQFMEFEKLSQFAAALE
 Nav1.9 VVNMYIAVILENFSVATEESAEPLEDDFEMFYEVWEKFDPDATQFMEFEKLSQFAAALE
 Nav1.2 VVNMYIAVILENFSVATEESAEPLEDDFEMFYEVWEKFDPDATQFIEFAKLSDFADALD
 Nav1.3 VVNMYIAVILENFSVATEESAEPLEDDFEMFYEVWEKFDPDATQFIEFSKLSDFAAALD
 Nav1.7 VVNMYIAVILENFSVATEESTEPLSEDDFEMFYEVWEKFDPDATQFIEFSKLSDFAAALD
 Nav1.6 VVNMYIAIILENFSVATEESADPLSEDDFETFYEIWEKFDPDATQFIEYCKLADFADALE
 Nav1.4 VVNMYIAIILENFNVATEESEPLGEDDFEMFYETWEKFDPDATQFIAYSRLSDFVDTLQ
 Nav1.5 VVNMYIAIILENFSVATEESTEPLSEDDFDMFYEIWEKFDPDATQFIEYSVLSDFADALS
 *****:*****:*****:*****:*****:*****:*****:*****:*****:

 Nav1.1 PPLNLQPQPNKLQLIAMDLPMSGDRIHCLDILFAFTKRVLGESGEMDALRIQMEERFMAS
 Nav1.8 PPLNLQPQPNKLQLIAMDLPMSGDRIHCLDILFAFTKRVLGESGEMDALRIQMEERFMAS
 Nav1.9 PPLNLQPQPNKLQLIAMDLPMSGDRIHCLDILFAFTKRVLGESGEMDALRIQMEERFMAS
 Nav1.2 PPLLIAKPNKVQLIAMDLPMSGDRIHCLDILFAFTKRVLGESGEMDALRIQMEERFMAS
 Nav1.3 PPLLIAKPNKVQLIAMDLPMSGDRIHCLDILFAFTKRVLGESGEMDALRIQMEDRFMAS
 Nav1.7 PPLLIAKPNKVQLIAMDLPMSGDRIHCLDILFAFTKRVLGESGEMDSLRSQMEERFMSA
 Nav1.6 HPLRVPKPNTIELIAMDLPMVGDRIHCLDILFAFTKRVLGDSGEVDILRQQMEERFVAS
 Nav1.4 EPLRIAKPNKIKLITDLPMVGDKIHCLDILFAFTKEVLGDSGEVDALKQTMEEKFMAA
 Nav1.5 EPLRIAKPNQISLINMDLPMVGDRIHCMDILFAFTKRVLGESGEMDALKIQMEEKFMAA
 ** :.*: :** :*****:***:*****:***:***:***:***:***:***:***:

 Nav1.1 NPSKVSYQPITTLKRKQEEVAIVIQRAYRRHLLKRTVKQASFTYNKNKIK--GGANLL
 Nav1.8 NPSKVSYQPITTLKRKQEEVAIVIQRAYRRHLLKRTVKQASFTYNKNKIK--GGANLL
 Nav1.9 NPSKVSYQPITTLKRKQEEVAIVIQRAYRRHLLKRTVKQASFTYNKNKIK--GGANLL
 Nav1.2 NPSKVSYEPITTLKRKQEEVSAIIQRAYRRYLLKQVKVVSSIYKKDKKGK--ECDGTP
 Nav1.3 NPSKVSYEPITTLKRKQEEVSAAIQRNFRCYLLKQRLKNISSNNKEAIK--GRIDLP
 Nav1.7 NPSKVSYEPITTLKRKQEDVSATVIQRAYRRYLRQNVKNISSIYIKDGR--D-DDLL
 Nav1.6 NPSKVSYEPITTLRKRQEEVSAV/LQRAYRGHLARR-----GFI
 Nav1.4 NPSKVSYEPITTLRKRKHEEVCAIKIQRAYRRHLLQRSMKQASYMYRHSHDG--SGDDAP
 Nav1.5 NPSKISYEPITTLRKRKHEEVSAMVIQRAFRHLLQRLKHASFLFRQQAGSGLSEEDAP
 ****:***:*****:***:***:***:***:***:***:***:***:***:

 Nav1.1 IKEDMIIDRI-----NENSITEKTDLTSTAACPSSYDRVTKPIVEK-----HE
 Nav1.8 IKEDMIIDRI-----NENSITEKTDLTSTAACPSSYDRVTKPIVEK-----HE
 Nav1.9 IKEDMIIDRI-----NENSITEKTDLTSTAACPSSYDRVTKPIVEK-----HE
 Nav1.2 IKEDTLIDKL-----NENSTPEKTDMTPSTTS-PPSYDSVTKPEKEK-----FE
 Nav1.3 IKQDMAIDKL-----NGNSTPEKTDGSSSTTS-PPSYDSVTKPDKEK-----FE
 Nav1.7 NKKDMAFDNV-----NENSSPEKTDATSSTTS-PPSYDSVTKPDKEK-----YE
 Nav1.6 CKKTTSNKLE-----NGGTHREKKESTPSTAS-LPSYDSVTKPEKEKQQR-----AE
 Nav1.4 EKEGLLANTMSKMYGHENGNSSPSPEEKGEAGDAGPTMGLMPISPSDT--A-----WP
 Nav1.5 EREGLIAYVMSN----FSRPLGPPSSSISSTSFPSSYDSVTRATSDNLQVRGSDYHS
 :: *:

Appendix

Nav1.1	QEGKDEKAKGK-----
Nav1.8	QEGKDEKAKGK-----
Nav1.9	QEGKDEKAKGK-----
Nav1.2	KDKSEKEDKGKDIRESKK
Nav1.3	KDKPEKESKGKEVRENQK
Nav1.7	QDRTEKEDKGKDSKESKK
Nav1.6	EGRRERAKRQKEVRESKC
Nav1.4	PAPPPGQTVRPGVKESLV
Nav1.5	EDLADFPPSPDRDRESIV

9.4 Curriculum Vitae

PERSONAL DETAILS	
First Name	Gowri Shankar
Last Name	Bagavananthem Andavan
Date of Birth	25 November 1983
Place of Birth	Chennai, India
Nationality	Indian
Email	gowri.bagavananthem.andavan@univie.ac.at

ACADEMIC PROFILE		
	INSTITUTE	YEAR
Primary and Secondary Schooling	Sindhi Model Senior Secondary School, Chennai India.	June 1988 - April 1999
Higher school Certificate	Jaigopal Garodia Higher Secondary School Chennai, India	June 1999 - April 2001
Bachelor of Technology	Centre for Biotechnology (CBT), Anna University, Chennai, India.	June 2001 - May 2005
Master of Science (Research)	University of Sydney, Sydney, Australia.	March 2006 - March 2007

GRANT

1. **First Contact Initiative Grant from European Society of Cardiology (ESC)**.Feb 2011-March 2011.

SCIENTIFIC PAPERS

1. **Voltage Gated Sodium Channels: mutations, channelopathies and subtype specific targets**
Gowri Shankar Bagavananthem Andavan and Rosa Lemmens-Gruber
Current Medicinal Chemistry, 2011, 18(3):377-97.

2. Essential structural features of TNF- α lectin-like domain derived peptides for activation of amiloride-sensitive sodium current in A549 cells.

Parastoo Hazemi, Susan J. Tzotzos, Bernhard Fischer, Gowri Shankar Bagavananthem Andavan, Hendrick Fischer, Helmut Pietschmann, Rudolf Lucas, Rosa Lemmens-Gruber.

Journal of Medicinal Chemistry, **2010**, 53(22):8021-9.

3. Cyclodepsipeptides from marine sponges: natural agents for drug research.

Gowri Shankar Bagavananthem Andavan and Rosa Lemmens-Gruber

Marine Drugs, **2010**, 8(3), 810-834.

4. A Structural and Phylogenetic Analysis of Cytochrome P450

B.A.Gowri Shankar, Michael Charleston, Michael Murray and David Hibbs

International Proceedings of the 15th International Conference on Cytochrome P450: Biochemistry, Biophysics, Functional Genomics, **2007**, 75-80.

5. Ion-pairs in non-redundant protein structures

B.A.Gowri Shankar, R.Sarani, Daliah Michael, P.Mridula, C.Vasuki Ranjani,

G.Sowmiya, B.Vasundhar, P.Sudha, J.Jeyakanthan, D.Velmurugan and K.Sekar. *J. Biosci.*, **2007**, 32(4), 693-704.

POSTER PRESENTATIONS

1. ESC Congress 2010, 28 August - 1 September, Stockholm, Sweden. **Title:** *Modulation of cardiac voltage gated sodium channel splice variants with its auxiliary subunit by Fyn tyrosine kinase.*

2. Frontiers in Cardiovascular Biology, Berlin, Germany, 16-19 July 2010, **Title:** *Cardiac sodium channel variants and fyn tyrosine kinase modulation.*

3. XXth World Congress of the International Society of Heart Research 2010, May 13-16 2010, Kyoto, Japan. **Title:** *Fyn tyrosine kinase modulation on cardiac voltage gated sodium channel splice variants.*

4. 54th Biophysical Society's Annual Meeting at The Moscone Convention Center 20-24 February 2010, San Francisco, California. **Title:** *Modulation of Na_v1.5 varients by Src tyrosine kinase.*

5. **15th International Conference on Intelligent System for Molecular Biology (ISMB) Jointly with European Conference on Computational Biology (ECCB)** on 21-25 July, 2007, Vienna, Austria.
6. **11th Annual International Conference on Research in Computational Molecular Biology (RECOMB 2007)**, 21-25 April, 2007, San Francisco Bay, California.
7. **Fifth Asia-Pacific Bioinformatics Conference**, 15-17 January, 2007, Hong Kong.
8. **4th Annual Rocky Mountain Bioinformatics Conference**, 1-6 December, 2006, Aspen/Snowmass, Colorado.
9. **Bioinformatics Australia 2006**, Sydney, 21-22 November, 2006.

SCHOLARSHIPS

1. Travel grant from the **ESC Council on Basic Cardiovascular Science** to attend ESC Congress 2010, Stockholm, Sweden.
2. International **ISHR Travel Grant** to attend XXth World Congress of the International Society of heart Research 2010, Kyoto, Japan.
3. International Travel Award from **Biophysical Society** to attend and present my data in 54th Annual Meeting at San Francisco, California.
4. Travel scholarship from **RECOMB 2007** committee, to attend RECOMB 2007 in San Francisco Bay, California, USA.
5. BioinfoSummer 2006, **ICE-EM Scholarship** to attend summer symposium in Bioinformatics, ANU, Canberra; Australia.
6. Travel scholarship to attend **PhD Winter School** in Data Mining & Bioinformatics, Lorne, Victoria, Australia
7. Travel scholarship to attend **APAC Summer School in Computational Science** 2006, Brisbane, Australia.
8. Chief Minister Meritorious Award to students to continue their undergraduate studies, Chennai, India.

TEACHING

- Demonstrating **Medicinal Chemistry** PHAR2632 in Faculty of Pharmacy, University of Sydney. (March 2007 – June 2007)
- Demonstrating **Medicinal Chemistry** PHAR2618 in Faculty of Pharmacy, University of Sydney. (July 2006 – November 2006)